Publication No. R76-42 Order No. 558

EFFECT OF DUCTILITY ON RESPONSE SPECTRA FOR ELASTO-PLASTIC SYSTEMS

by

SAMIR SEHAYEK

Supervised by
José M. Roesset

September 1976

Sponsored by the National Science Foundation
Division of Advanced Environmental Research
and Technology
Grant GI-43106

Additional Copies May be Obtained from
National Technical Information Service
U. S. Department of Commerce
5285 Port Royal Road
Springfield, Virginia 22151

Massachusetts Institute of Technology
Department of Civil Engineering
Constructed Facilities Division
Cambridge, Massachusetts 02139

EFFECT OF DUCTILITY ON RESPONSE SPECTRA FOR ELASTO-PLASTIC SYSTEMS

by

SAMIR SEHAYEK

Supervised by

José M. Roesset

September 1976

Sponsored by National Science Foundation
Division of Advanced Environmental Research and Technology
Grant GI-43106

Research Report R76-42

der No. 558

ABSTRACT

EFFECT OF DUCTILITY ON RESPONSE SPECTRA
FOR ELASTO-PLASTIC SYSTEMS

The purpose of this work is to evaluate two procedures used to estimate response spectra for inelastic systems subjected to earthquakes. The first, which is a set of rules suggested by Newmark, derives the inelastic response spectrum for the elastic one. The second is a procedure which replaces the nonlinear spring of the system by an equivalent linear one with stiffness and damping obtained as functions of a characteristic strain.

It is concluded that Newmark's procedure, although approximate, performs quite satisfactorily. The second procedure, although not as satisfactory as Newmark's, reproduces the general trends of spectra quite well also.

PREFACE

The work described in this report is based on the thesis by Samir Sehayek, presented to the Civil Engineering Department at M.I.T. in partial fulfillment of the requirements for the degree of Master of Science. The research was supervised by Professor José M. Roesset and was made possible through Grant GI-43106 from the National Science Foundation, Division of Advanced Environmental Research and Technology.

This is the third of a series of reports published under this grant. The first two were:

1. Research Report R76-37, by Tarek S. Aziz: "Inelastic Dynamic Analysis of Building Frames," August 1976.

2. Research Report R76-38, by Kenneth Mark: "Nonlinear Dynamic Response of Reinforced Concrete Frames," August 1976.

TABLE OF CONTENTS

source of information in earthquake design. It is clear, however, that there is no reason to assume that the earthquake that might occur in any given location would have precisely the same characteristics multiplied throughout the whole range of frequencies by a constant factor.

One approach towards a better characterization of strong motions was taken by Newmark, recognizing seven distinct ranges in the response spectrum (Fig. 1-5).

a) A range of very small frequencies in which the relative displacement of the 1-DOF system is practically equal to the maximum ground displacement (in other words the structure is so flexible that it remains practically at rest).

b) A transition range.

c) A range of frequencies over which the maximum relative displacement of the 1-DOF system does not change very much in the average and can be assumed as constant, function of damping.

d) An intermediate range of frequencies over which the maximum relative velocity of the 1-DOF system does not change very much and can be assumed to be a constant, function of damping.

e) A range of frequencies over which the maximum absolute acceleration of the 1-DOF system does not change very much in the average and can be assumed to be a constant, function of damping.

f) A second transition zone.

g) A range of high frequencies for which the absolute acceleration of the 1-DOF system is practically equal to the maximum ground acceleration (in other words the structure is so stiff that it follows practically the motion of the ground).

Figure 1-5 shows the basic Newmark spectrum as defined above. To

TABLE OF CONTENTS

CHAPTER 1 - INTRODUCTION

Earthquake considerations have always represented special problems in the design of buildings. Due to the unpredictable nature and magnitude of earthquakes, their effects can be treated only in an approximate way through sets of simplified rules. Within the last two decades, however, our knowledge and understanding of the subject have greatly improved due to new analytical methods, the aid of computational tools, and intense study and research undertaken by universities in this country and abroad.

Our aim in this report is to study and investigate some of these analytical methods and rules and if possible to come up with some conclusions and recommendations as how to best use and apply these methods in design practice.

Basically, our only means of studying the effects of an earthquake is through an earthquake record. Such a record, recorded by a strong motion accelerograph, reproduces the variation of the ground acceleration to be given by a function of the form:

$$\ddot{y}_s = \begin{cases} 0 & \text{for } t \leq 0 \\ f(t) & 0 \leq t \leq T_d \\ 0 & T_d \leq t \end{cases}$$

the response of a single degree-of-freedom system (Fig. 1-1), to a base motion represented by an acceleration $\ddot{y}_s = f(t)$ could be determined using Duhamel's integral. This integral is given as

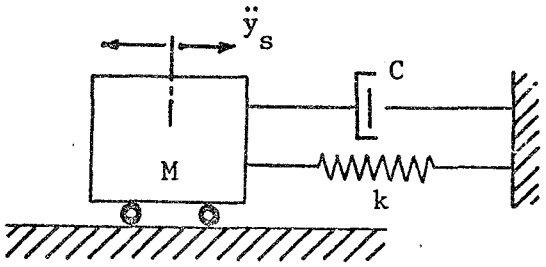

Figure 1-1
Linear Elastic 1 D.O.F. System

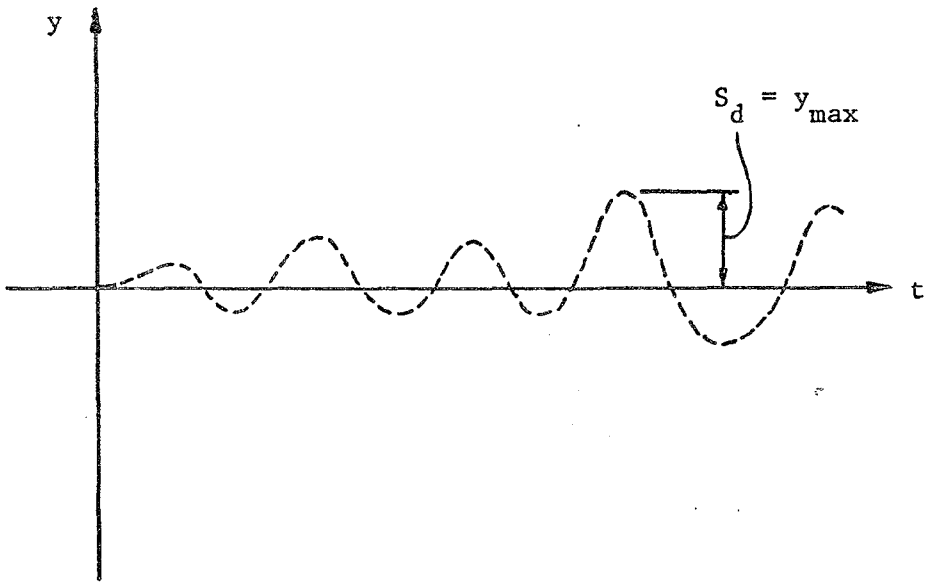

Figure 1-2

Response of a Single D.O.F. System
with a Given ω and β to Earthquake Record

$$u(t) = -\frac{1}{\omega} \int_0^t f(\tau)\, e^{-\beta(t-\tau)} \sin \omega_D(t-\tau_D)d \qquad (1)$$

where ω_D = damped natural frequency

$= \omega^2 - \beta^2 = \omega^2(1-p^2)$

$\beta = \omega p$

p = fraction of critical damping.

Now we can define the maximum value of $u(t)$ as

$$S_d(\omega,p) = \text{max. over } t \left| u(t) \right|$$

For a given value of p, S_d is known as the <u>displacement response spectrum</u>. In a similar way one can define a velocity response spectrum for $\dot{u}(t)$ and an acceleration response spectrum for $\ddot{y}(t)$.

The maximum relative velocity of a single D.O.F. system is very close to ω times the maximum relative displacement except for small values of ω. It is thus more common to define a pseudo velocity as $\omega|u(t)|$ and pseudo velocity response spectrum as

$$S_v(\omega,p) = \omega\, S_d(\omega,p)$$

In the same way we define a pseudo acceleration response spectrum as

$$S_a(\omega,p) = \omega S_v(\omega,p) = \omega^2\, S_d(\omega,p) \qquad (2)$$

Hence it is obvious that once we compute one of these spectra (corresponding to a given value of damping), the other two are immediately determined using relation (2).

What is usually done in practice is to subject the single D.O.F. system with a given natural period and critical damping (Fig. 1-1) to

the earthquake under study. The mass will undergo a maximum displacement relative to the fixed reference frame, which is usually the ground (Fig. 1-2).

Similarly by subjecting a large number of 1-DOF systems with different frequencies and corresponding to a given value of damping to this same record, their maximum response can be computed. A displacement response spectrum is then plotted as the maximum relative displacement versus the natural period or frequency of the system.

Following the same procedure, response spectra for different values of damping can be obtained (Fig. 1-3), thus providing all the necessary information for the elastic design of 1-DOF systems.

Because of the direct relationship between the displacement, pseudo velocity and pseudo acceleration response spectra, it has become customary to plot the pseudo velocity spectrum as a function of period or frequency on a double logarithmic scale. Fig. 1-4 shows the spectrum of the 1940 El Centro earthquake plotted this way. Horizontal lines correspond to constant pseudo velocity values. Lines inclined at 45 degrees (with + ve slope) represent the constant relative displacement values. Those with the negative slope are of constant pseudo acceleration values. It is thus possible from this plot to read simultaneously the values of these three components corresponding to any value of period or frequency of the 1-DOF system.

The set of response spectra used in practice was for a long time that of the 1940 El Centro earthquake. This earthquake has been thoroughly documented and for some time was considered a sufficient and reliable

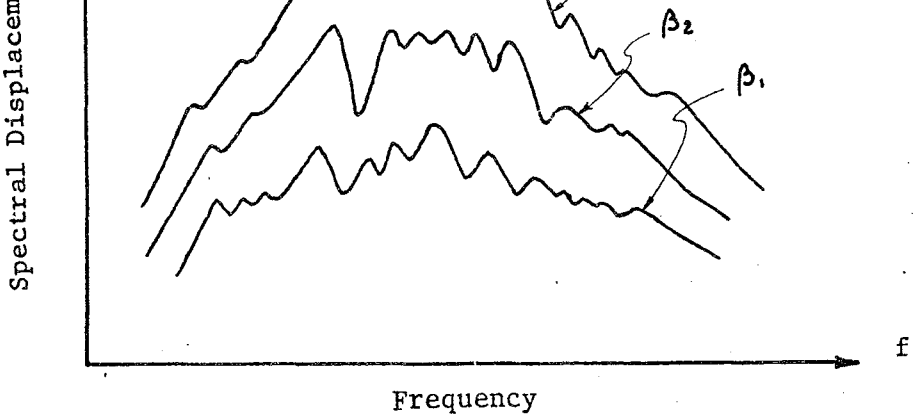

Figure 1-3

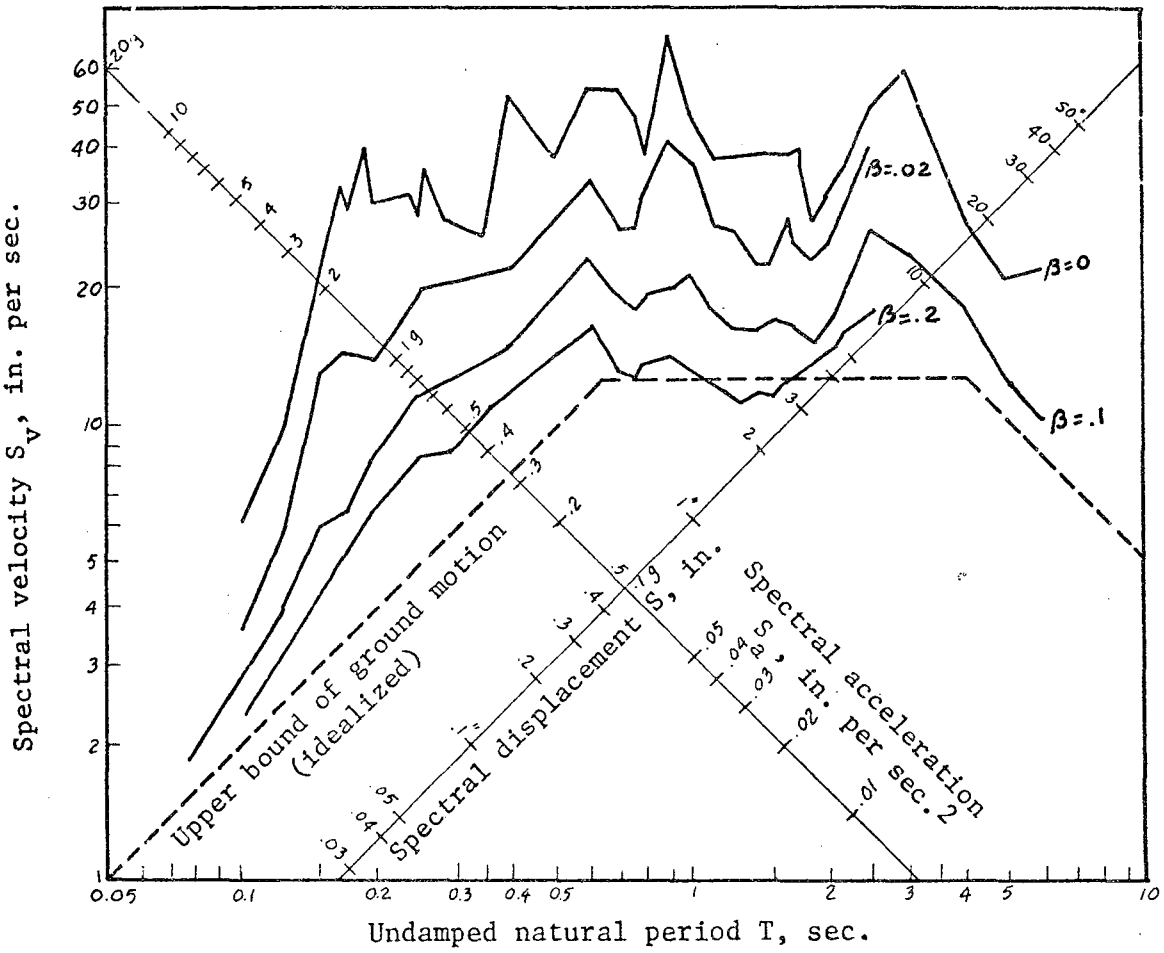

Response Spectra for Elastic Systems, 1940 El Centro Earthquake

Figure 1-4

source of information in earthquake design. It is clear, however, that there is no reason to assume that the earthquake that might occur in any given location would have precisely the same characteristics multiplied throughout the whole range of frequencies by a constant factor.

One approach towards a better characterization of strong motions was taken by Newmark, recognizing seven distinct ranges in the response spectrum (Fig. 1-5).

a) A range of very small frequencies in which the relative displacement of the 1-DOF system is practically equal to the maximum ground displacement (in other words the structure is so flexible that it remains practically at rest).

b) A transition range.

c) A range of frequencies over which the maximum relative displacement of the 1-DOF system does not change very much in the average and can be assumed as constant, function of damping.

d) An intermediate range of frequencies over which the maximum relative velocity of the 1-DOF system does not change very much and can be assumed to be a constant, function of damping.

e) A range of frequencies over which the maximum absolute acceleration of the 1-DOF system does not change very much in the average and can be assumed to be a constant, function of damping.

f) A second transition zone.

g) A range of high frequencies for which the absolute acceleration of the 1-DOF system is practically equal to the maximum ground acceleration (in other words the structure is so stiff that it follows practically the motion of the ground).

Figure 1-5 shows the basic Newmark spectrum as defined above. To

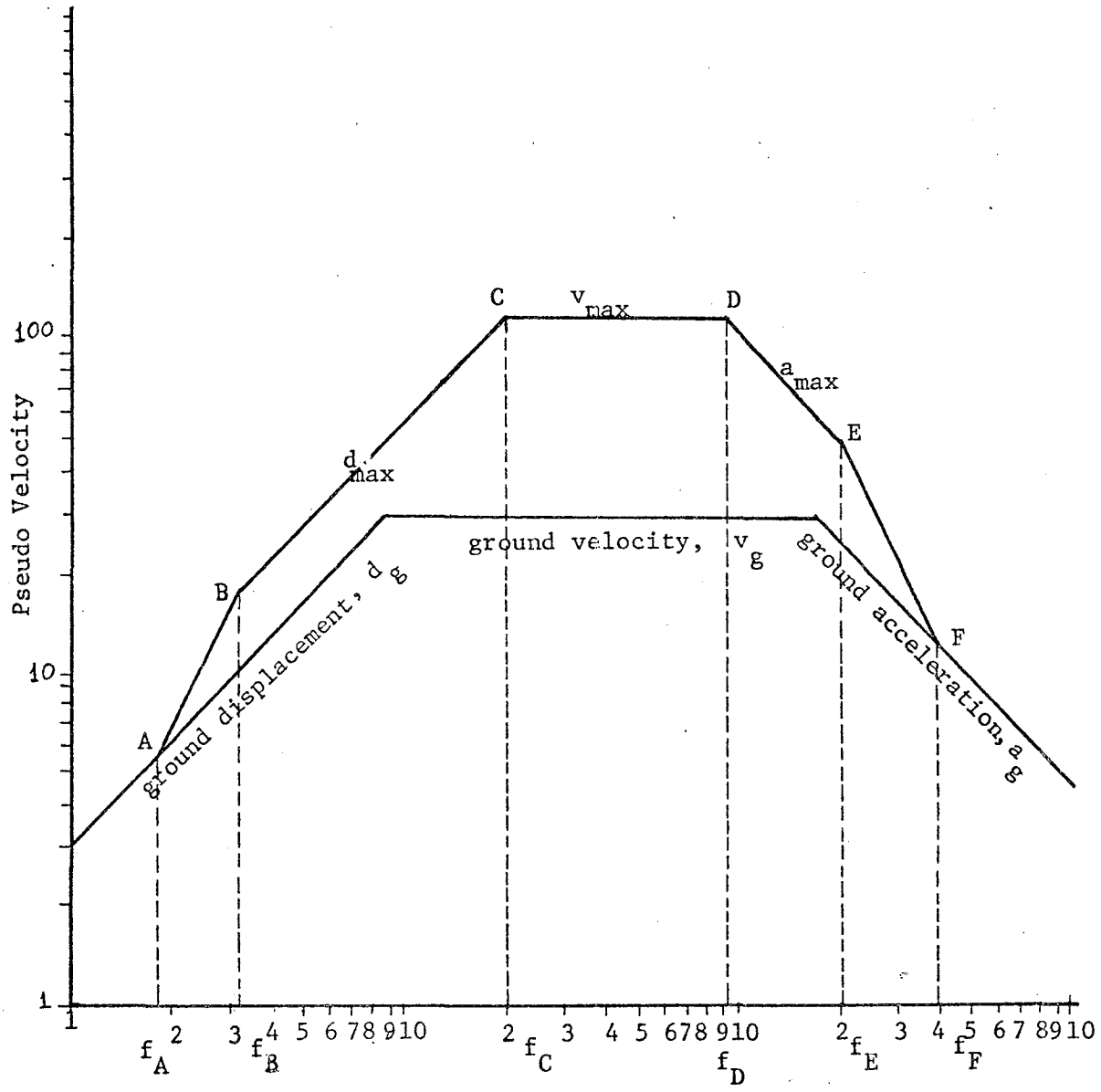

NEWMARK'S BASIC SPECTRUM

Fig. 1-5

construct design spectra of this nature, it is thus necessary to:

1) Define the design earthquake by means of its ground acceleration, velocity and displacement.

2) Once these three parameters have been characterized, the design spectrum for a given percentage of critical damping requires the specifications of seven quantities. The quantities suggested by Newmark are the ratios of:

$$d_{max}/d_G \quad , \quad f_C/f_B \quad , \quad f_F/f_D$$
$$v_{max}/v_G \quad , \quad f_C/f_A$$
$$a_{max}/a_G \quad , \quad f_E/f_D$$

On the basis of the 1940 El Centro response spectra, newmark suggests:

$$f_C/f_B = 4 \quad , \quad f_E/f_D = 4$$
$$f_C/f_A = 10 \quad , \quad f_F/f_D = 10$$

And the ratios of d_{max}/d_G, v_{max}/v_G and a_{max}/a_G for different values of damping are given as:

Damping %	d_{max}/d_G	v_{max}/v_G	a_{max}/a_G
0	2.5	4.0	6.4
0.5	2.2	3.6	5.8
1	2.0	3.2	5.2
2	1.8	2.8	4.3
5	1.4	1.9	2.6
7	1.2	1.5	1.9
10	1.1	1.3	1.5
20	1.0	1.1	1.2

Garcia (ref. 1) extended Newmark's work by considering the records of five earthquakes (El Centro 1940, Taft, Olympia, Helena and Golden Gate). The average values suggested by Garcia are:

Damping %	d_{max}/d_G	v_{max}/v_G	a_{max}/a_G
0	2.10	4.50	9.00
0.5	2.01	3.52	5.95
1	1.91	3.25	5.00
2	1.82	2.80	4.03
5	1.56	2.08	3.01
10	1.33	1.59	2.26
20	1.08	1.13	1.67

While these values are only slightly different from those of Newmark, the frequency ratios were on the other hand somewhat different, thus suggesting slight modification over those proposed by Newmark. Garcia suggested that the values of f_B and f_E could be computed from the equation

$$f_C/f_B = 6.1\ (1 + 300\beta)^{-.17}$$

$$f_E/f_D = 2.1 + 0.283 \log\ (1 + 450\beta)$$

thus showing damping dependence instead of taking $f_C/f_B = f_E/f_D = 4$ as suggested by Newmark.

Since Newmark's set of proposed data is the one that is still used in practice, it will be the one we will be referring to in succeeding chapters.

The preceding discussion provided us with some information concerning elastic 1-DOF systems. Using modal analysis and some approximations, this information provides the basis for the design of linear multi-DOF systems.

Modal analysis involves the determination of the responses in each mode separately and the use of superposition to provide the total response. The total response is normally approximated by using the square root of

the sum of the squares of the maximum responses determined for each normal mode.

The approximation introduced by superimposing maxima (or the square of the sum of the squares) is an area which is under discussion and will not be dealt with here. Rather, we will shift our discussion to the behavior of nonlinear 1-DOF systems under strong ground motion.

Under a severe earthquake, design codes recognize that a structure may not remain elastic and that a certain amount of yielding and plastic deformation may take place in different components (except maybe for rather flexible structures).

The mathematical determination of the dynamic response of inelastic systems, once a nonlinear model has been selected, offers little problem and requires only a step-by-step numerical integration of the equation of motion. The significant questions in this area relate to:

a) The modeling of the structure; i.e., selection of nonlinear springs which will properly reproduce the behavior of different structural components, and the determination of which type of nonlinear effects is really significant.

b) The interpretation of results and their generalization into design guidelines.

Some of the mathematical models describing nonlinear systems often used are shown in Fig. 1-6.

A substantial amount of work has been carried out trying to determine the variation of maximum effects as a function of earthquake intensity, elastic or ultimate strength and natural period. The first step in this

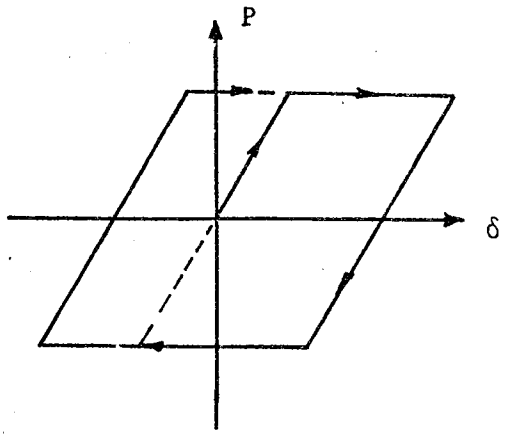

a - Elasto-Plastic

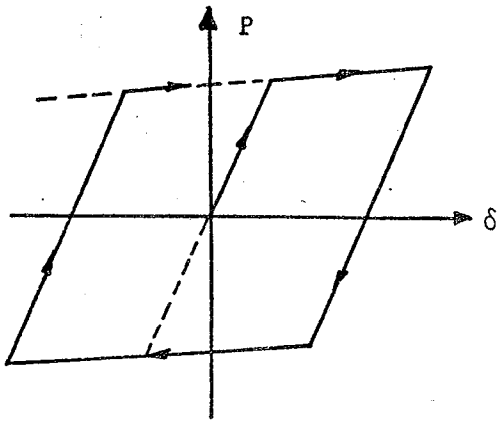

b - Bilinear

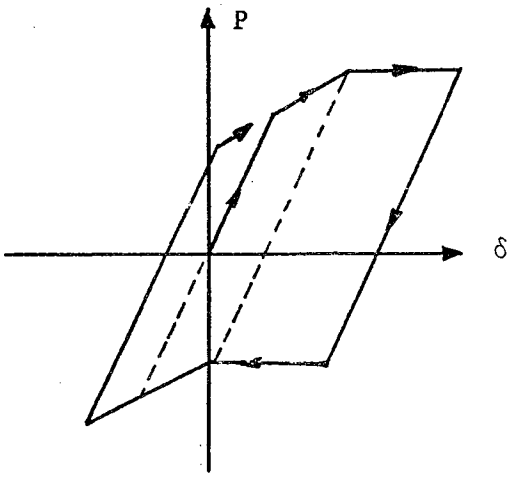

c - Trilinear

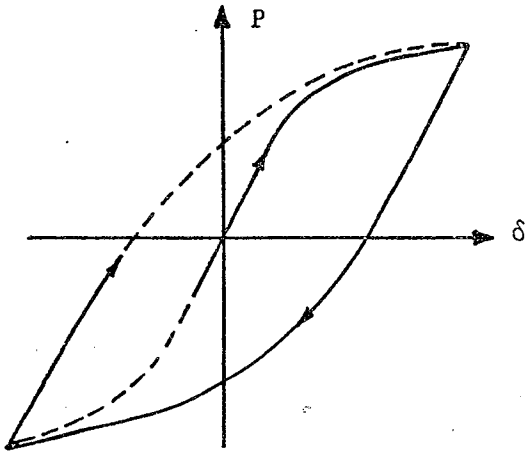

d - Ramberg Osgood

Figure 1-6 Mathematical Models Describing Nonlinear Systems

direction was the determination of inelastic response spectra. Figs. 1.7 and 1.8 show response spectra for elastoplastic systems with zero and 10% damping under the NS component of the 1940 El Centro earthquake as reported by Blume, Newmark and Corning (ref. 2). Note that each spectrum corresponds to a fixed value of the ductility factor μ (ductility being defined as the ratio of the maximum distortion in the spring to the limit elastic distortion).

Response spectra for other nonlinear systems have been obtained by Veletsos (ref. 3). The results are often interpreted in a simple way by comparing the response of a nonlinear system to that of an "equivalent" linear system. There are two main effects which characterize the response of a single D.O.F. system in the inelastic range:

a) a reduction in the instantaneous or equivalent stiffness with increasing deformation;

b) a loss of energy through hysteretic loops.

The first effect represents an increase in the natural period (or a decrease in the natural frequency), while the second can be interpreted as an increase in damping.

The purpose of the present work is to consider an elastoplastic system (Fig. 1.6a) and subject it to five different earthquakes with a total of 9 components (El Centro 1940 NS, El Centro 1940 EW, Taft NW, Taft SW, Helena NS, Helena EW, Golden Gate, Olympia NW, Olympia NE). Using a numerical integration procedure, the response spectra of each record for different values of ductility μ are obtained. These spectra are then used to evaluate:

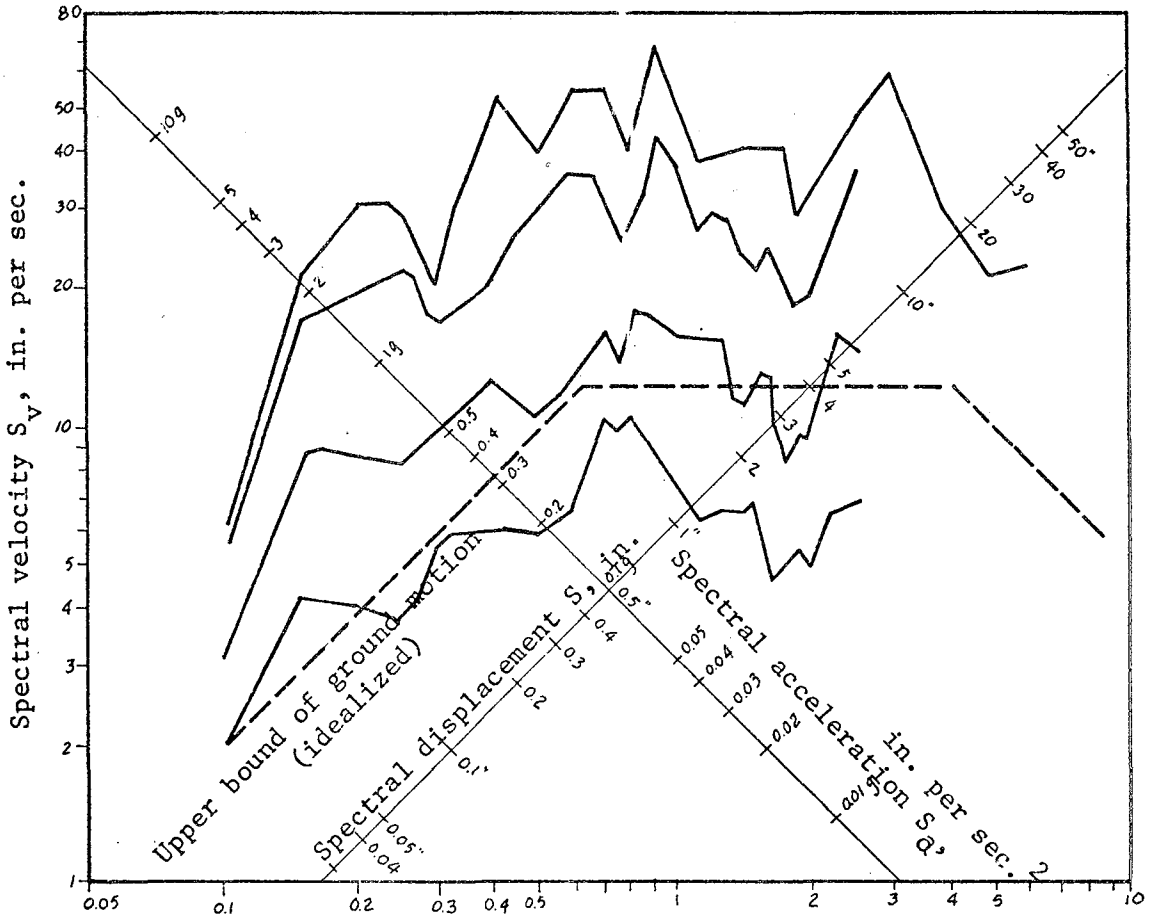

RESPONSE SPECTRA FOR UNDAMPED ELASTO-PLASTIC SYSTEMS,
1940 EL CENTRO EARTHQUAKE

Fig. 1-7

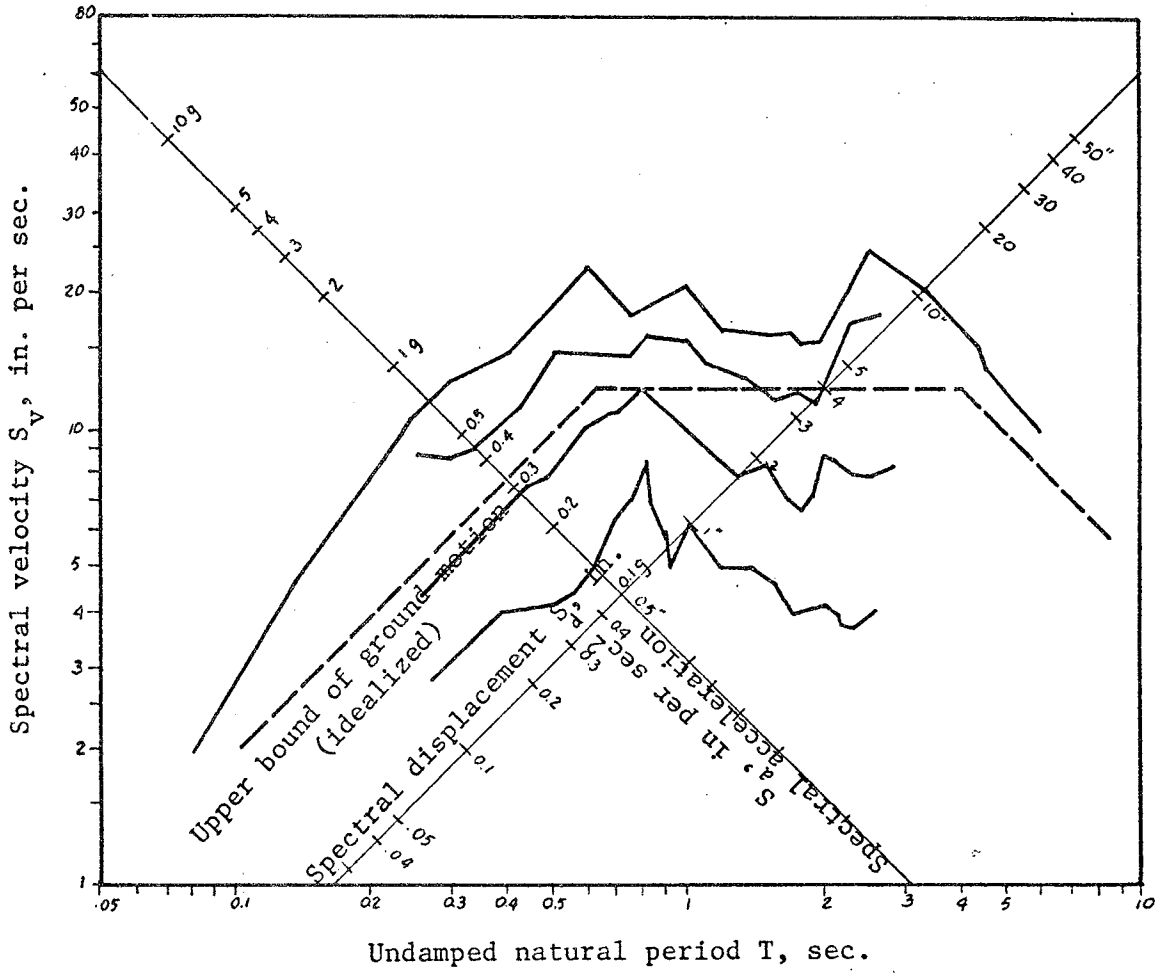

RESPONSE SPECTRA FOR ELASTO-PLASTIC SYSTEMS WITH
10 PERCENT CRITICAL DAMPING, 1940 EL CENTRO EARTHQUAKE

Fig. 1-8

(1) A procedure suggested by Newmark for shifting from the elastic response spectra ($\mu = 1$) to any level of desired ductility for nonlinear systems. The details of this procedure are described in Chapter 2.

(2) A procedure often used in practice to determine the response of inelastic systems by replacing the nonlinear system by an equivalent linear system. This, too, is described in Chapter 2.

Chapter 2 covers the details of the two procedures mentioned above and also the procedure followed to obtain the actual inelastic response spectra for levels of ductility from $\mu = 1$ to 10. Since we used nine earthquake records, then nine different sets of plots were obtained, one corresponding to each earthquake.

Similar plots were obtained using the approximate method.

In Chapter 3 Newmark's rule is defined. The analytical procedure used to evaluate it is then described. This is followed by a discussion on the results obtained and an evaluation of the above mentioned rule. Chapter 4 follows the same procedure for the approximate method.

And finally, conclusions and recommendations concerning these two methods are discussed in Chapter 5.

CHAPTER 2

Newmark's Inelastic Response Spectra

The procedure suggested by Newmark for obtaining inelastic response spectra of single D.O.F. systems for any level of ductility is illustrated graphically in Fig. 2.1.

These response spectra are intended to define the pseudo (or maximum absolute) acceleration, S_a, of the mass of the single D.O.F. system as a function of damping and frequency. In order to determine the inelastic response spectra for the maximum relative displacement, the curve obtained by these rules is multiplied by the ductility factor μ over the complete range of frequencies. Clearly for an inelastic system it is no longer possible to read acceleration, velocity and displacement from a unique curve.

Newmark's procedure consists basically of the following steps:

a) The elastic response spectra ($\mu = 1$) of the single D.O.F. system is divided into seven distinct ranges, as shown on Fig. 1.5. This is shown as the curve for $\mu = 1$ on Fig. 2.1.

b) For the frequency range covered by R1, R2, R3 and R4, the procedure is to multiply the S_v values by a factor of $1/\mu$, thus making a downward vertical shift of the curve only. This implies that in this range the maximum relative displacement is the same as for an elastic system independently of the ductility ratio μ.

c) The S_v values of R5 are multiplied by a factor of $1/\sqrt{2\mu - 1}$.

d) A transition line is drawn from the limiting frequency of R5 to the elastic spectrum at the limit of R6.

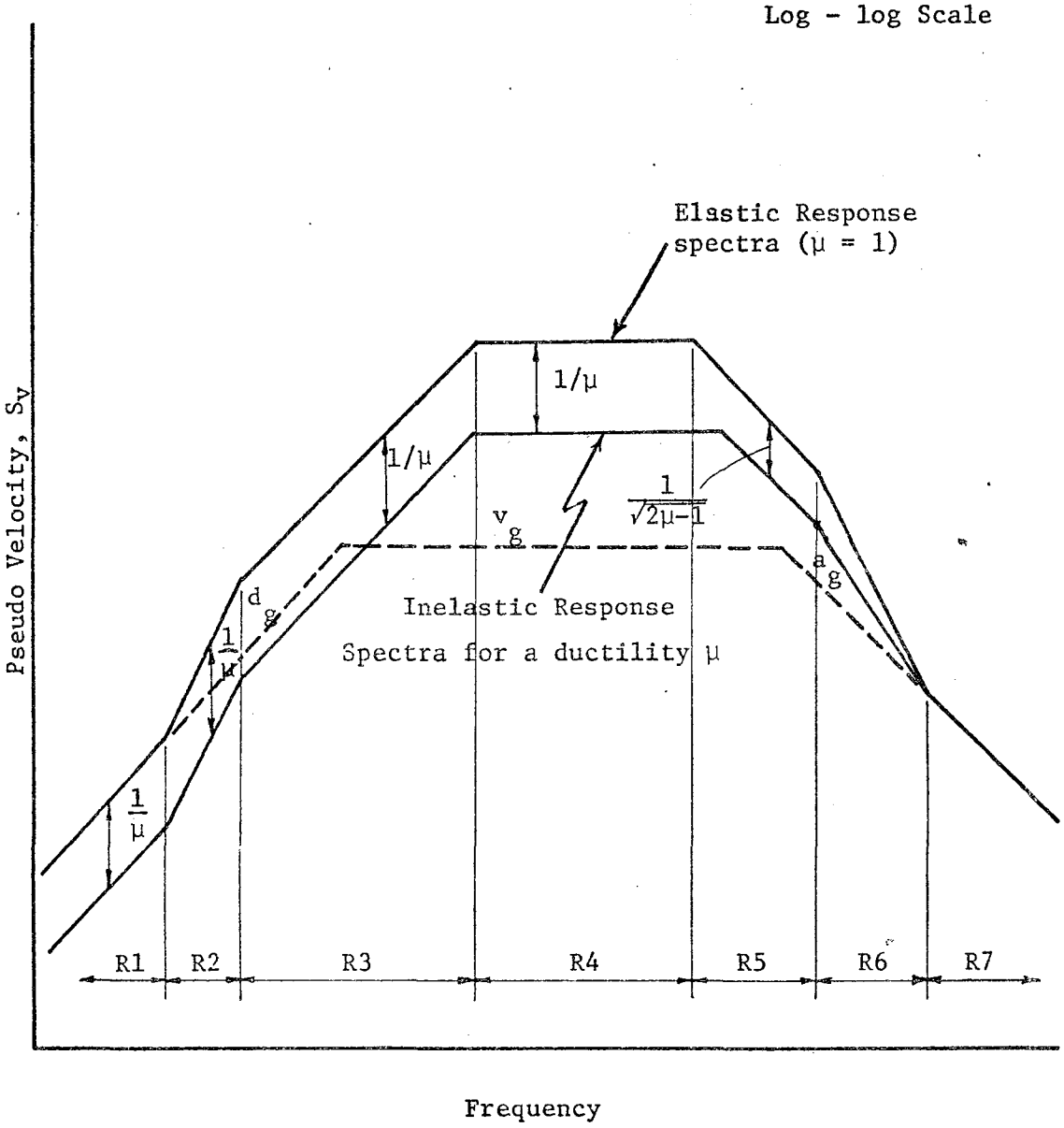

Figure 2-1 Newmark's Inelastic Response Spectra

While the assumption of equal maximum relative displacement (an acceleration ratio of $1/\mu$) is intuitively clear for small frequencies, the suggested ratio in range 5 is based on energy considerations, as shown on Fig. 2.2.

If we let Energy of Elastoplastic system = Energy of Elastic system, we can write:

$$1/2k\ u_{me}^2 = k\ u_y\ u_m - 1/2\ ku_y^2$$

Replacing $u_m = \mu u_y$ and rearranging terms, we obtain

$$\frac{u_y}{u_{me}} = \frac{1}{\sqrt{2\mu - 1}}$$

In the range of high frequencies, on the other hand, Newmark suggests that the ductility requirements increase so rapidly with earthquake intensity that systems should be designed to remain elastic. This leads to the rule that the acceleration is constant independently of the ductility factor μ.

Inelastic Response Spectra Using Equivalent Elastic Systems

Another approach which is sometimes used in determining the inelastic response of a single D.O.F. system is to replace the inelastic system by an elastic system with an equivalent stiffness and damping factor (Fig. 2.3).

The equivalent stiffness and damping factors are given as

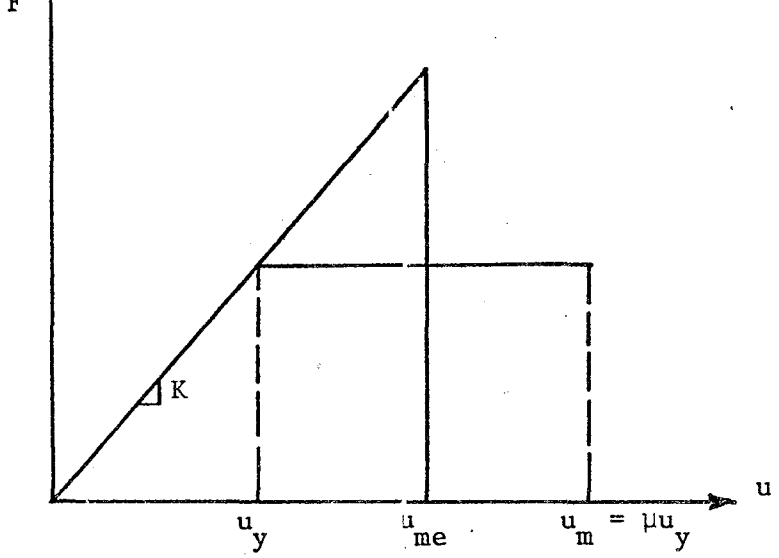

Figure 2-2 Elasto-Plastic system with an Equivalent Elastic System

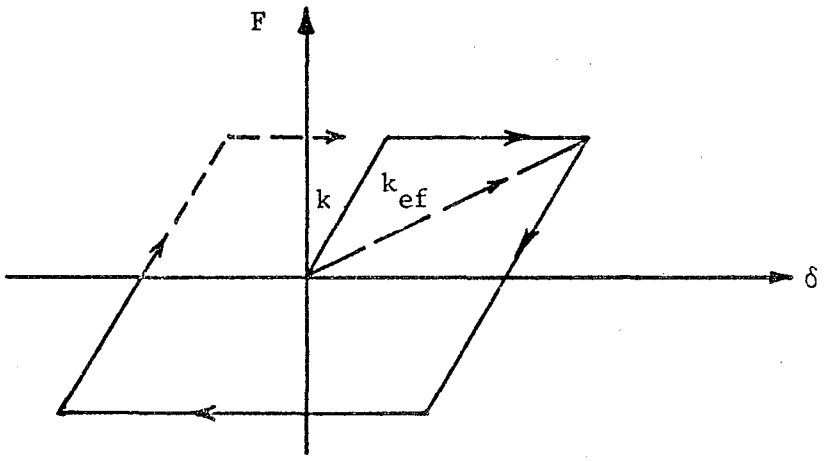

Figure 2-3 Elasto-Plastic System Showing Actual Stiffness with a Modified Equivalent Stiffness

$$k_{ef} = \frac{k}{\mu_{char}}$$

$$\beta_{ef} = \beta + \frac{2}{\pi}\left(1 - \frac{1}{\mu_{char}}\right)$$

where: k = actual stifness factor of elastoplastic system

μ_{char} = ductility factor corresponding to a characteristic displacement or strain. For a steady-state response, μ_{char} is the maximum μ. For a transient response on the other hand, μ_{char} is taken as a fraction of the maximum ductility, μ, typically $2/3\mu$.

β = viscous damping of the elastoplastic system.

Processing of Earthquakes

Our proceeding study and analysis will be based on the basis of nine earthquake records available at M.I.T.

Earthquake	Component	Maximum Recorded Ground Acceleration
El Centro 1940	N-S	.319g
El Centro 1940	E-W	.218g
Taft 1952	N-69-W	.157g
Taft 1952	S-21-W	.178g
Helena 1935	N-S	.140g
Helena 1935	E-W	.152g
Golden Gate 1957	S-80-E	.128g
Olympia 1949	N-10-W	.184g
Olympia 1949	N-80-E	.318g

These records were selected because they are normally considered as representing typical motions on firm ground. This assumes that the motion generated by each of them is based on a record registered on firm ground. It does not therefore account for the effect of local soil conditions which may in fact exist and thus distort the records.

The records had a standard base line correction applies to them, as suggested by Berg and Housner (ref. 4).

Determination of Response Spectra

The nonlinear system considered in this work is the elastoplastic system shown in Fig. 2.4. The equation of motion for the 1 D.O.F. system shown subjected to a ground acceleration is

$$M\ddot{u} + c\dot{u} + kF(u) = - M\ddot{u}_g$$

or

$$\ddot{u} + 2p\,\omega\,\dot{u} + \omega^2 F(u) = - \ddot{u}_g \qquad (2\text{-}1)$$

where

M = mass of the 1 D.O.F. system

u = displacement of the mass relative to ground

$F(u)$ = spring force divided by initial stiffness

k = initial stiffness of the spring

c = coef. of viscous damping

$p = \dfrac{c}{2\sqrt{kM}}$ = percentage of critical damping

$\ddot{u}_g$ = ground acceleration

Equation (2-1) can be transformed to a nondimensional form by defining a dimensionless response z as

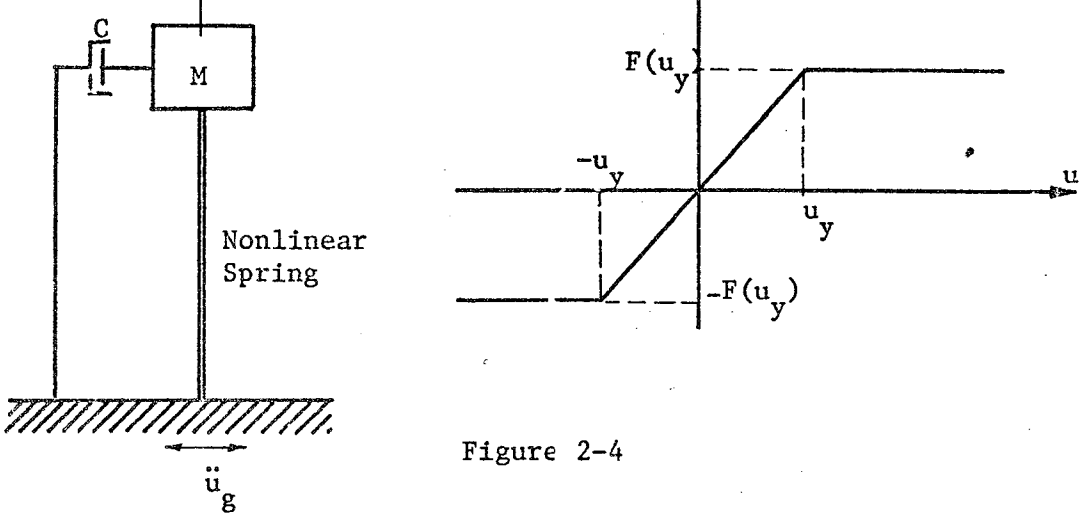

Figure 2-4

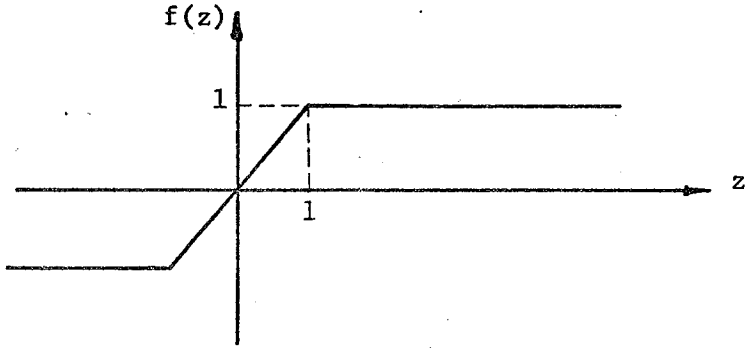

Figure 2-5

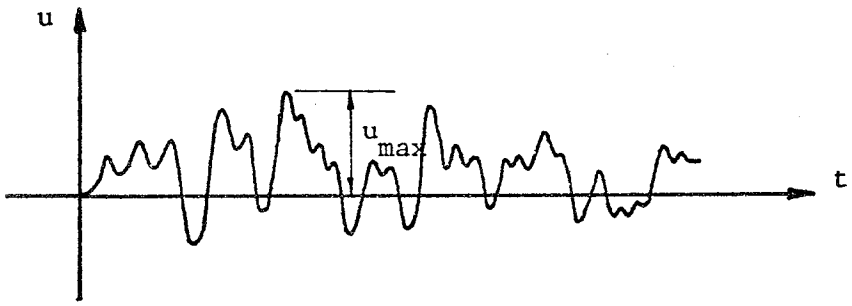

Figure 2-6

$$z = \frac{u}{u_y}$$

where $u > u_y$ and $z_{max} = \frac{u_{max}}{u_y} = \mu$

and by defining $f(z) = \frac{F(u)}{u_y}$ as shown in Fig. 2.5.

Note that $f(z) = z$ for $z \leq 1$

$= 1$ for $z \geq 1$

Substituting for z in Eq. (2-1), we obtain

$$u_y\ddot{z} + 2p\omega u_y\dot{z} + \omega^2 u_y f(z) = -\ddot{u}_g$$

or

$$\ddot{z} + 2p\omega\dot{z} + \omega^2 f(z) = -\frac{\ddot{u}}{u_y}$$

$$= -k\left(\frac{\ddot{u}_g}{F_y}\right)$$

$$= -\omega^2\left(\frac{M\ddot{u}_g}{f_y}\right) \qquad (2\text{-}2)$$

From Eq. (2-2) we see that the dimensionless response $z = \frac{u}{u_y}$ of a nonlinear system depends on

a) The fraction of critical damping, p.

b) The initial undamped natural period of the system, $T = \frac{2\pi}{\omega}$ or its frequency ω.

c) The ratio $M\ddot{u}_g/F_y$.

Simply, $z = f(\beta, T, M\ddot{u}_g/F_y)$.

Through numerical integration of the equation of motion, using the available earthquake records, the time history response of the system could be obtained.(Fig. 2.6). The nine records used were digitized at

sponse obtained defines the maximum response of the system u_{max}, which in turn defines the ductility of the system $\mu = u_{max}/u_y$.

This maximum response is defined for one given single D.O.F. system with a given β, T, F_y, M and subjected to a given ground acceleration u_g. By varying F_y we can end up with a plot of u_{max} vs. Mu_{gmax}/F_y defined for certain T and β as shown in Fig. 2.7.

We can repeat the same procedure for different values of natural period. From the generated plots we can extract by interpolation plots of the acceleration ratio $\ddot{u}_{max}/\ddot{u}_{gmax}$ versus frequency (Fig. 2-8) for different damping factors.

Computer Program and Generation of Plots

The amount of effort to be spent on computations and generation of plots made the use of the computer necessary. The numerical integration procedure used in generating the maximum response was based on a central difference formula.

Equation (2-1) can be rewritten as:

$$M \ddot{u}_n + 2 \beta \omega M \dot{u}_n + F(u_n) = - M \ddot{u}_{gn} \qquad (2\text{-}3)$$

where

$$\ddot{u}_n = \frac{u_{n+1} - 2u_n + u_{n-1}}{\Delta t^2}$$

$$\dot{u}_n = \frac{u_{n+1} - u_{n-1}}{2\Delta t}$$

Substituting for $\ddot{u}_n$ and $\dot{u}_n$ in Equation (2-3) and rearranging terms, we obtain the recurrence formula:

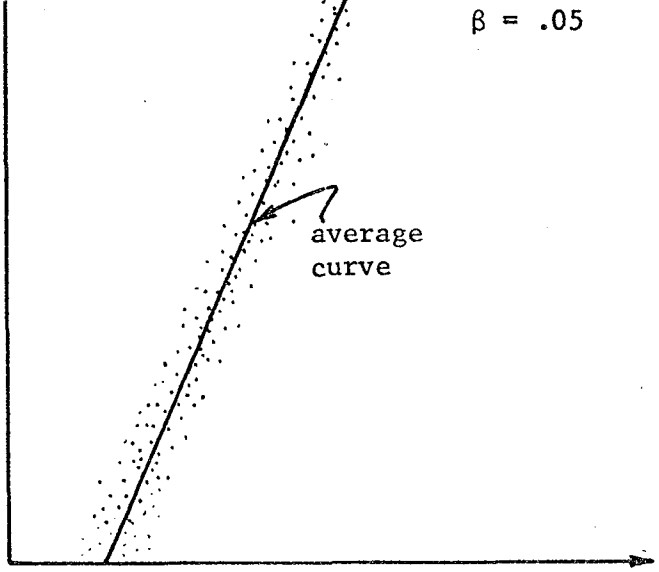

$$\frac{M\ddot{u}_g}{F_y} = \frac{\ddot{u}_g}{\ddot{u}_{max}}$$

Figure 2-7

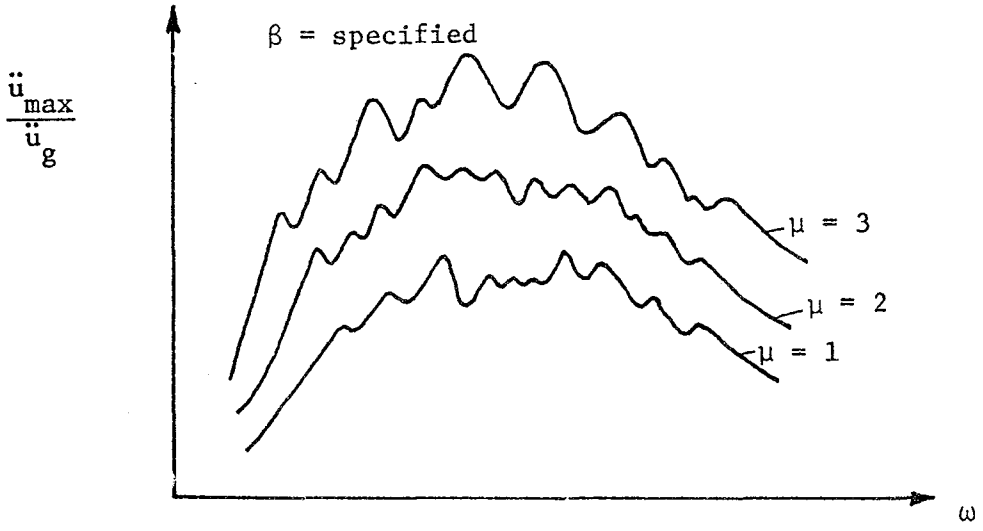

$\frac{\ddot{u}_{max}}{\ddot{u}_g}$

Figure 2-8

Since u_{n-1} is not defined at t = 0, we assume a linear acceleration during the first time interval to obtain:

$$u_1 = -\frac{1}{6}\Delta t^2 u_{go}\frac{2+\beta\omega\Delta t}{1+\beta\omega\Delta t+(1/6)\omega^2\Delta t^2} - \frac{1}{6}\Delta t^2 \ddot{u}_{g1}\frac{1}{1+\beta\omega\Delta t+1/6\omega^2\Delta t^2}$$

Using then the recurrence formula for a given set of values of $\ddot{u}_g$ corresponding to an earthquake record, the maximum response u_{max} was calculated. Plots similar to those of Fig. (2-7) and (2-8) could then be extracted.

The computer was used to determine all the desired spectral curves and to generate plots similar to that of Fig. 2-8. Plots of pseudo velocity ratio versus frequency and displacement ratio versus frequency were also generated. Having these three sets of plots thus furnished all the necessary information needed to proceed with the analysis and comparisons. This is the topic of the next chapter.

Additional Considerations

The computer program developed for this study was assigned to take a standard range of frequencies .03 to 20.0 cycles per second with 57 points uniformly spaced on a logarithmic scale. The value of damping considered was .05. Although other values of damping could be considered, the choice of only one value seemed to provide sufficient information as far as the intention of this work is concerned--that is, evaluating Newmark's procedure for obtaining inelastic response spectra and the second procedure used by replacing the nonlinear system with a linear one with modified effective stiffness and damping factors.

Evaluation of Newmark's Rule

As described in Chapter 1, for an elastic system the pseudo acceleration S_a, defined as $\omega^2 S_d$, will be a very close approximation to the maximum absolute acceleration for usual values of viscous damping. In a similar way the pseudo velocity will represent a good estimate of the maximum relative velocity except in the low frequency range. (Notice that the velocity is not an important design parameter). Thus the possibility of reading displacement, velocity and acceleration from a unique diagram.

For an elasto-plastic system, on the other hand, if u_y is the yield displacement, f_y the yield force, M the mass and k_o the initial or elastic stiffness, for values of the ductility ratio μ larger than 1 the maximum acceleration is limited to $\frac{f_y}{M}$.

With $$\omega_o^2 = \frac{k_o}{M}$$

$$\ddot{y}_{max} = \frac{f_y}{M} = \frac{k_o u_y}{M} = \omega_o^2 u_y$$

Whereas $$u_{max} = \mu u_y.$$

Defining thus the maximum acceleration, or pseudo-acceleration as $\omega_o^2 u_y$ in order to read the maximum relative displacement from the same diagram, it is necessary to multiply the displacement scale by the appropriate factor μ. This is consistent with Newmark's procedure.

In these conditions it might be more appropriate to plot directly

the pseudo-acceleration versus frequency, rather than the pseudo-velocity (defined now as ωu_y). Such a plot is shown in Figure 3.1 for the E-W component of the 1940 El Centro earthquake. These plots could now be used in two different ways:

a) for a given one-degree-of-freedom system with known characteristics k_o, M, f_y one could find for the particular earthquake considered the ductility requirements by interpolating the value of μ.

b) for a system with known k_o, M and a desired design ductility μ one could read the pseudo-acceleration and obtain the necessary value of the yield force f_y to guarantee this ductility.

Notice that in Fig. 3.1 the acceleration $\ddot{y}_{max}$ is divided by the maximum ground acceleration of the earthquake $\ddot{u}_g$, to give a dimensionless amplification ratio as was done in Garcia's work.

While these plots might be simpler to use for design purposes, plots of pseudo-velocity (scaled also by dividing by the maximum ground velocity) were also obtained. These plots are the ones usually shown for elastic spectra and permit thus an easier comparison. In addition it is easier to visualize in these plots the seven spectral ranges defined by Newmark. Of course both kinds of plots are directly related, the second one being simply the first divided by ω_o at each frequency. Figure 3.2 shows the normalized pseudo velocity spectra corresponding to Fig. 3.1. Because of the normalization the factor to pass from Fig. 3.1 to Fig. 3.2 would be $\ddot{u}_{gmax}/\omega_o\dot{u}_{gmax}$, where $\dot{u}_{gmax}$ is the maximum ground velocity of the earthquake. This normalization is of no consequence, however, to the remainder of the work.

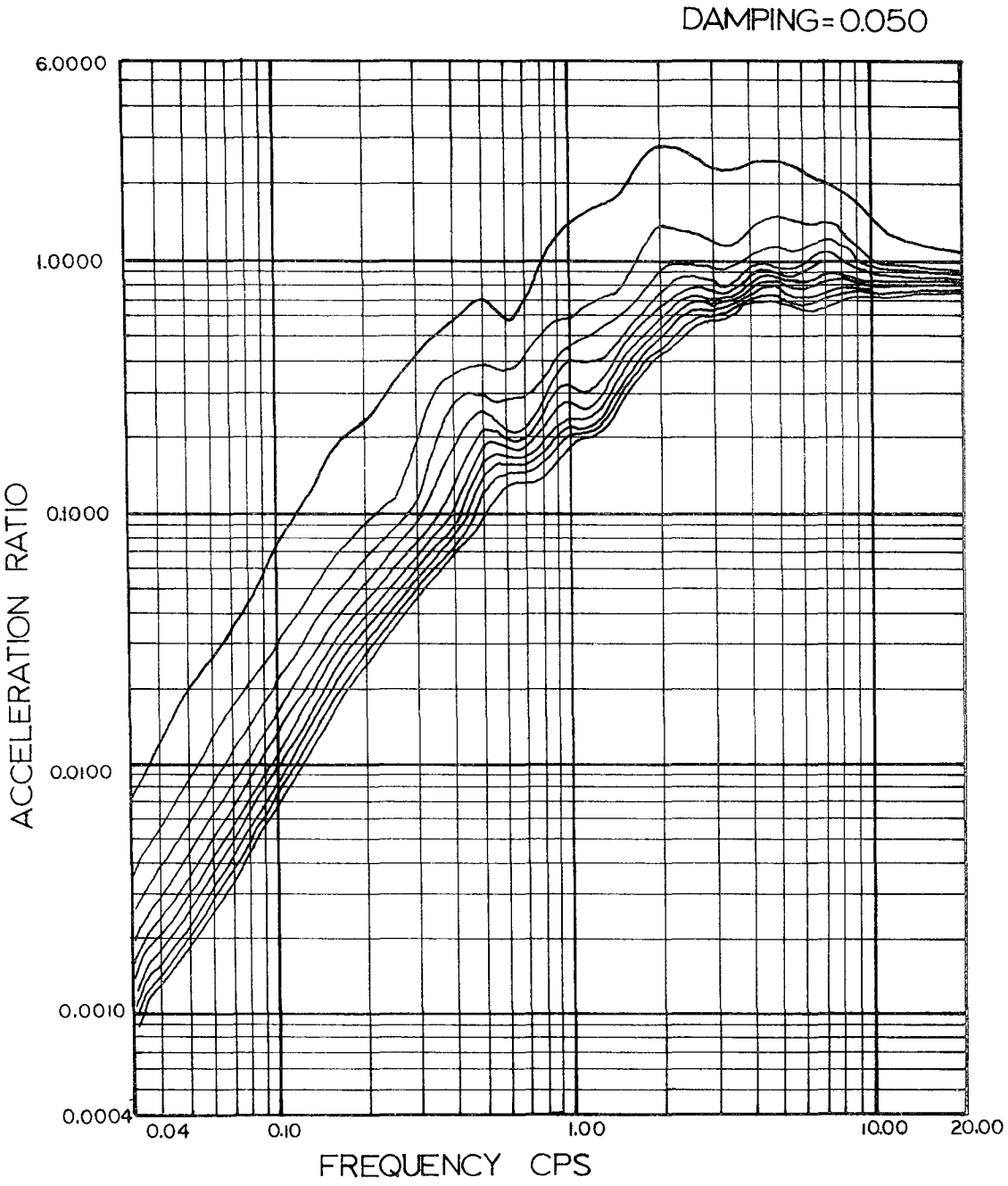
DAMPING=0.050
6.0000
1.0000
0.1000
0.0100
0.0010
0.0004
ACCELERATION RATIO
0.04
0.10
1.00
10.00
20.00
FREQUENCY CPS

FIGURE 3.1

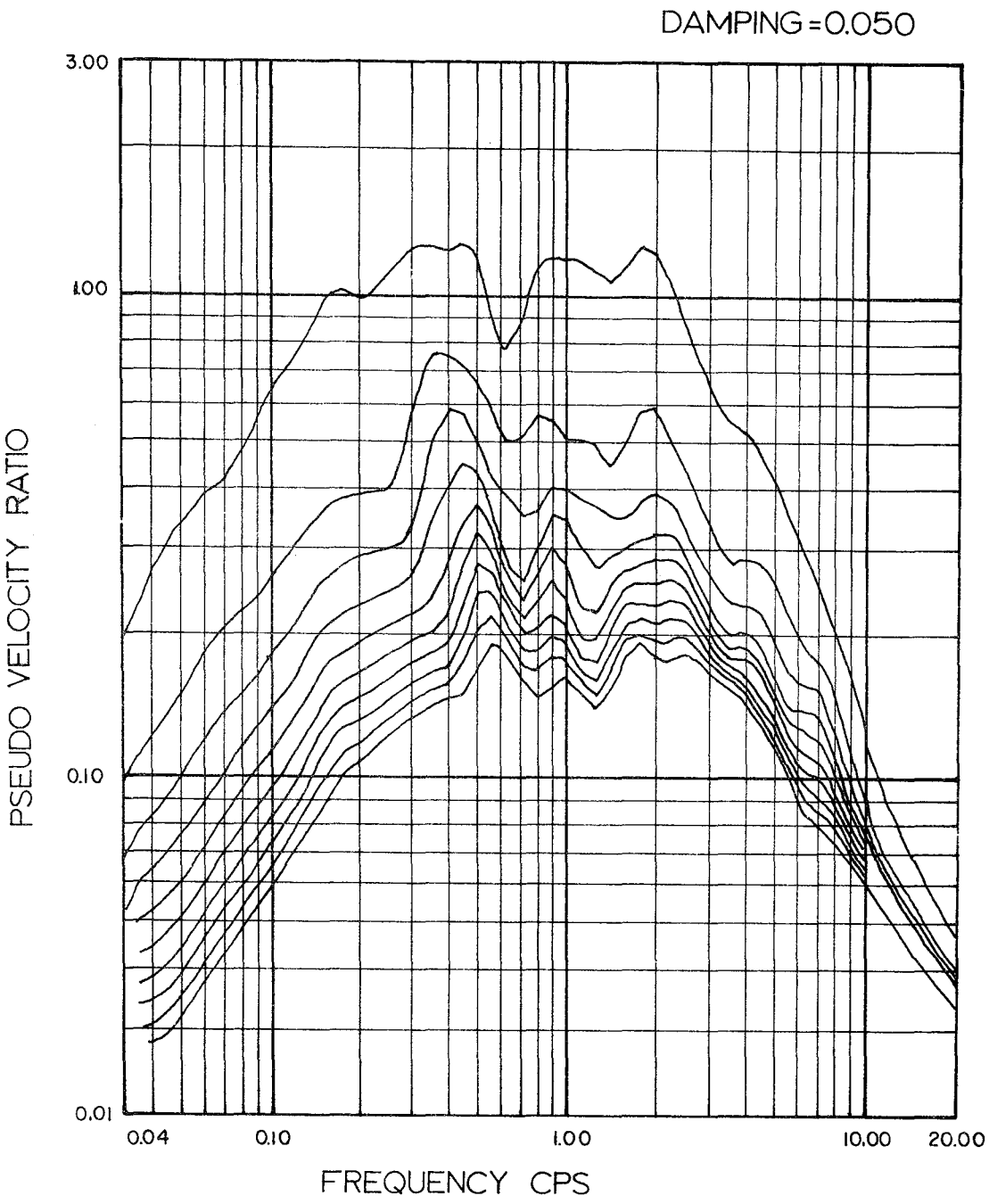
DAMPING = 0.050
3.00
1.00
0.10
0.01
PSEUDO VELOCITY RATIO
0.04
0.10
1.00
10.00
20.00
FREQUENCY CPS

FIGURE 3.2

Similar plots were obtained for each of the nine accelerograms considered. Each diagram, corresponding to a given ductility factor μ, was then treated individually and an envelope was drawn with the seven ranges of Newmark's spectrum. For each range the ratio was then obtained between the elastic spectral value ($\mu = 1$) and the particular curve considered. Fig. 3.3 illustrates the envelope for $\mu = 1$ and Fig. 3.4 the corresponding one for $\mu = 5$. The resulting ratios are shown in Tables 3.1 to 3.7 for the seven ranges. It should be pointed out that for some of the eqrthquakes the extreme ranges could not be located within the frequency range studied (0.03 to 20 cps).

For each one of the ranges the ratios were then plotted as a function of ductility factor μ for all accelerograms. Figures 3.5 to 3.11 show the resulting upper and lower bounds, the average curves, Newmark's recommended curve, and the curve that would best fit the average. It is important to notice that a lower value of the ratio (as corresponding to the lower bound) represents a more strict requirement (larger ductility for a given f_y or larger value of f_y for a desired ductility).

The best fit curves shown in these figures were obtained by a trial and error procedure. An equation of the form

$$R = [\alpha(\mu-1) + 1]^{\gamma} \qquad (3\text{-}1)$$

was assumed to apply. This functional form would of course include Newmark's factors, μ for the first four range, $(2\mu-1)^{1/2}$ for the fifth range, and one for the last range.

The average values for the nine accelerograms were then plotted in

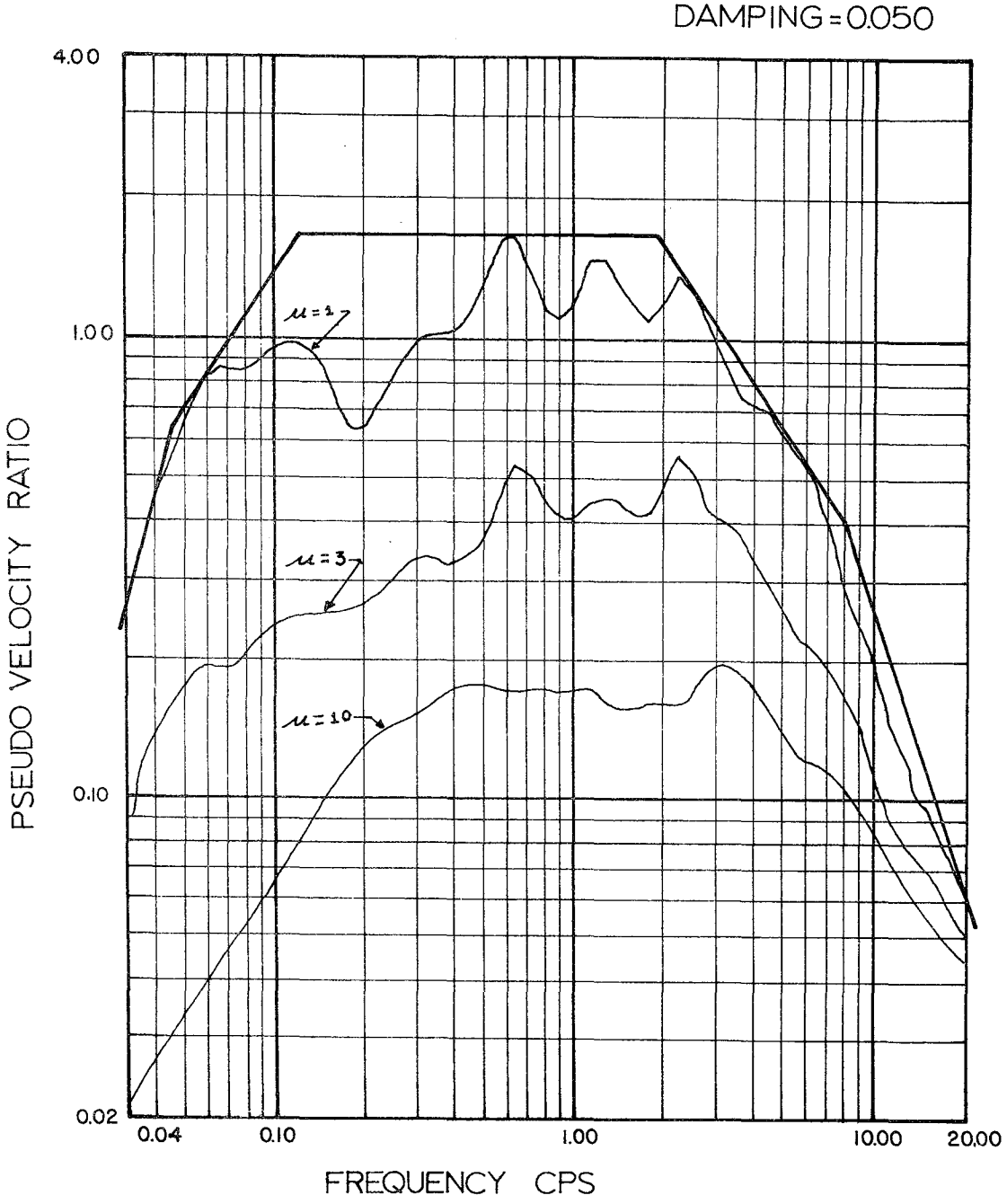
DAMPING = 0.050
4.00
1.00
0.10
0.02
PSEUDO VELOCITY RATIO
μ = 1
μ = 3
μ = 10
0.04
0.10
1.00
10.00
20.00
FREQUENCY CPS

FIGURE 3.3

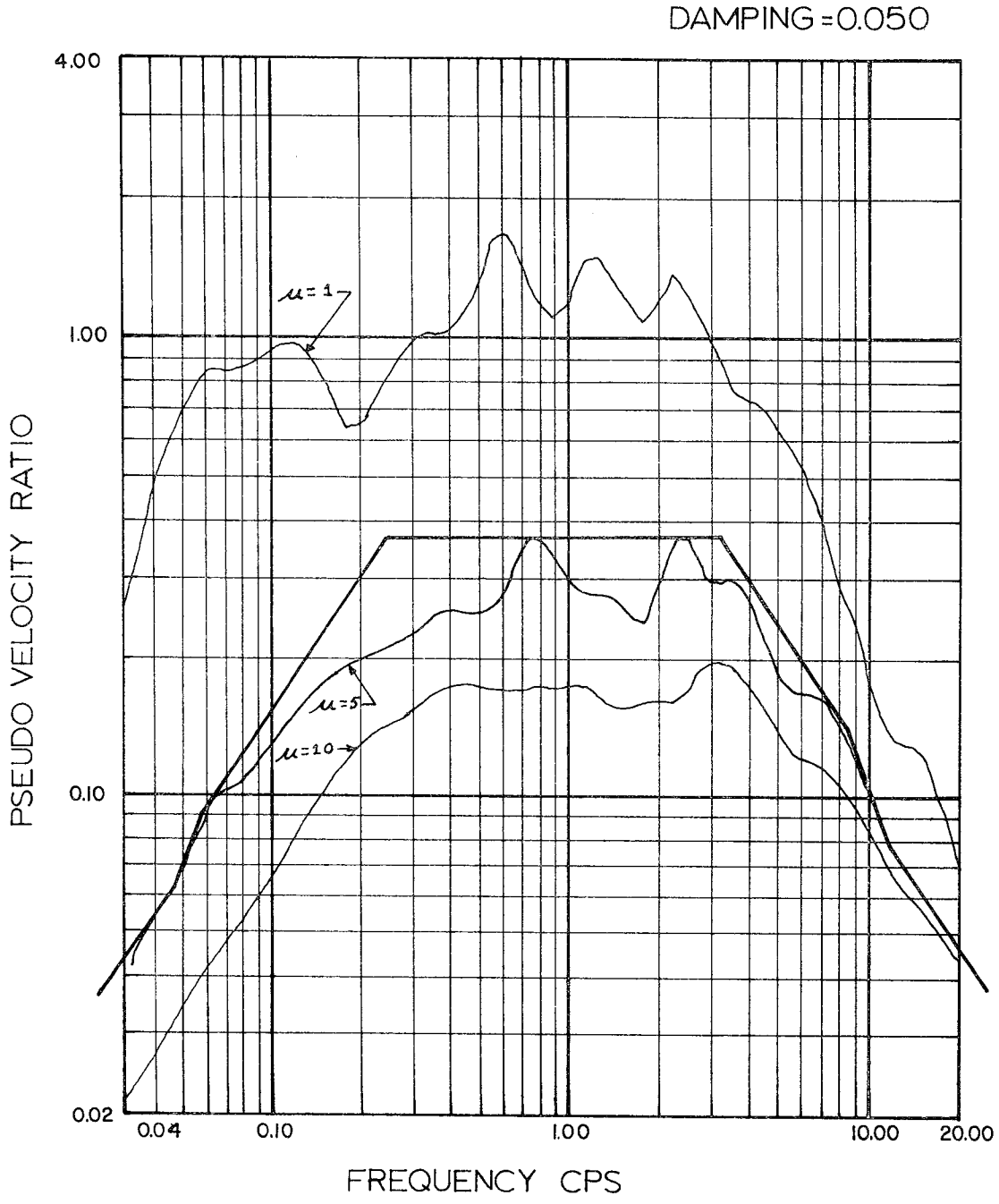
DAMPING = 0.050
4.00
1.00
0.10
0.02
PSEUDO VELOCITY RATIO
μ = 1
μ = 5
μ = 10
0.04
0.10
1.00
10.00
20.00
FREQUENCY CPS

FIGURE 3.4

log-log paper versus $\alpha(\mu-1) + 1$ for different values of α and a straight line was fitted through them. In this way, an optimum value of α was determined visually for each range, then the corresponding value of γ measured as the slope of the straight line. For range 1, $R = \mu$ was still found to be the best fit. For range 2 a straight line with $\alpha = 1.16$ was also seen to be satisfactory directly from Fig. 3.6. For the other five ranges the plots are shown in Figs. 3.12 to 3.16. It should be noticed that the decision on the best values is somewhat arbitrary and in fact different sets of values of α and γ can provide very similar results. The final values chosen are shown in Table 3.8.

Discussion of Results

Figures 3.5 to 3.11 permit now an evaluation of Newmark's suggested procedure. Range 1 corresponding to low frequencies has very little scatter and shows that the assumption of $R = \mu$ (same maximum displacement for the elastic and inelastic systems) is quite satisfactory. From an intuitive point of view this has to be so, since the system being very flexible remains essentially at rest.

This rule is still satisfactory for range 2, although the scatter increases considerably and a value of $\alpha = 1.16$ would provide a better fit. Newmark's procedure would provide, however, a reasonable answer, slightly more conservative than the average of the nine records.

For range 3 it can be seen that Newmark's rule coincides almost with the lower bound, being therefore more conservative than for the two previous cases. The average is still well fitted by a straight line, but the

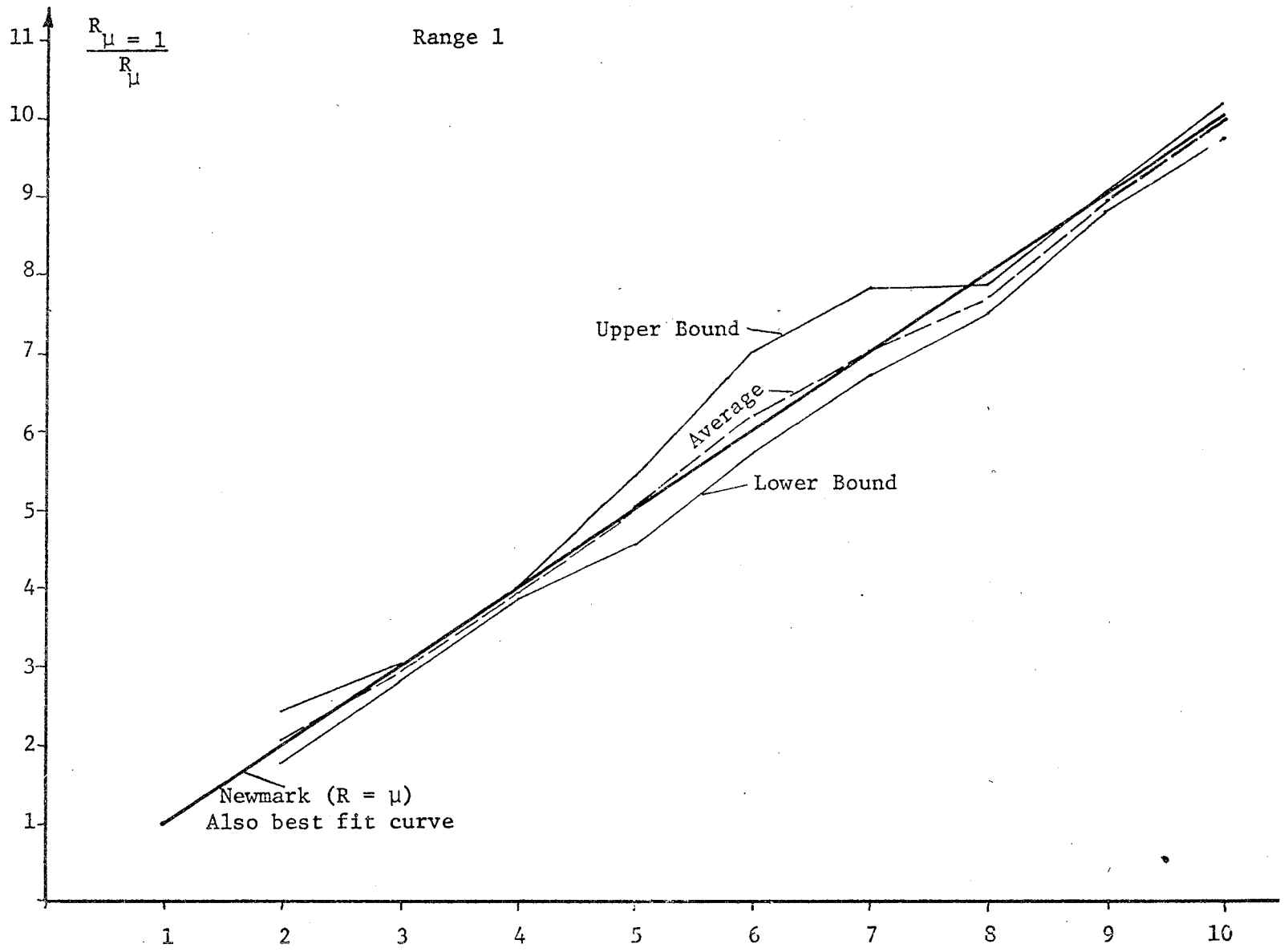
$\frac{R_{\mu = 1}}{R_{\mu}}$
Range 1
11
10
9
8
7
6
5
4
3
2
1
Upper Bound
Average
Lower Bound
Newmark (R = μ)
Also best fit curve
1
2
3
4
5
6
7
8
9
10

Figure 3-5

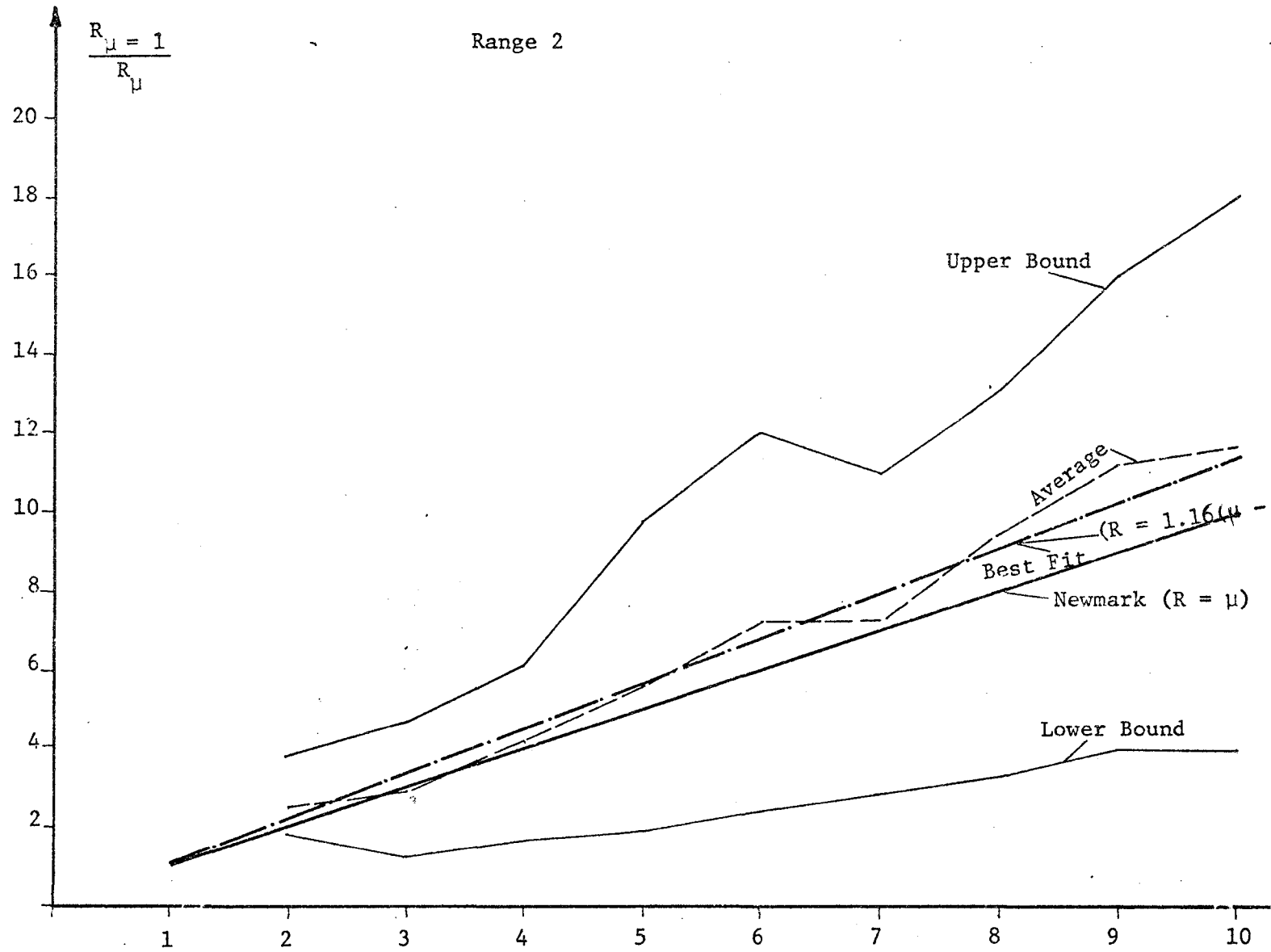
$\frac{R_\mu = 1}{R_\mu}$
Range 2
20
18
16
14
12
10
8
6
4
2
1
2
3
4
5
6
7
8
9
10
Upper Bound
Average
(R = 1.16(μ
Best Fit
Newmark (R = μ)
Lower Bound

Figure 3-6

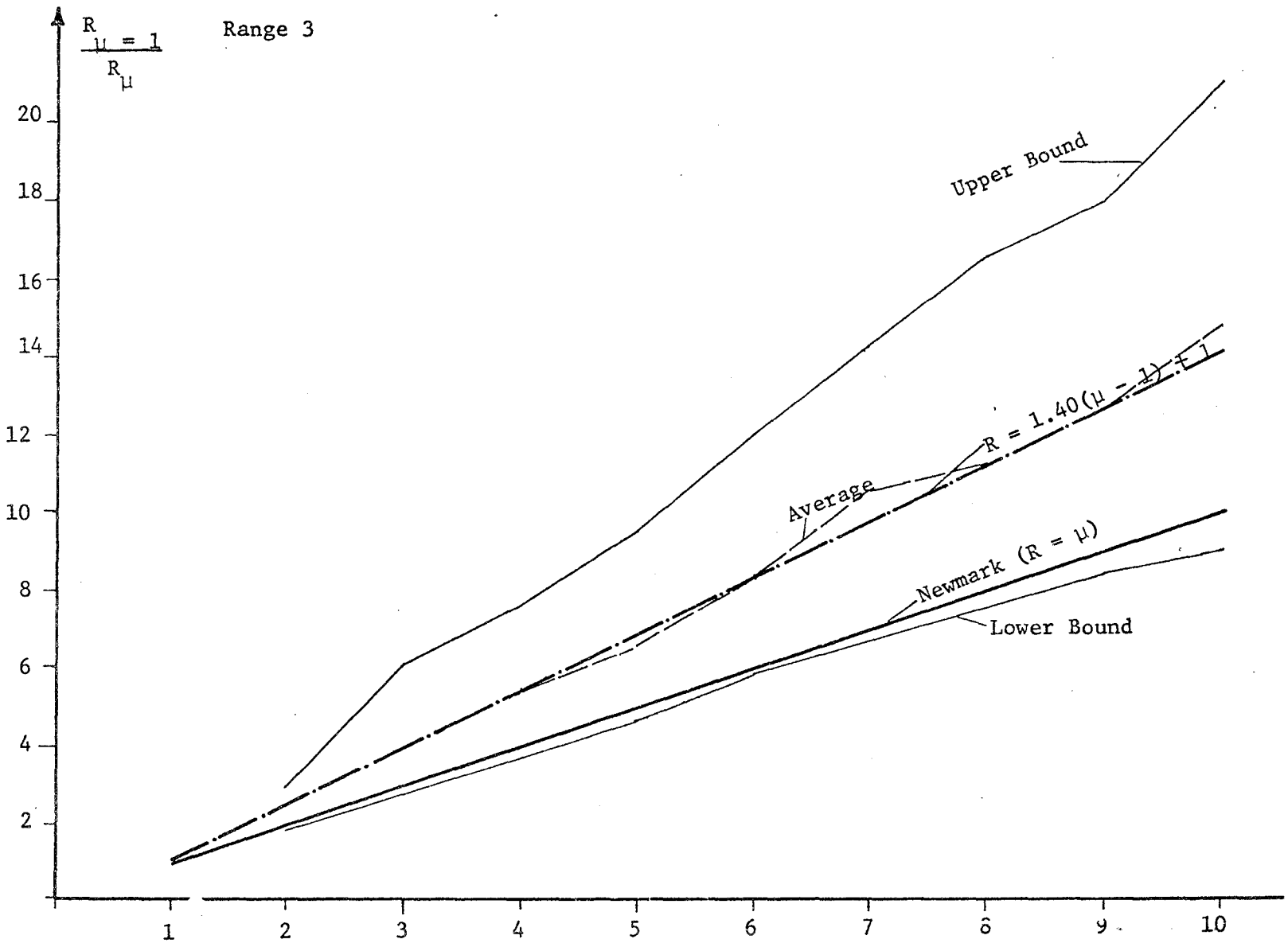
R
μ = 1
R
μ
Range 3
20
18
16
14
12
10
8
6
4
2
1
2
3
4
5
6
7
8
9
10
Upper Bound
R = 1.40(μ - 1) + 1
Average
Newmark (R = μ)
Lower Bound

Figure 3-7

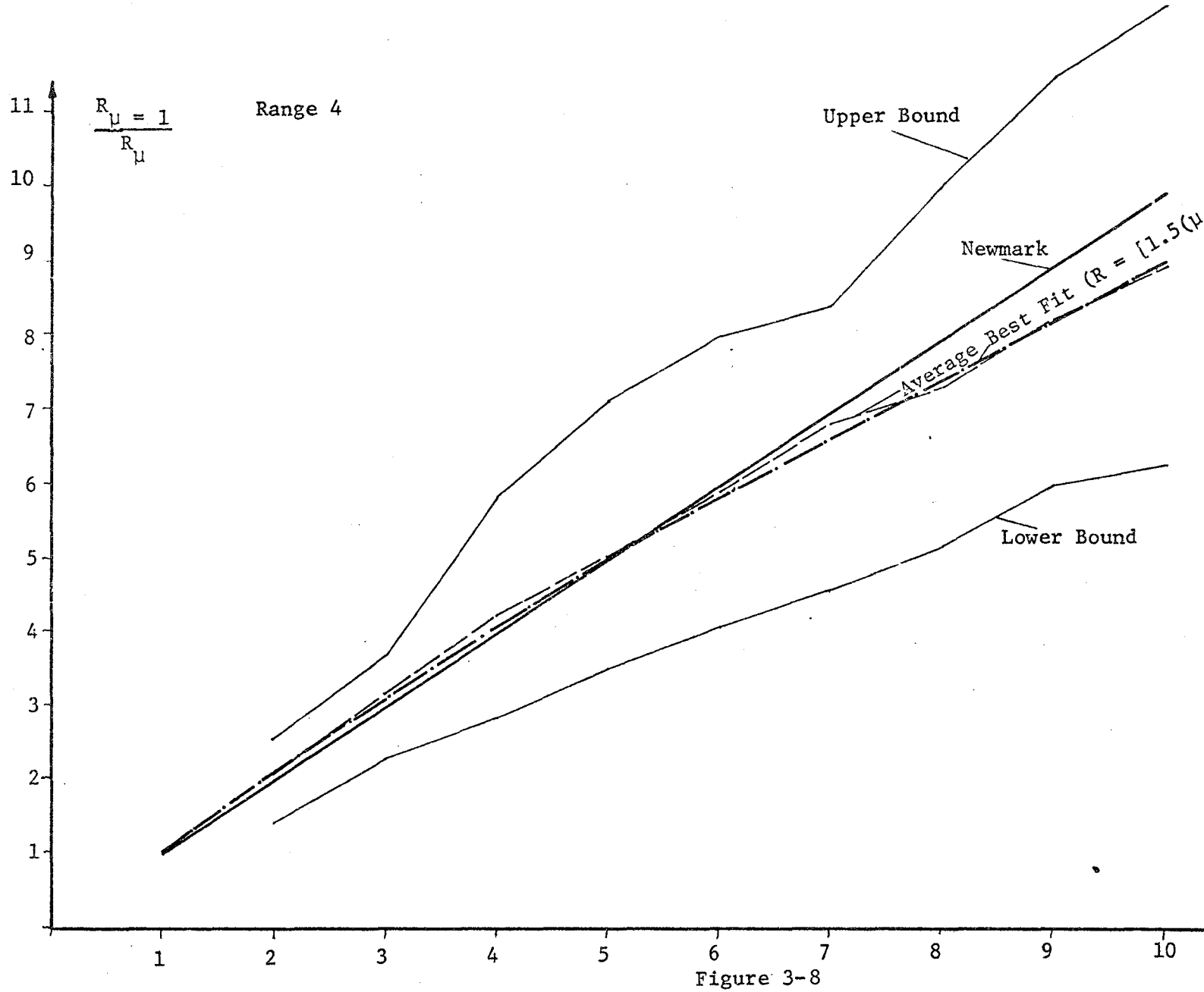
$\frac{R_\mu = 1}{R_\mu}$
Range 4
Upper Bound
Newmark
Average Best Fit (R = [1.5(μ
Lower Bound
11
10
9
8
7
6
5
4
3
2
1
1
2
3
4
5
6
7
8
9
10

Figure 3-8

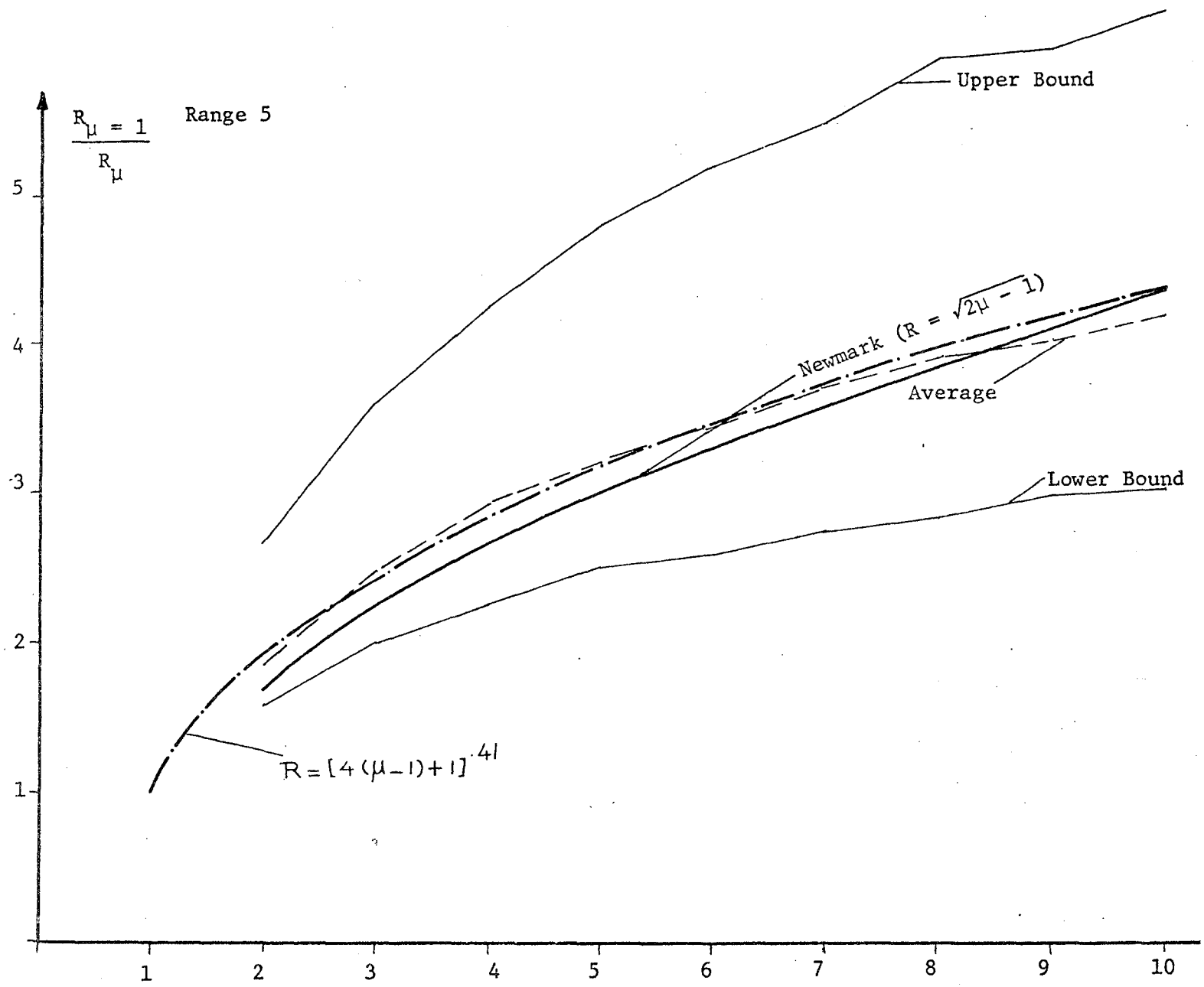
Range 5
$\frac{R_\mu = 1}{R_\mu}$
Upper Bound
Newmark ($R = \sqrt{2\mu - 1}$)
Average
Lower Bound
$R = [4(\mu - 1) + 1]^{.41}$
5
4
3
2
1
1
2
3
4
5
6
7
8
9
10

Figure 3-9

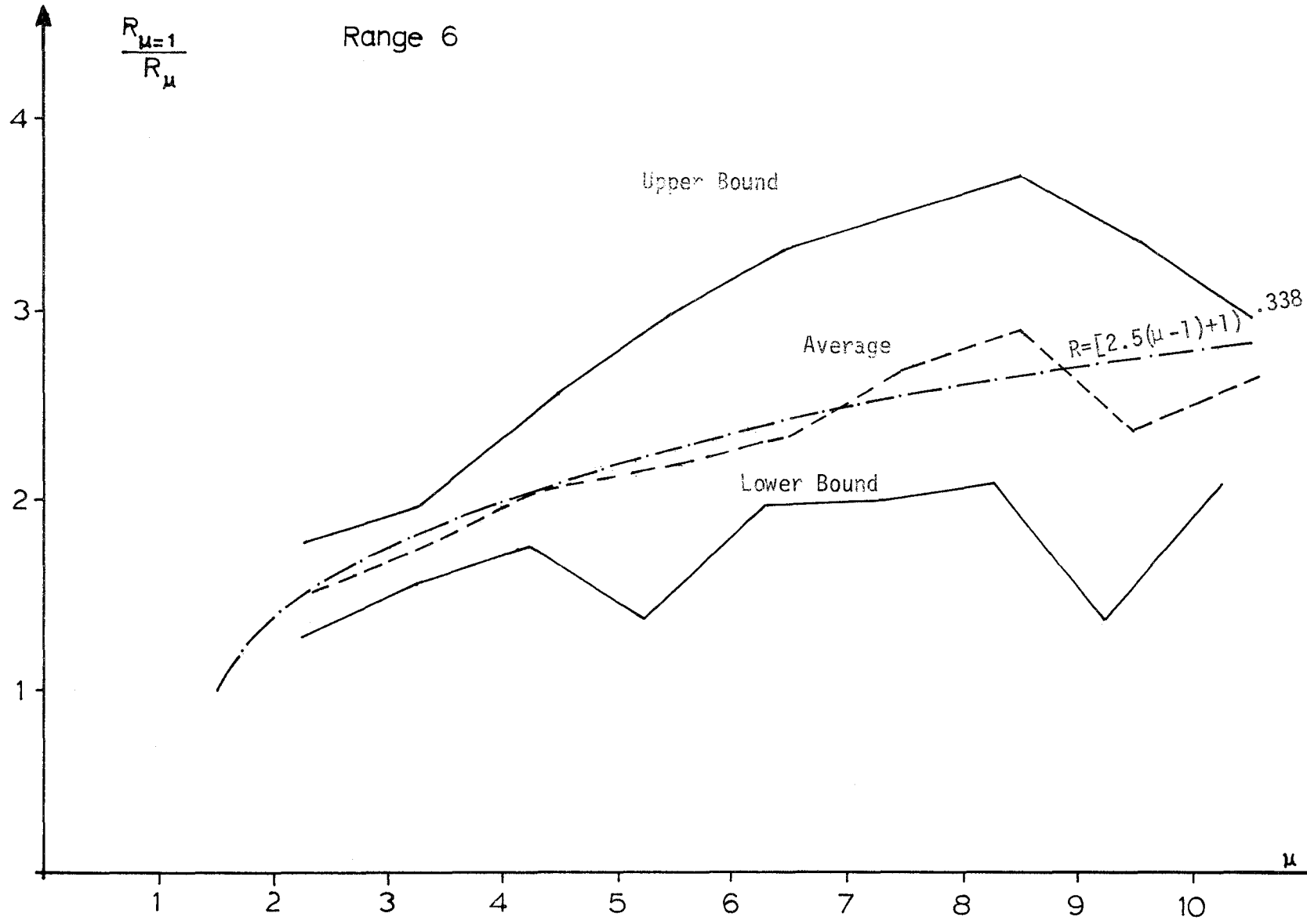
$\frac{R_{\mu=1}}{R_\mu}$
Range 6
Upper Bound
Average
Lower Bound
R=[2.5(μ-1)+1)
.338
μ
4
3
2
1
1
2
3
4
5
6
7
8
9
10

FIGURE 3-10

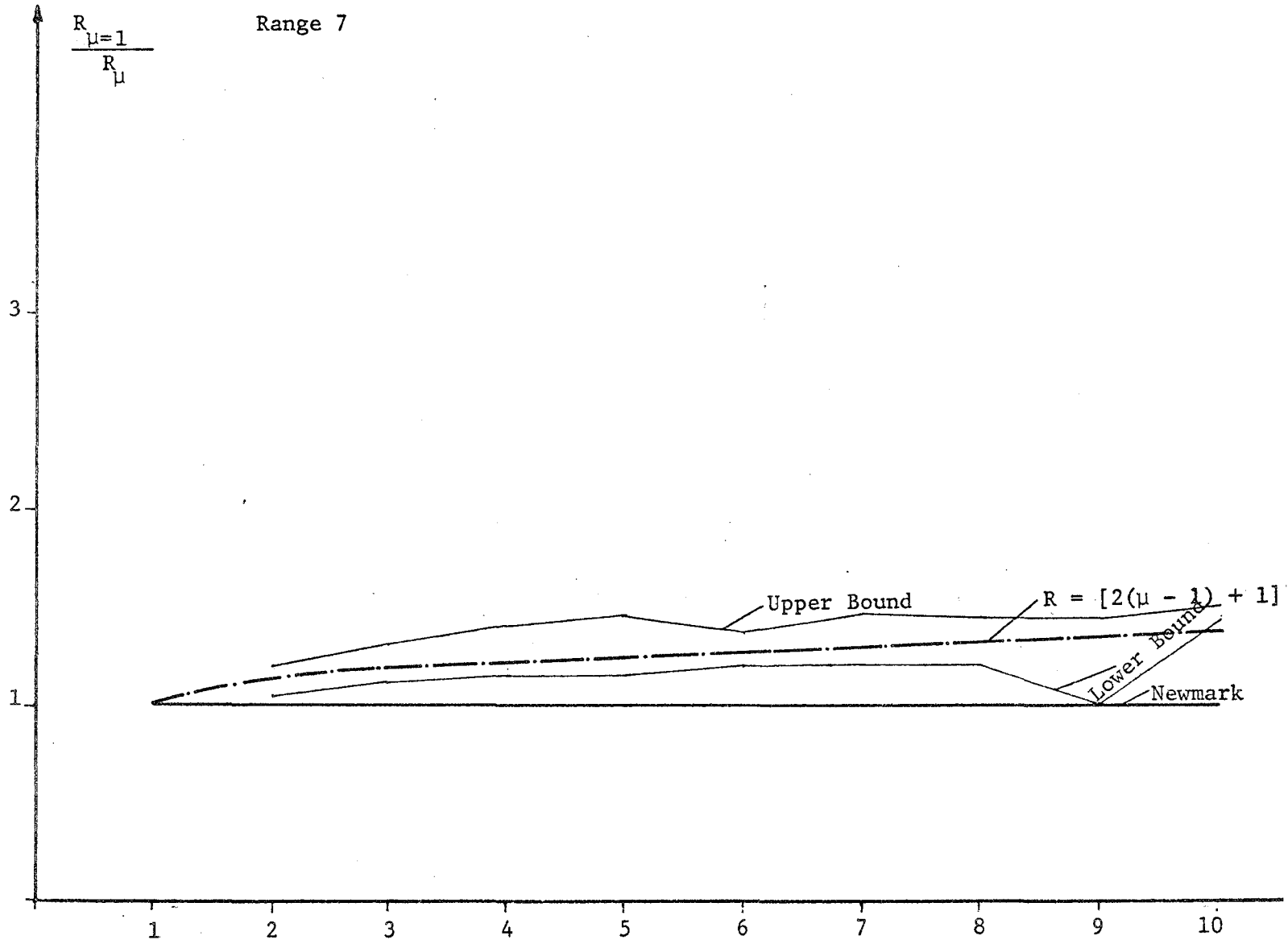
$\frac{R_{\mu=1}}{R_\mu}$
Range 7
3
2
1
Upper Bound
R = [2(μ - 1) + 1]
Lower Bound
Newmark
1
2
3
4
5
6
7
8
9
10

Figure 3-11

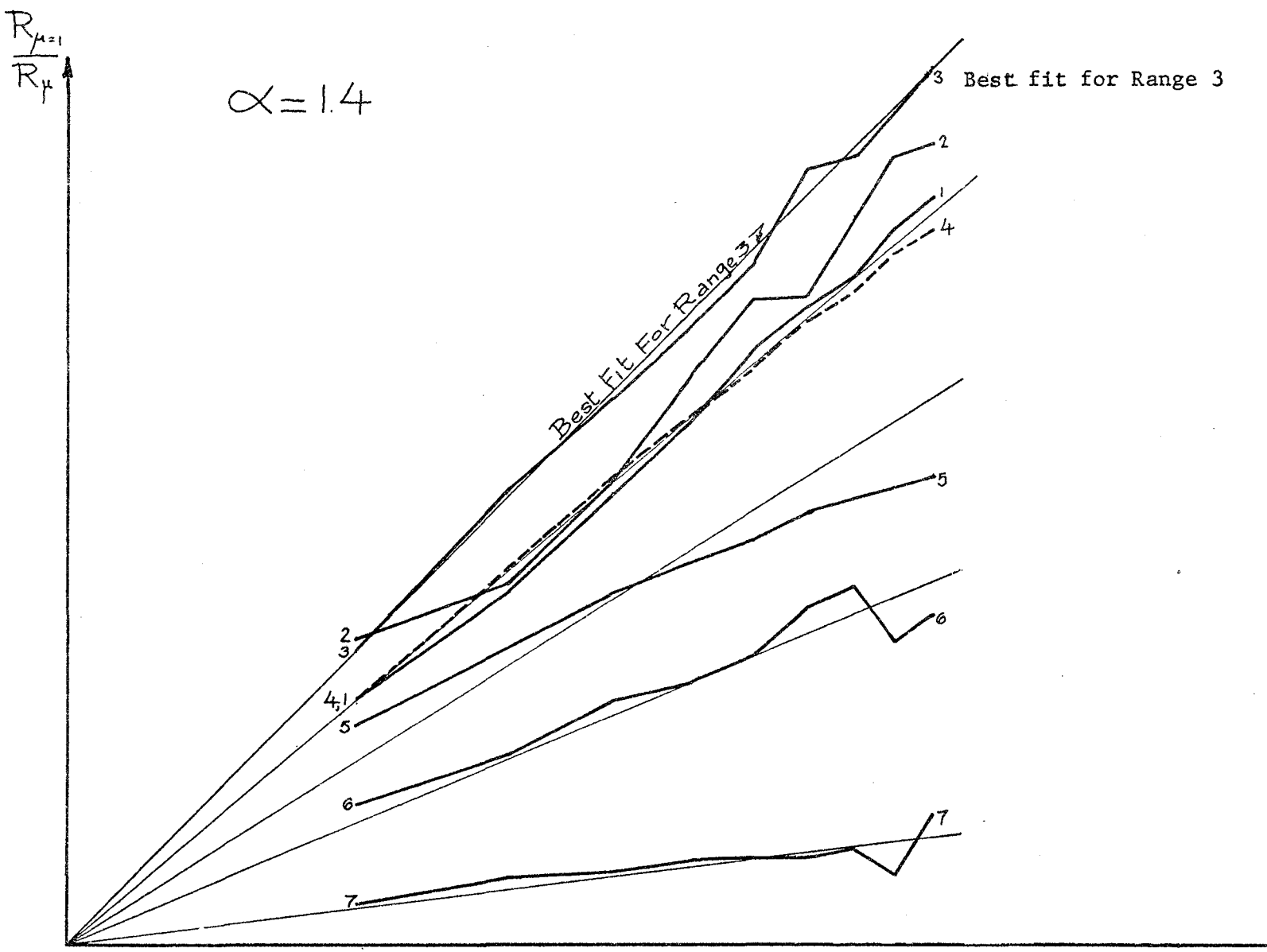
$\frac{R_{\mu=1}}{R_\mu}$
$\alpha = 1.4$
3 Best fit for Range 3
2
1
4
Best Fit For Range 3
5
2
3
4,1
5
6
6
7
7
1.4

Figure 3-12

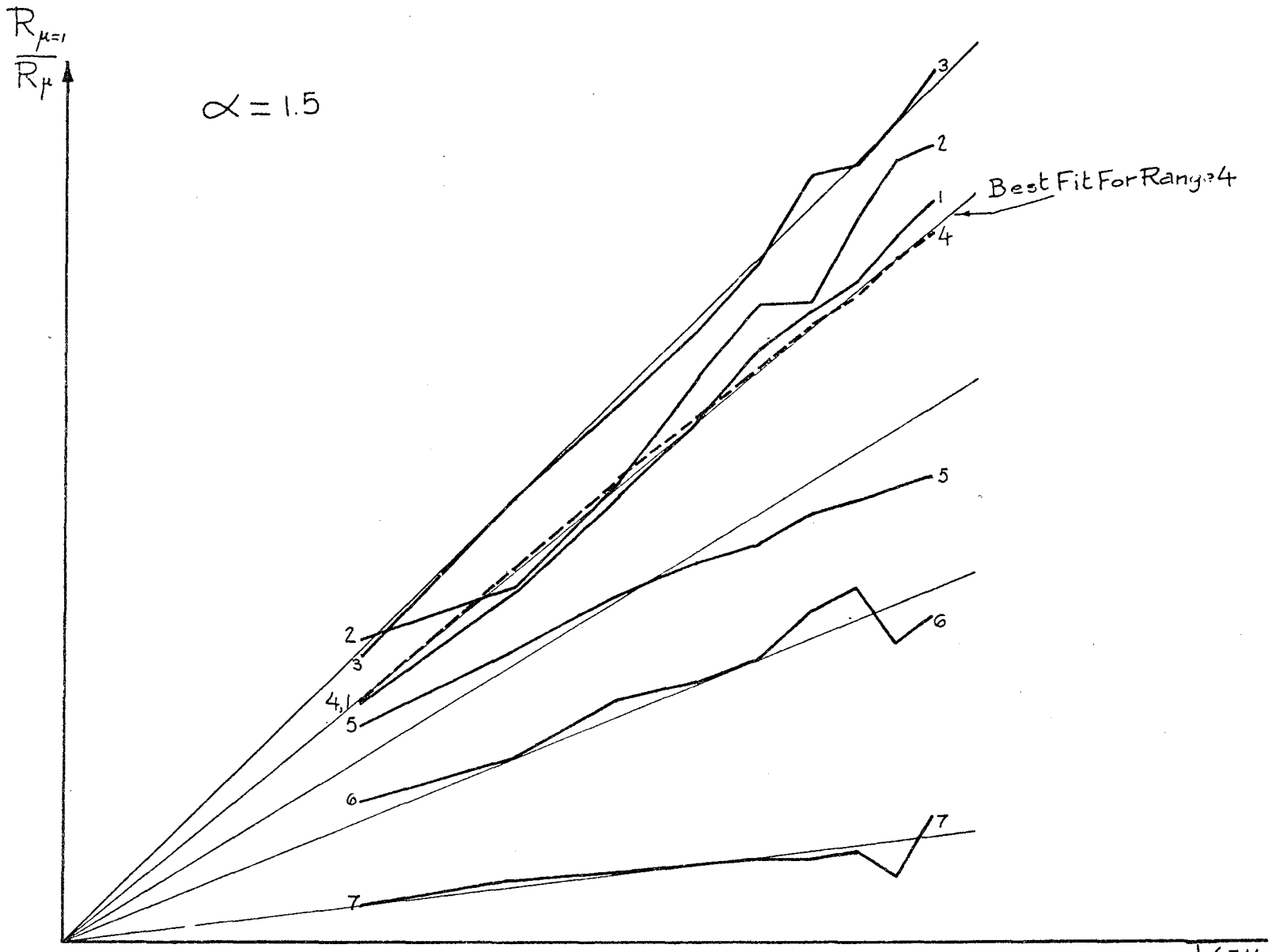
$\frac{R_{\mu=1}}{R_\mu}$
$\alpha = 1.5$
3
2
1
4
Best Fit For Range 4
5
6
7
2
3
4,1
5
6
7
$\frac{1}{2}(3\mu$

Figure 3-13

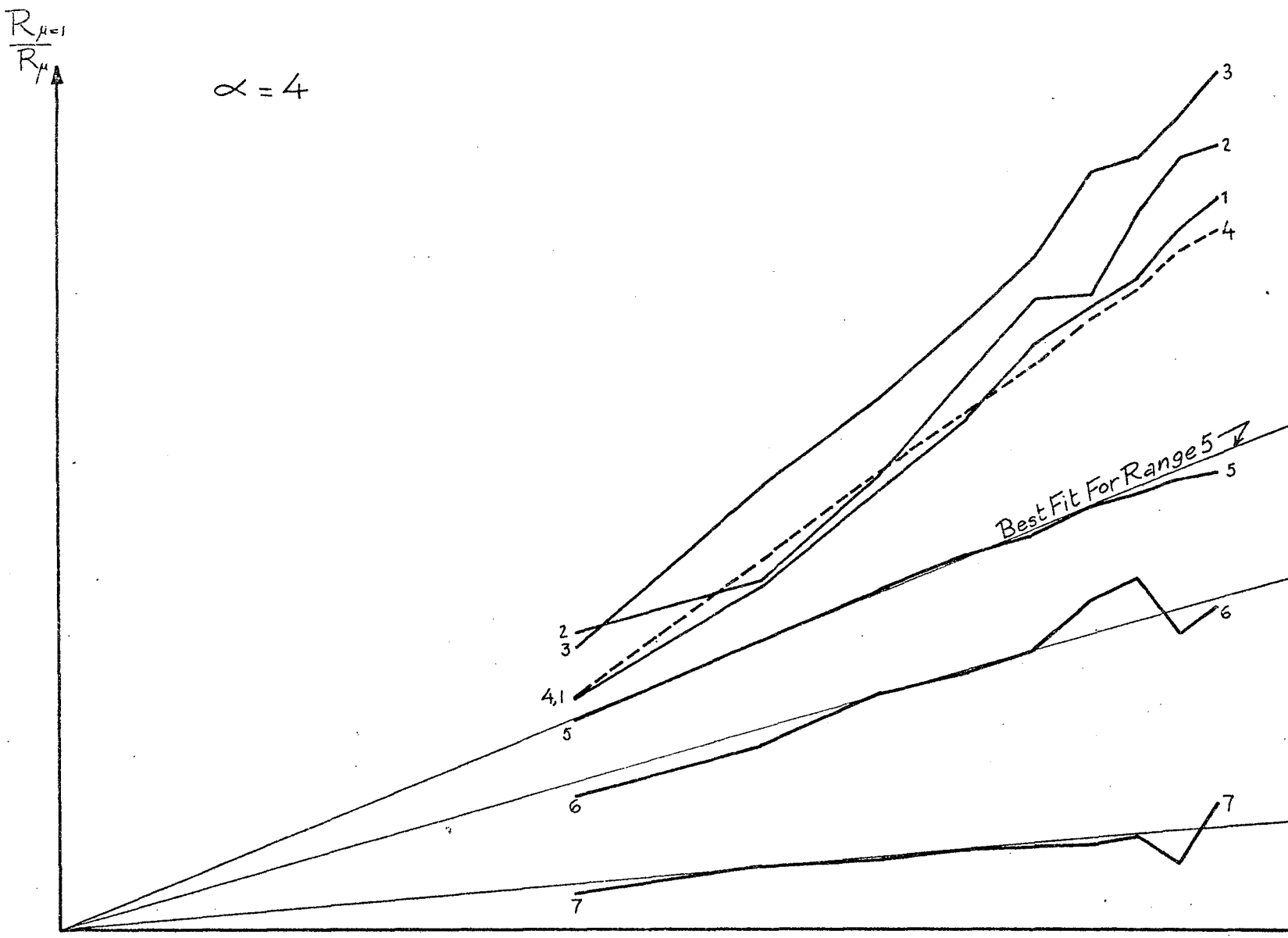

Figure 3-14

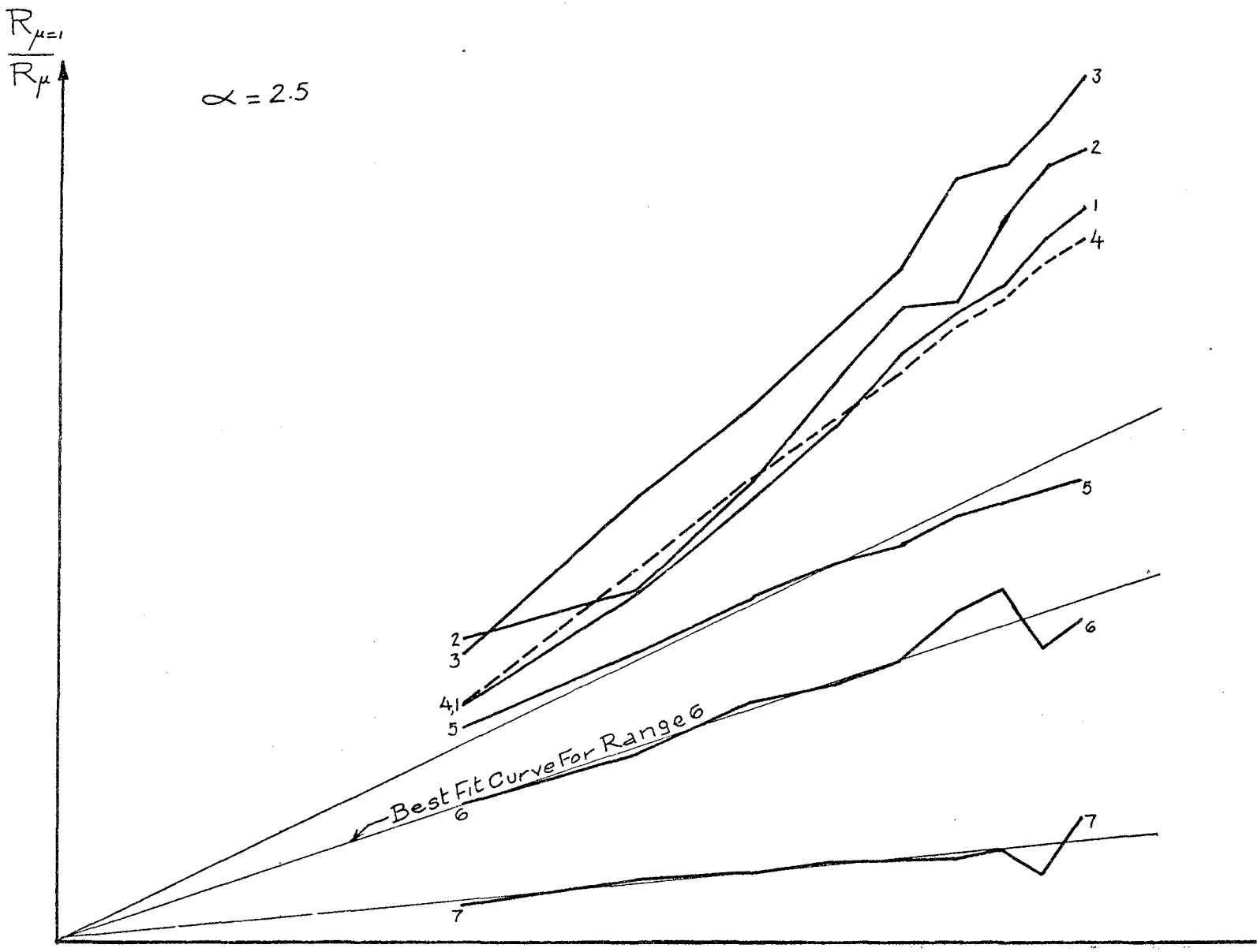
$\frac{R_{\mu=1}}{R_\mu}$
$\alpha = 2.5$
3
2
1
4
5
6
7
2
3
4,1
5
6
7
Best Fit Curve For Range 6
$\frac{1}{2}(5\mu$

Figure 3-15

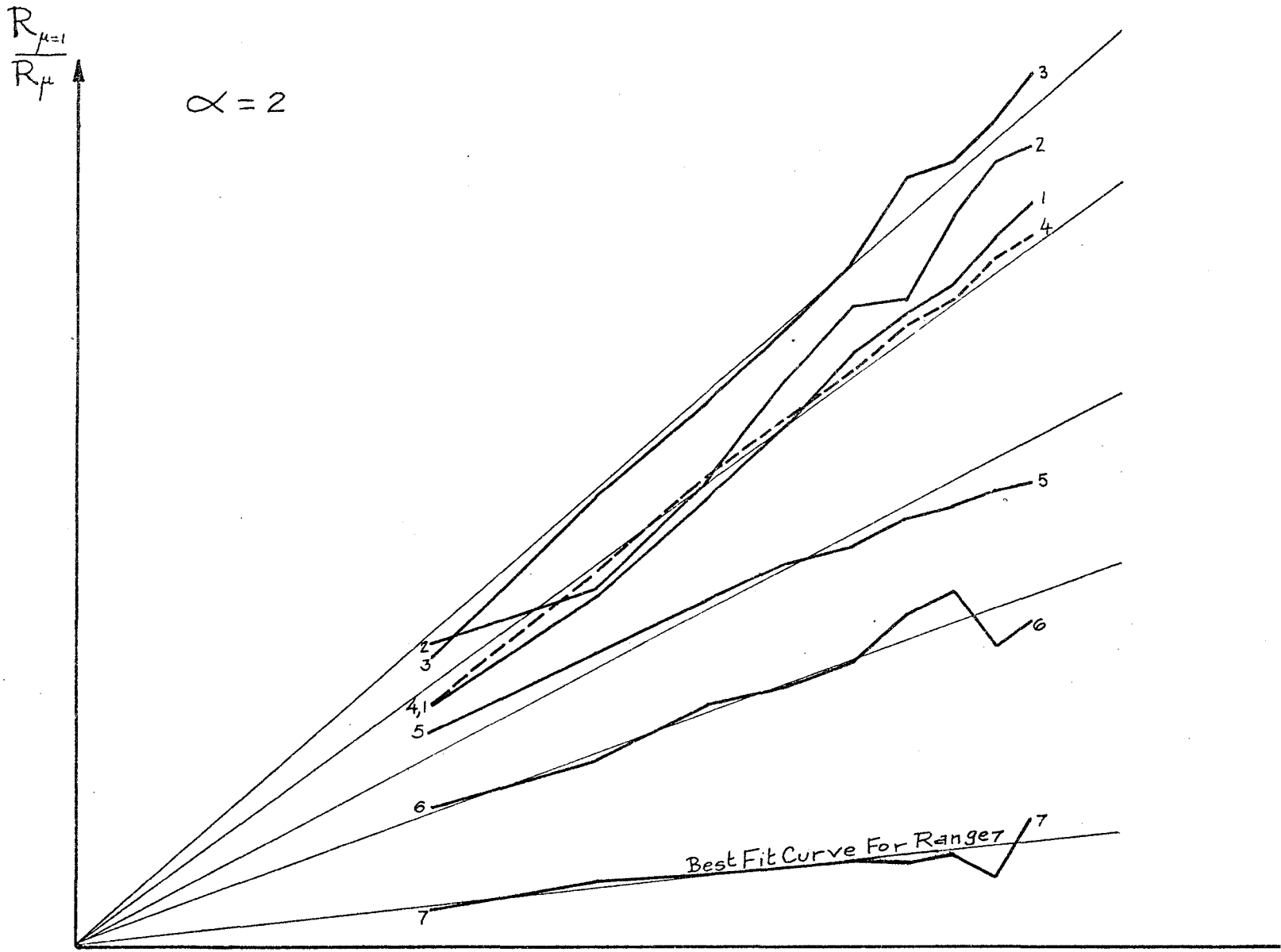

Figure 3-16

coefficient α becomes now 1.4. This indicated that in this range the displacements of the inelastic system will generally be smaller than those of an elastic system, something that would never happen in Newmark's procedure.

Newmark's rule fits again reasonably well the average in range 4, but becomes slightly less conservative, particularly for high values of μ.

In range 5 there is once more relatively good agreement between Newmark's factor $(\sqrt{2\mu-1})$ and the average curve, although expressions of the form $R = (4\mu-3)^{.41}$ or $(5\mu-4)^{.38}$ seem to provide a better fit for the data set used.

In range 6 Newmark's rule suggests a linear transition and there is not therefore a unique expression for the spectral ratio independent of frequency. In range 7 Newmark's rule becomes again conservative. It should be noticed, however, that R changes much more slowly with increasing ductility, suggesting, as pointed out by Newmark, that ductility requirements increase very rapidly with earthquake intensity. While there is still a functional relationship between R and μ (as it should physically), the curve is extremely flat and not very different from Newmark's horizontal line.

In order to visualize better the relationship between these ratios and the displacements of the system, plots were also obtained of the ratio of the maximum inelastic displacement for different values of μ to the maximum displacement of an elastic system as a function of frequency. These plots shown in Figs. 3.17 to 3.25 show clearly that for low frequencies, this ratio is essentially 1, becomes smaller than 1 particularly

in the 3rd range, then increases somewhat, and in the final two ranges it increases monotonically and very fast. These figures show actually the upper and lower bounds of the results obtained for ductility ratios μ from 1 to 10. In the high frequency range the upper bound corresponds to $\mu = 10$ and the lower bound to $\mu = 1$. This is not true, however, over the complete frequency range.

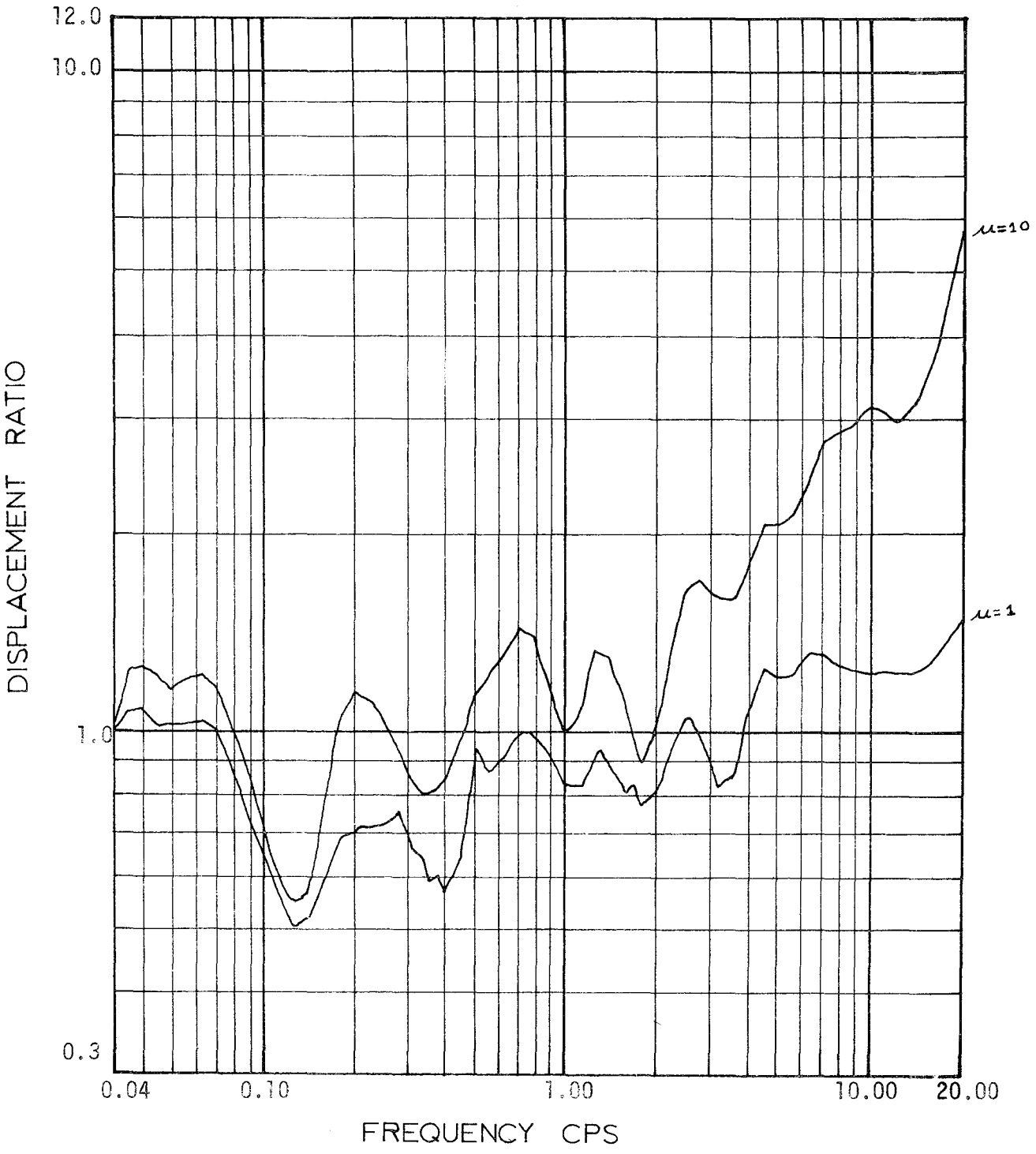
12.0
10.0
1.0
0.3
DISPLACEMENT RATIO
μ=10
μ=1
0.04
0.10
1.00
10.00
20.00
FREQUENCY CPS

FIGURE 3.17

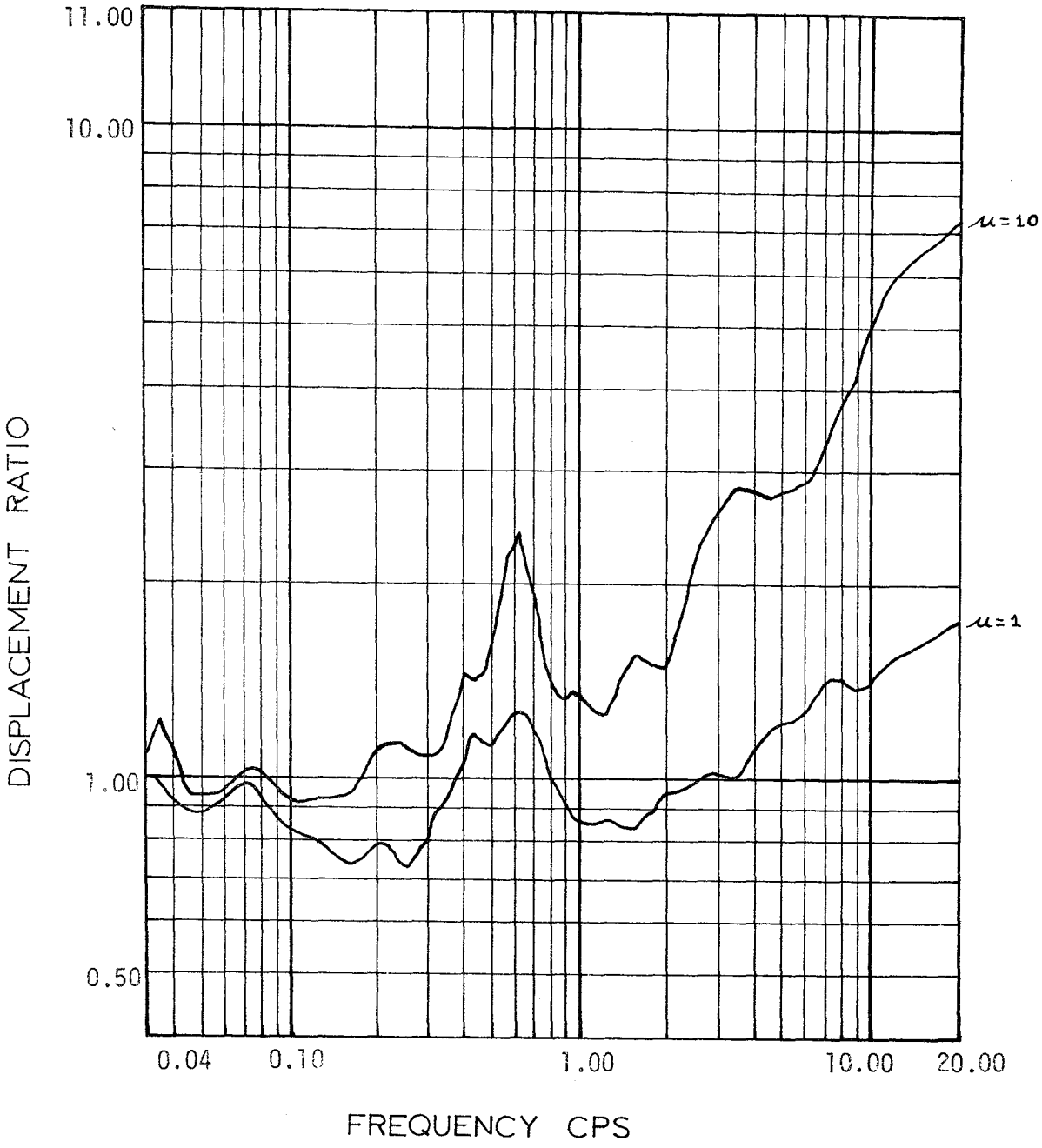
11.00
10.00
1.00
0.50
DISPLACEMENT RATIO
μ=10
μ=1
0.04
0.10
1.00
10.00
20.00
FREQUENCY CPS

FIGURE 3.18

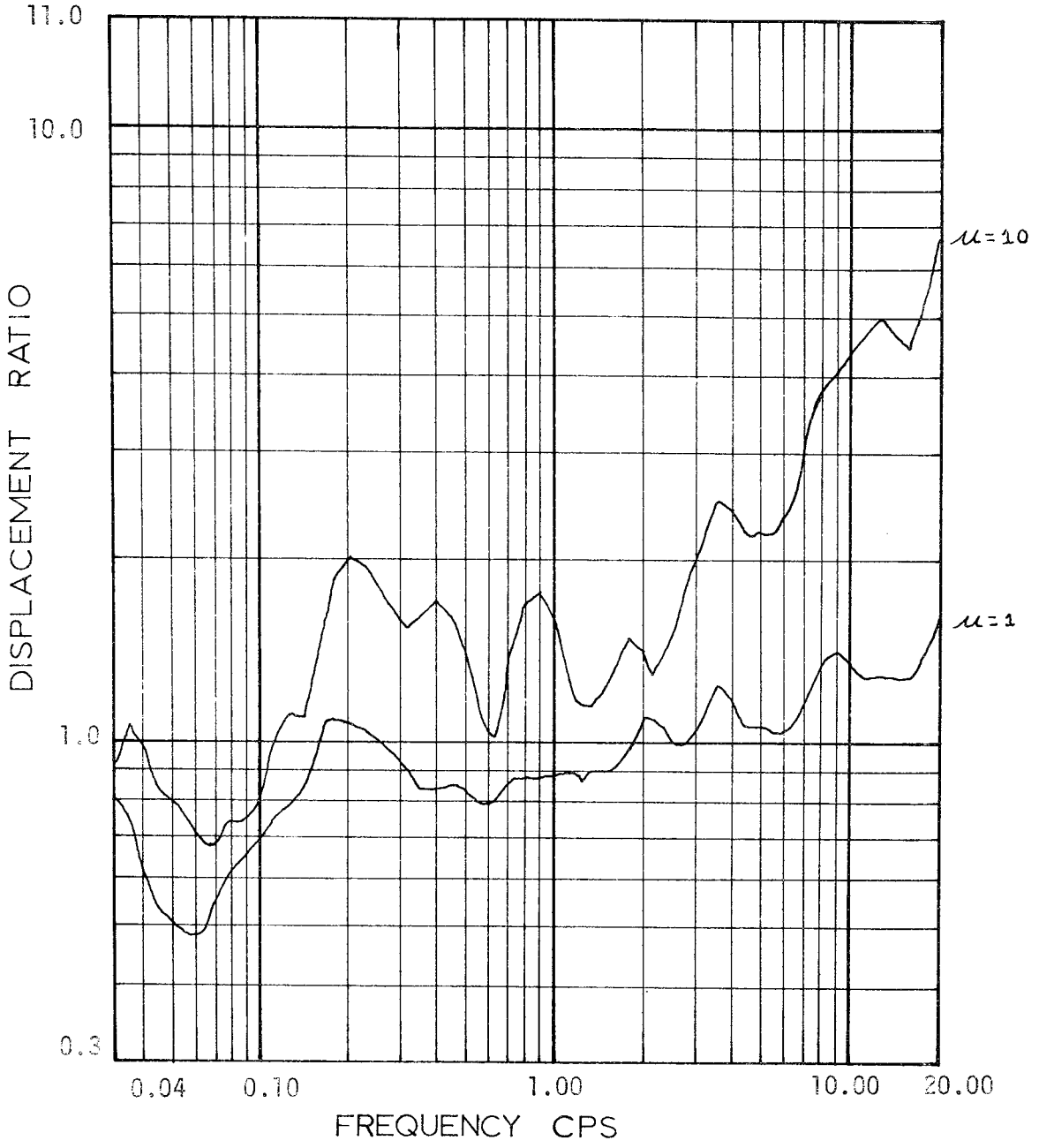
11.0
10.0
1.0
0.3
DISPLACEMENT RATIO
μ=10
μ=1
0.04
0.10
1.00
10.00
20.00
FREQUENCY CPS

FIGURE 3.19

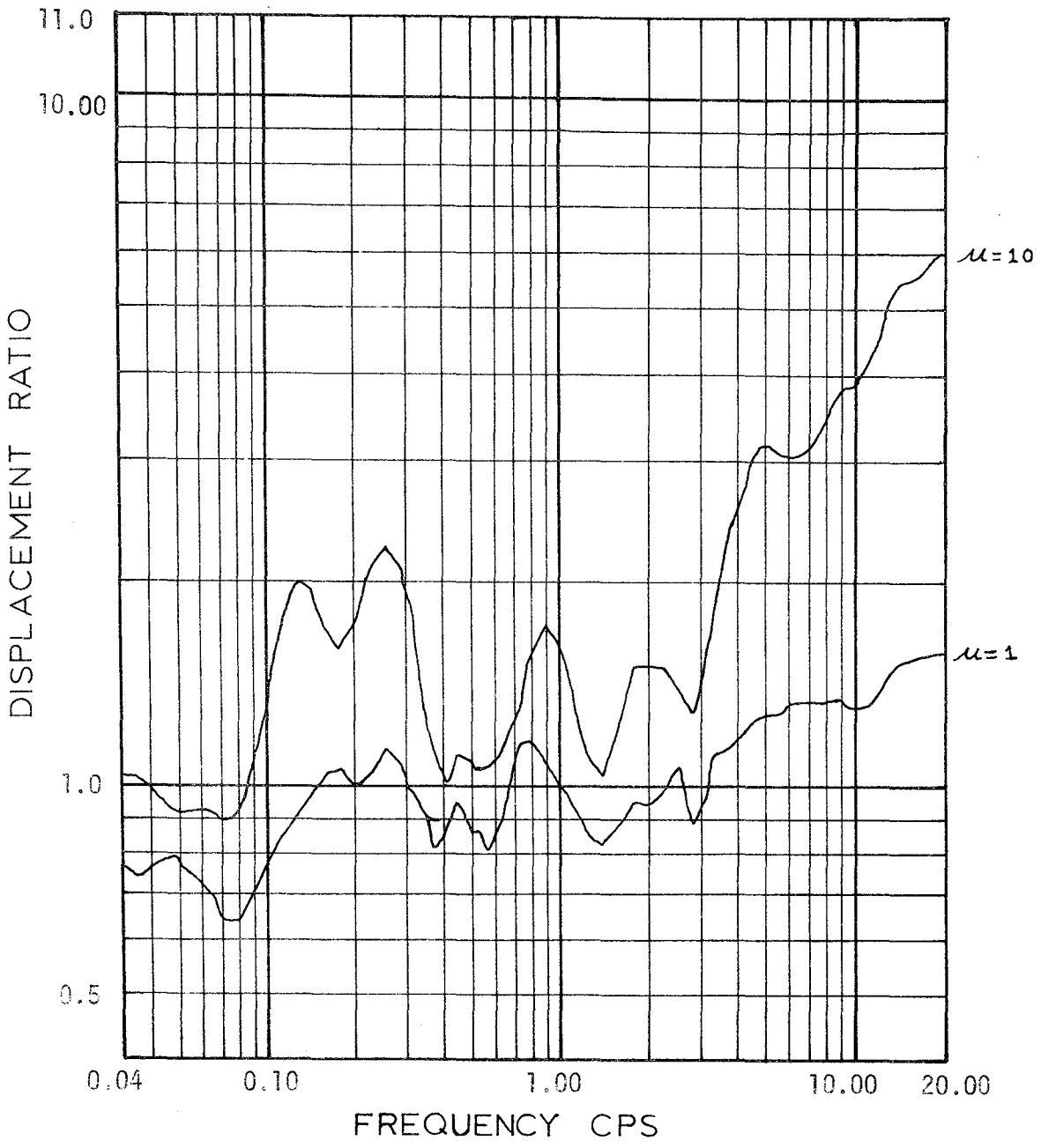
11.0
10.00
1.0
0.5
DISPLACEMENT RATIO
μ=10
μ=1
0.04
0.10
1.00
10.00
20.00
FREQUENCY CPS

FIGURE 3.20

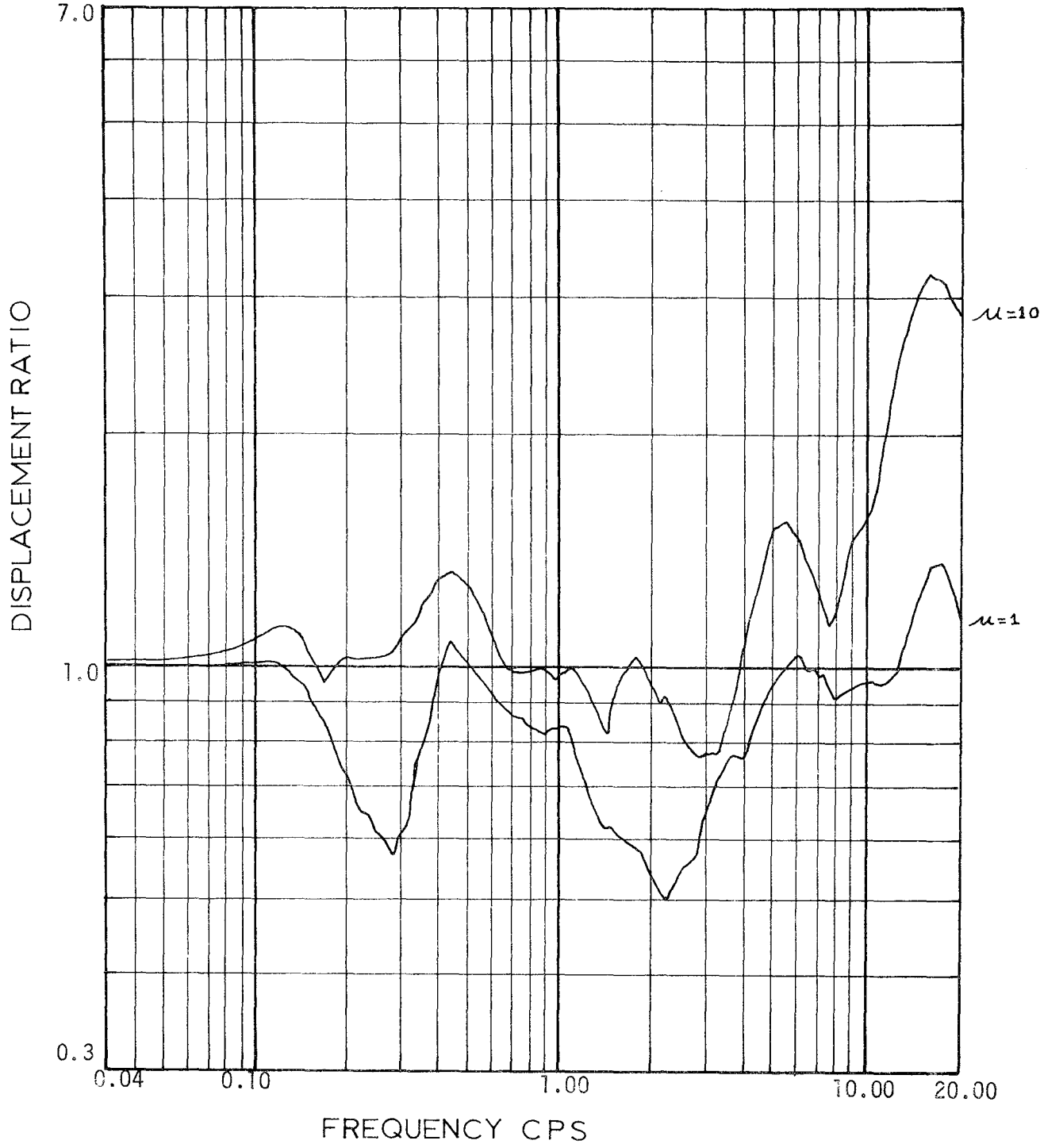
7.0
1.0
0.3
DISPLACEMENT RATIO
μ=10
μ=1
0.04
0.10
1.00
10.00
20.00
FREQUENCY CPS

FIGURE 3.21

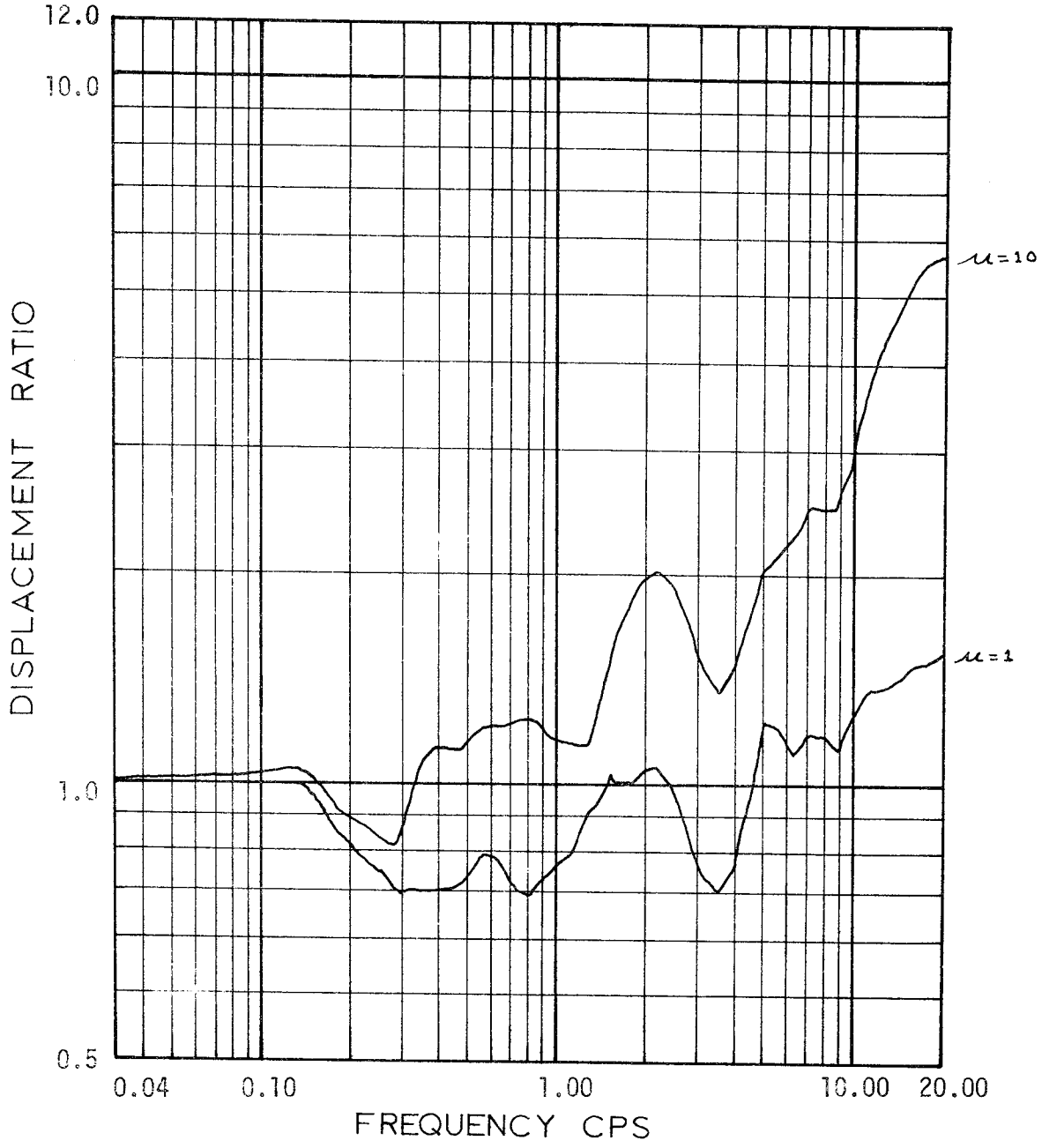
12.0
10.0
1.0
0.5
DISPLACEMENT RATIO
μ=10
μ=1
0.04
0.10
1.00
10.00
20.00
FREQUENCY CPS

FIGURE 3.22

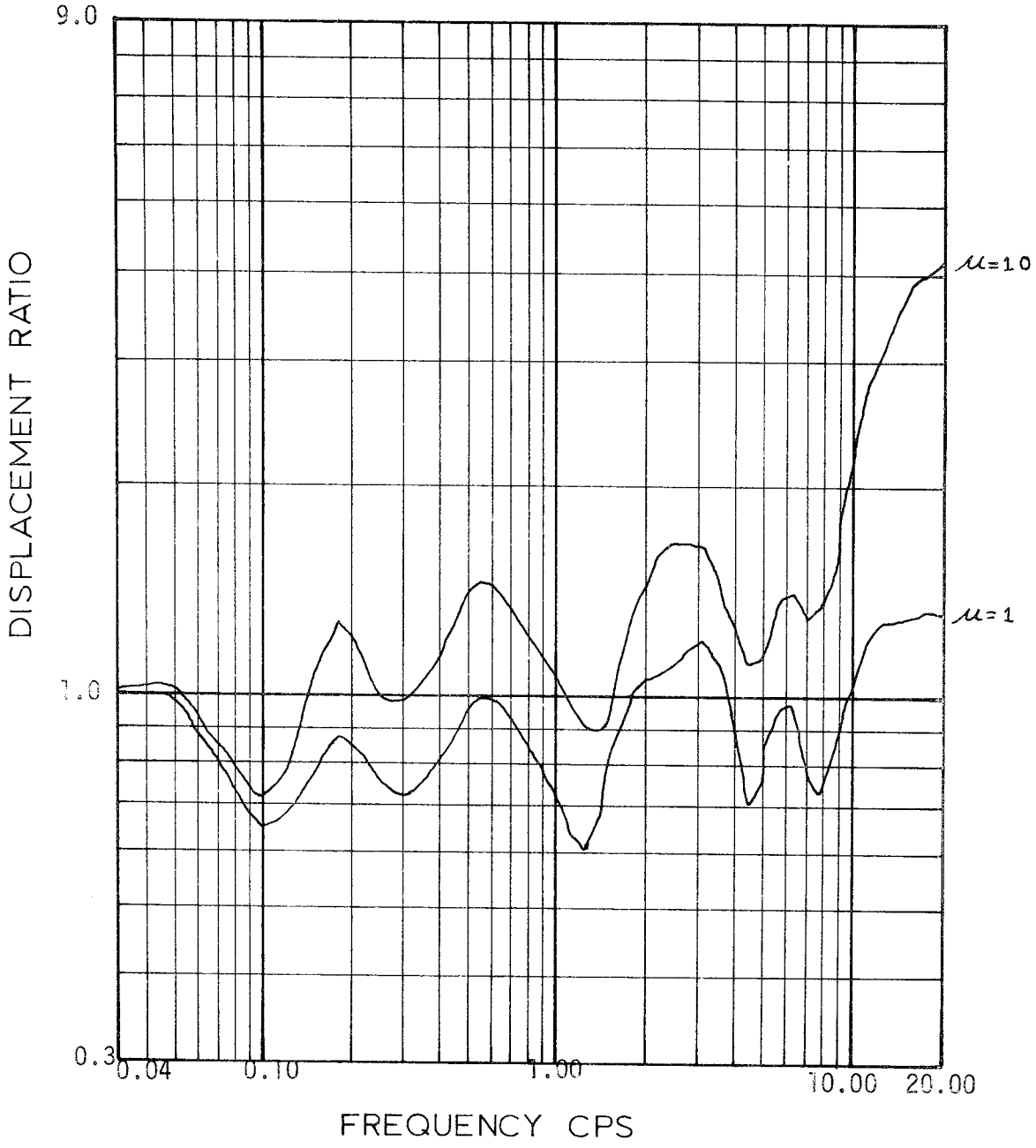
9.0
1.0
0.3
DISPLACEMENT RATIO
μ=10
μ=1
0.04
0.10
1.00
10.00
20.00
FREQUENCY CPS

FIGURE 3.23

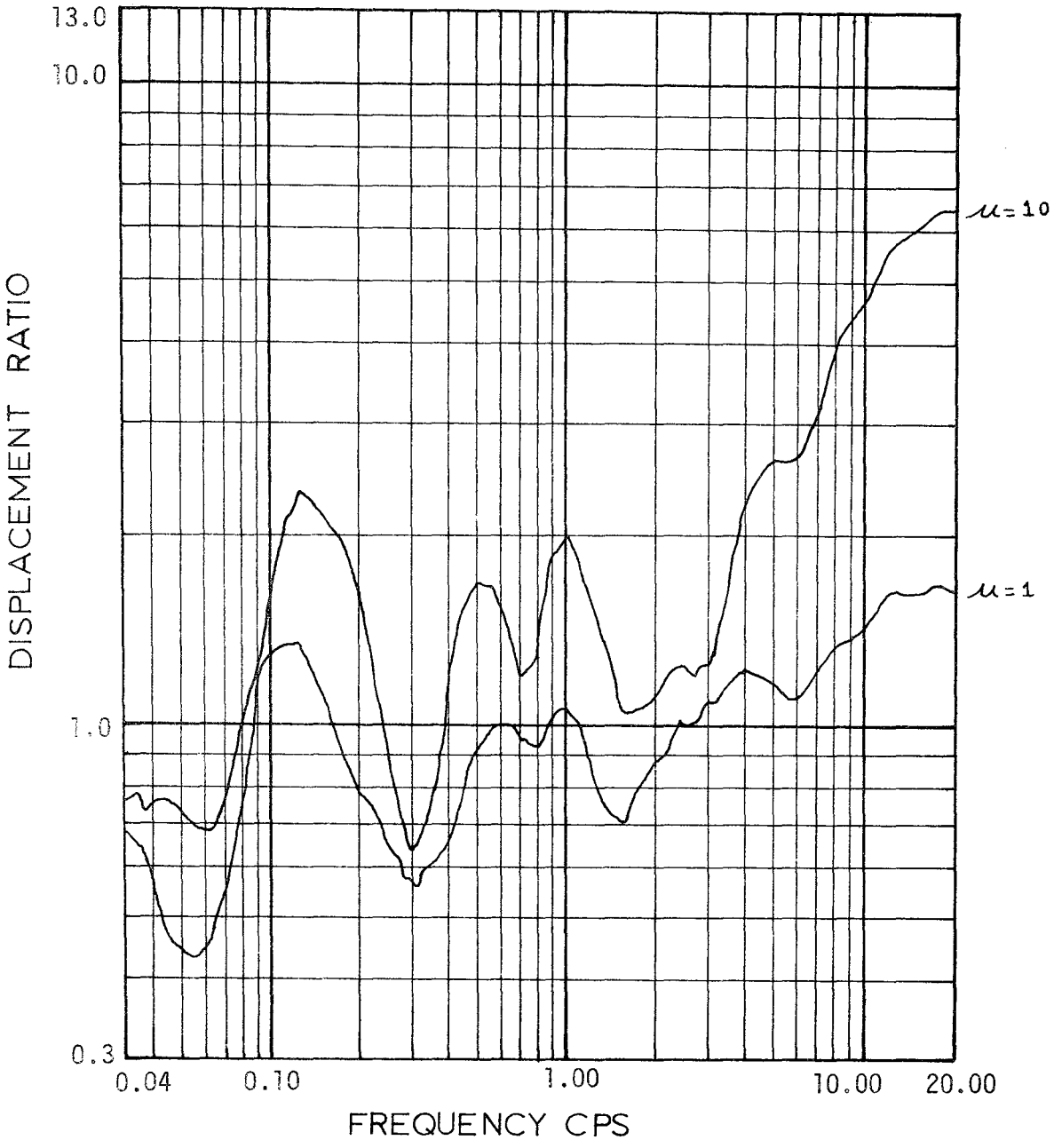
13.0
10.0
1.0
0.3
DISPLACEMENT RATIO
μ=10
μ=1
0.04
0.10
1.00
10.00
20.00
FREQUENCY CPS

FIGURE 3.24

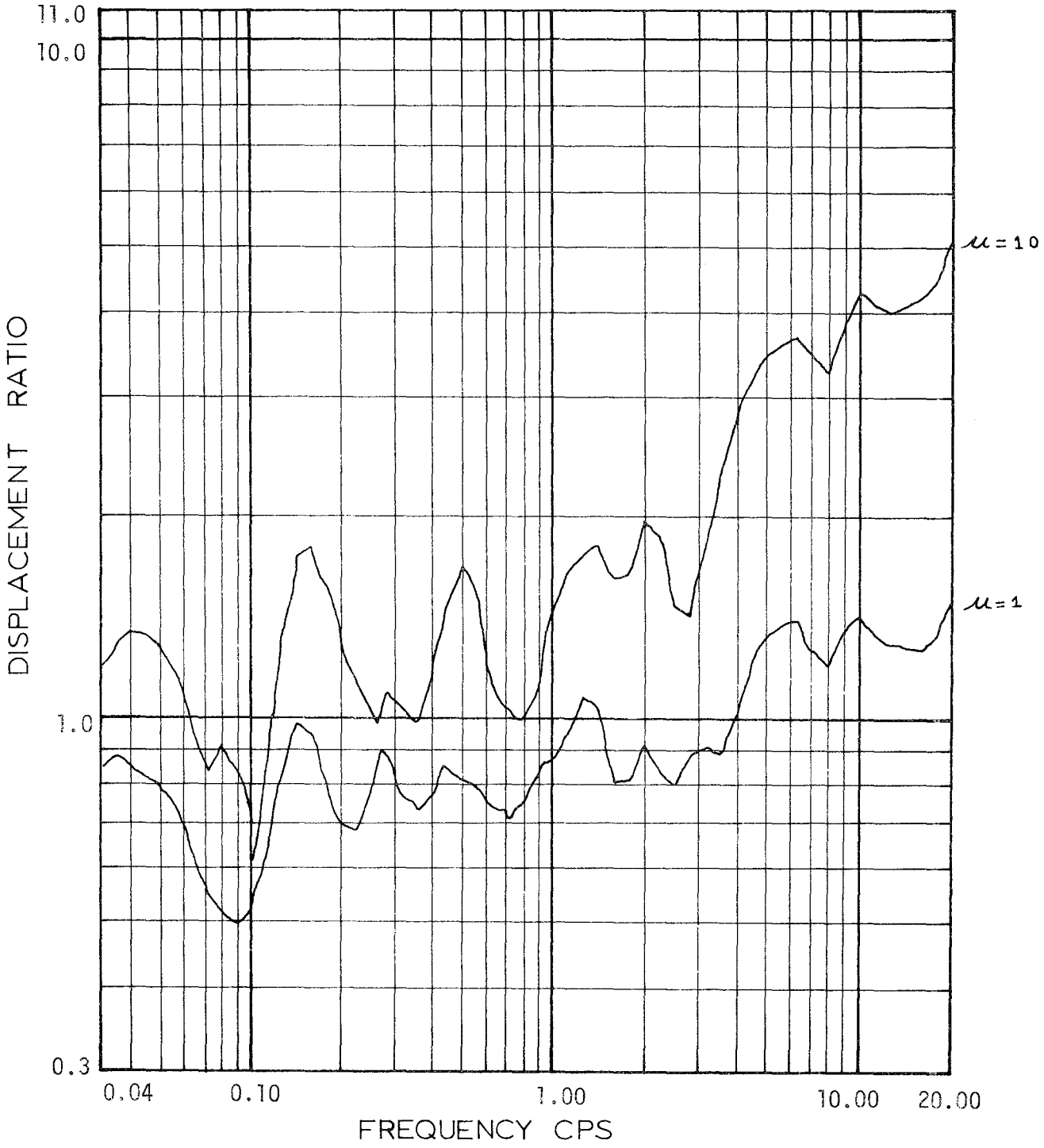
11.0
10.0
1.0
0.3
DISPLACEMENT RATIO
μ = 10
μ = 1
0.04
0.10
1.00
10.00
20.00
FREQUENCY CPS

FIGURE 3.25

	Earthquake No.									
μ	1	2	3	4	5	6	7	8	9	Average
2	2.33	2.10	-	-	2.00	-	1.85	1.8	2.4	2.08
3	-	-	-	-	2.85	-	3.00	-	-	2.93
4	-	-	4.0	-	3.85	-	4.00	-	-	3.95
5	-	-	5.4	-	4.90	-	4.60	-	-	4.97
6	-	-	7.0	-	5.90	-	5.70	6.2	-	6.20
7	-	-	7.8	6.8	6.70	-	6.80	-	-	7.00
8	-	-	-	7.8	7.80	-	7.50	-	-	7.70
9	-	-	-	9.05	9.00	-	8.80	-	-	8.95
10	-	-	-	10.10	10.00	-	9.70	-	-	9.93

TABLE 3.1 - RATIO = $R_{\mu=1}/R_{\mu}$ FOR RANGE 1

	Earthquake No.									
μ	1	2	3	4	5	6	7	8	9	Average
2	4.1	2.5	2.10	1.85	1.9	-	3.1	2.3	2.7	2.560
3	1.2	2.9	3.00	2.90	3.3	-	4.6	1.8	4.0	2.960
4	1.6	3.7	5.00	4.10	4.3	-	6.0	2.2	6.0	4.125
5	1.9	4.7	9.70	5.70	6.4	-	7.2	3.5	6.8	5.670
6	2.4	5.5	12.00	7.10	7.9	-	9.0	4.5	8.8	7.150
7	2.8	6.0	8.50	8.50	8.5	-	11.0	5.6	11.0	7.240
8	3.2	6.5	-	10.00	11.5	-	13.0	10.0	11.5	9.400
9	4.0	7.6	-	11.50	13.0	-	16.0	14.0	12.5	11.200
10	4.0	7.6	-	13.00	16.0	-	18.0	10.5	13.0	11.730

TABLE 3.2 - RATIO = $R_{\mu=1}/R_{\mu}$ FOR RANGE 2

	Earthquake No.									
μ	1	2	3	4	5	6	7	8	9	Average
2	2.50	2.25	2.6	2.6	1.9	2.0	3.0	2.35	2.65	2.43
3	4.20	3.30	4.0	3.7	2.8	3.0	4.0	4.70	6.00	3.97
4	5.80	4.10	6.3	4.8	3.8	3.9	5.2	6.00	7.60	5.28
5	7.25	5.00	9.0	5.7	4.7	5.0	6.2	7.20	9.50	6.62
6	9.20	5.90	12.0	7.0	6.0	6.0	7.8	8.20	11.50	8.20
7	11.00	6.80	14.0	7.8	7.1	6.8	9.1	10.00	12.50	10.57
8	12.50	7.60	16.5	9.1	8.5	8.0	11.5	13.00	13.50	11.13
9	14.50	8.50	18.0	10.0	10.0	8.9	12.5	16.50	15.00	12.65
10	16.00	9.00	20.5	11.5	11.5	10.0	14.0	21.00	20.00	14.83

TABLE 3.3 - RATIO = $R_{\mu=1}/R_{\mu}$ FOR RANGE 3

	Earthquake No.									
μ	1	2	3	4	5	6	7	8	9	Average
2	1.40	1.67	2.33	2.45	2.50	1.75	2.33	2.50	1.80	2.08
3	3.33	2.25	3.00	3.25	3.63	2.50	3.60	3.60	3.10	3.14
4	3.80	2.80	3.75	4.00	5.80	4.15	4.50	4.25	4.40	4.16
5	4.40	3.50	4.60	4.50	7.10	6.00	5.40	5.20	4.90	5.02
6	5.55	4.10	5.05	5.05	8.00	6.80	6.40	6.20	5.50	5.85
7	7.50	4.60	6.10	5.90	8.90	7.60	7.40	6.60	6.40	6.78
8	8.00	5.20	7.60	7.00	10.05	8.30	8.10	7.00	7.00	7.47
9	8.70	6.00	7.90	8.00	11.50	9.00	8.80	7.40	7.25	8.28
10	9.10	6.65	8.50	9.00	12.50	9.40	9.50	8.00	8.10	8.97

TABLE 3.4 - RATIO = $R_{\mu=1}/R_{\mu}$ FOR RANGE 4

	Earthquake No.									
μ	1	2	3	4	5	6	7	8	9	Average
2	1.65	1.9	1.75	1.85	2.15	1.65	2.65	1.70	1.70	1.89
3	2.00	2.3	2.40	2.60	2.75	2.05	3.60	2.00	2.35	2.45
4	2.35	2.6	2.45	3.00	3.33	2.60	4.25	2.25	2.90	2.89
5	2.80	2.9	2.90	3.20	3.85	2.85	4.80	2.50	3.05	3.21
6	3.10	3.2	3.00	3.35	4.20	3.00	5.20	2.60	3.15	3.42
7	3.50	3.5	3.25	3.60	4.80	3.30	5.50	2.75	3.30	3.72
8	3.80	3.6	3.50	3.90	5.00	3.35	5.90	2.85	3.30	3.90
9	4.00	3.8	3.65	4.00	5.00	3.50	6.00	3.00	3.60	4.06
10	4.10	3.8	3.85	4.10	5.35	3.65	6.25	3.05	3.65	4.20

TABLE 3.5 - RATIO = $R_{\mu=1}/R_{\mu}$ FOR RANGE 5

	Earthquake No.									
μ	1	2	3	4	5	6	7	8	9	Average
2	1.60	1.30	1.45	1.45	1.65	1.45	1.8	1.60	1.50	1.53
3	1.90	1.70	1.60	1.75	1.95	1.65	2.0	1.75	1.65	1.77
4	2.15	1.80	2.45	2.60	2.15	1.85	2.2	1.90	2.00	2.10
5	2.30	1.45	2.50	2.85	2.25	2.05	2.5	2.00	2.00	2.23
6	2.35	2.05	2.70	3.40	2.35	2.15	-	2.15	2.05	2.40
7	3.00	2.20	3.00	3.60	2.75	-	-	2.10	-	2.77
8	-	-	3.20	3.80	2.80	-	-	2.20	-	3.00
9	-	-	-	3.50	2.80	-	-	2.20	1.50	2.50
10	-	-	-	-	3.10	-	-	2.25	2.85	2.73

TABLE 3.6 - RATIO = $R_{\mu=1}/R_{\mu}$ FOR RANGE 6

	Earthquake No.									
μ	1	2	3	4	5	6	7	8	9	Average
2	-	1.05	-	1.10	-	1.20	1.10	-	1.15	1.12
3	-	1.10	-	1.20	-	1.25	1.30	-	1.20	1.21
4	-	1.15	1.15	1.25	-	1.30	1.40	-	1.20	1.24
5	-	1.15	1.15	1.30	-	1.35	1.45	-	1.25	1.28
6	-	1.20	1.20	1.35	-	1.35	-	-	1.35	1.29
7	1.35	1.20	1.20	1.45	-	-	-	-	-	1.30
8	-	-	-	1.45	-	-	-	-	-	1.33
9	-	-	-	1.45	-	-	-	1.0	-	1.23
10	-	-	-	1.45	-	-	-	-	1.50	1.48

TABLE 3.7 - RATIO = $R_{\mu=1}/R_{\mu}$ FOR RANGE 7

Range	α	γ	$R = [\alpha(\mu-1) + 1]^{\gamma}$
1	1	1	$R = \mu$
2	1	1	$R = 1.16\ (\mu-1) + 1$
3	1.4	1	$R = 1.4\ (\mu-1) + 1$
4	1.5	.825	$R = [1.5\ (\mu-1) + 1]^{.825}$
5	4	.41	$R = [4\ (\mu-1) + 1]^{.41}$
	5	.38	$R = [5\ (\mu-1) + 1]^{.38}$
6	2.5	.335	$R = [2.5\ (\mu-1) + 1]^{.338}$
7	2	.11	$R = [2\ (\mu-1) + 1]^{.11}$

TABLE 3.8 - SUGGESTED EQUATIONS

The Equivalent Linear System Approach

In order to evaluate this approach a separate computer program was implemented. For a system with an initial frequency ω_o and a ductility ratio μ larger than 1, a characteristic ductility of $2\mu/3$ was selected and the frequency and damping of an equivalent system were computed as indicated in Chapter 2. The response of this equivalent system to the desired earthquake was then computed by numerical integration. The same series of plots were obtained as for the inelastic systems.

In this case the pseudo acceleration of the system will be

$$S_a = \omega_{eq}^2 S_d = \frac{\omega_o^2}{\mu_{char}} S_d \qquad (4\text{-}1)$$

and since

$$S_d = \mu u_y \qquad (4\text{-}2)$$

$$S_a = \omega_o^2 u_y \frac{\mu}{\mu_{char}} \qquad (4\text{-}3)$$

Notice, however, that the equivalent viscous damping, computed from the area of the hysteresis loop and added to the original viscous damping of 5% of critical, results now in large values of p, particularly for large ductility ratios. Under these conditions the agreement between the pseudo-acceleration and the maximum absolute acceleration of the system deteriorates. Results obtained were, however, the pseudo-acceleration, since this is what would be normally used in practice.

The same procedure described in Chapter 3 was repeated in this case, obtaining for each spectrum its envelope and determining in each range the ratio between elastic ($\mu = 1$) and inelastic values. In this case, however, the extreme ranges could not be found within the range of frequencies studied except for a few cases, and the inelastic spectra showed only clearly the intermediate ranges 3, 4, and 5. For most buildings those are nevertheless the important ranges.

Tables 4.1 to 4.3 show the ratios obtained for the nine accelerograms in these ranges, and Figs. 4.1 to 4.3 show the upper and lower bounds, the average and the best fit curve obtained in Chapter 3. Figures 4.4 to 4.6 show the upper and lower bounds obtained for this approach and for the actual inelastic systems (Chapter 3), indicating the common region.

In range 3 the approximate metnod provides reasonably good results, in fact slightly on the conservative side. In range 4 on the other hand the approximate results seem somewhat unconservative (above the true results), but the common region is still a substantial part of the total area between bounds. (Notice that the trend is similar to that observed with Newmark's method, although the values are different). In this range accelerations would be on the average underestimated by maybe 20%. In range 5 again the approximate method seems conservative for large values of the ductility ratio and only slightly unconservative for ductilities around 3. In the overall, the procedure exhibits the right trend and the estimates of accelerations (or required yield level f_y) are probably acceptable considering the variation from one earthquake to another (as illustrated by the scatter in the results) and the uncertainties involved in selecting a design earthquake.

	Earthquake No.									
μ	1	2	3	4	5	6	7	8	9	Average
2	2.33	1.60	2.20	2.15	1.5	1.40	1.90	2.20	2.07	1.91
3	3.80	2.50	4.60	4.00	2.3	2.05	3.05	4.00	4.25	3.40
4	5.15	3.30	6.15	5.50	3.2	2.75	4.15	6.15	6.15	4.72
5	9.30	5.10	7.75	7.10	4.0	3.25	5.00	8.00	7.40	6.32
6	7.70	5.00	9.30	8.80	4.8	4.00	5.10	10.00	8.80	7.20
7	9.00	5.80	9.40	10.00	5.5	4.70	7.20	10.20	8.90	7.85
8	10.00	5.80	12.50	11.50	6.2	5.30	8.00	12.50	11.50	9.26
9	11.70	7.40	14.00	13.00	7.0	6.10	9.10	14.50	12.50	10.60
10	12.50	8.15	15.00	14.50	7.8	6.60	10.00	16.50	14.50	11.73

TABLE 4.1 - RATIO = $R_{\mu=1}/R_{\mu}$ FOR RANGE 3

	Earthquake No.									
μ	1	2	3	4	5	6	7	8	9	Average
2	2.20	1.90	2.35	2.55	2.40	1.70	2.70	3.05	1.80	2.29
3	4.15	3.25	4.00	4.15	4.20	3.00	5.10	5.60	3.30	4.08
4	5.80	4.30	5.10	5.40	5.40	3.75	7.00	7.15	4.50	5.90
5	6.90	5.20	6.10	6.60	6.50	4.50	8.80	8.75	5.50	6.54
6	7.90	6.00	7.00	7.30	7.20	5.15	10.00	10.00	6.30	7.43
7	8.70	6.80	7.70	8.25	8.15	5.90	11.50	11.50	7.30	8.42
8	10.00	7.50	8.40	9.15	9.00	6.40	12.00	12.00	8.00	9.16
9	10.50	8.15	9.15	10.00	9.90	7.00	12.50	13.00	8.80	9.90
10	11.50	8.70	9.90	11.5	11.00	7.40	14.00	14.00	9.20	10.80

TABLE 4.2 - RATIO = $R_{\mu=1}/R_{\mu}$ FOR RANGE 4

	Earthquake No.									
μ	1	2	3	4	5	6	7	8	9	Average
2	1.70	1.85	2.25	2.40	2.40	2.0	2.25	2.25	1.60	2.10
3	2.40	2.75	2.75	3.15	3.45	2.7	3.15	3.00	2.20	2.84
4	2.60	3.00	3.10	3.45	-	2.7	3.50	3.25	2.45	3.00
5	3.00	3.00	3.20	3.45	-	2.8	3.60	3.30	2.50	3.10
6	3.00	3.00	3.20	3.60	-	3.0	3.90	3.35	2.60	3.20
7	3.00	3.15	3.40	3.56	-	2.0	4.20	3.50	2.60	3.30
8	3.00	2.90	3.35	3.60	-	3.0	4.50	3.50	2.62	3.31
9	3.00	3.15	3.30	3.60	-	3.1	4.50	3.50	2.65	3.36
10	3.10	3.15	3.40	3.60	-	3.0	4.60	3.50	2.70	3.38

TABLE 4.3 - RATIO = $R_{\mu=1}/R_{\mu}$ FOR RANGE 5

It is interesting, however, to compare also maximum displacements. Figures 4.7 to 4.15 show the ratio of the maximum inelastic to the maximum elastic displacement, the first one being obtained by the approximate method. Comparing these figures to Figs. 3.17 to 3.25, it can be seen that, while the overall trend is again correct, maximum displacements seem to be consistently underestimated by the approximate method, the accuracy being worse than for the accelerations. This is logical, considering that if S_a is correct, S_d will now be $\mu_{char}\ (S_a/\omega_o^2)$ instead of (S_a/ω_o^2). If the resulting displacements were multiplied by the factor μ/μ_{char}, in our case 1.5, the agreement would be much better.

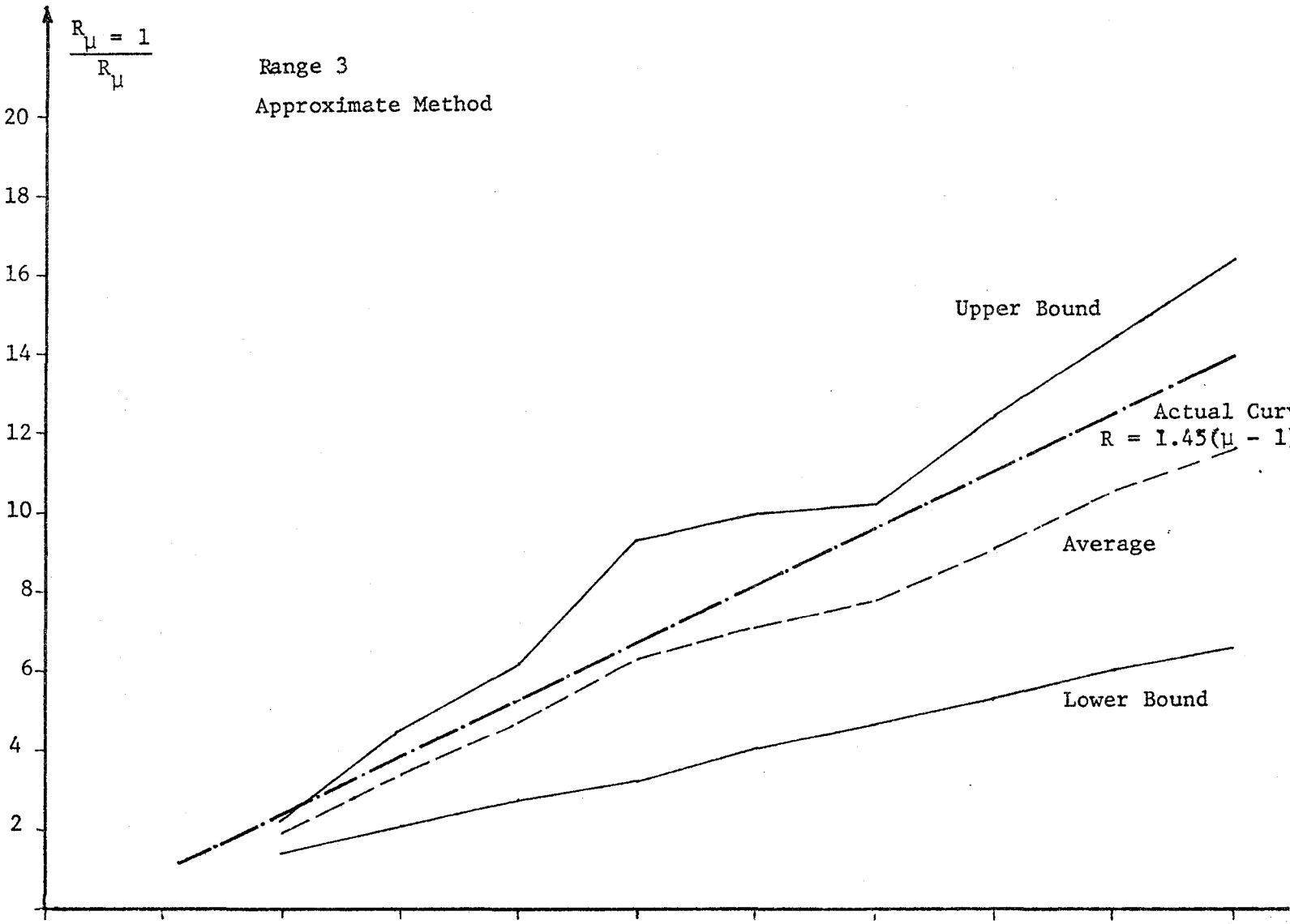
$\frac{R_\mu = 1}{R_\mu}$
Range 3
Approximate Method
20
18
16
14
12
10
8
6
4
2
1
2
3
4
5
6
7
8
9
10
Upper Bound
Actual Cur
R = 1.45(μ - 1
Average
Lower Bound

Figure 4-1

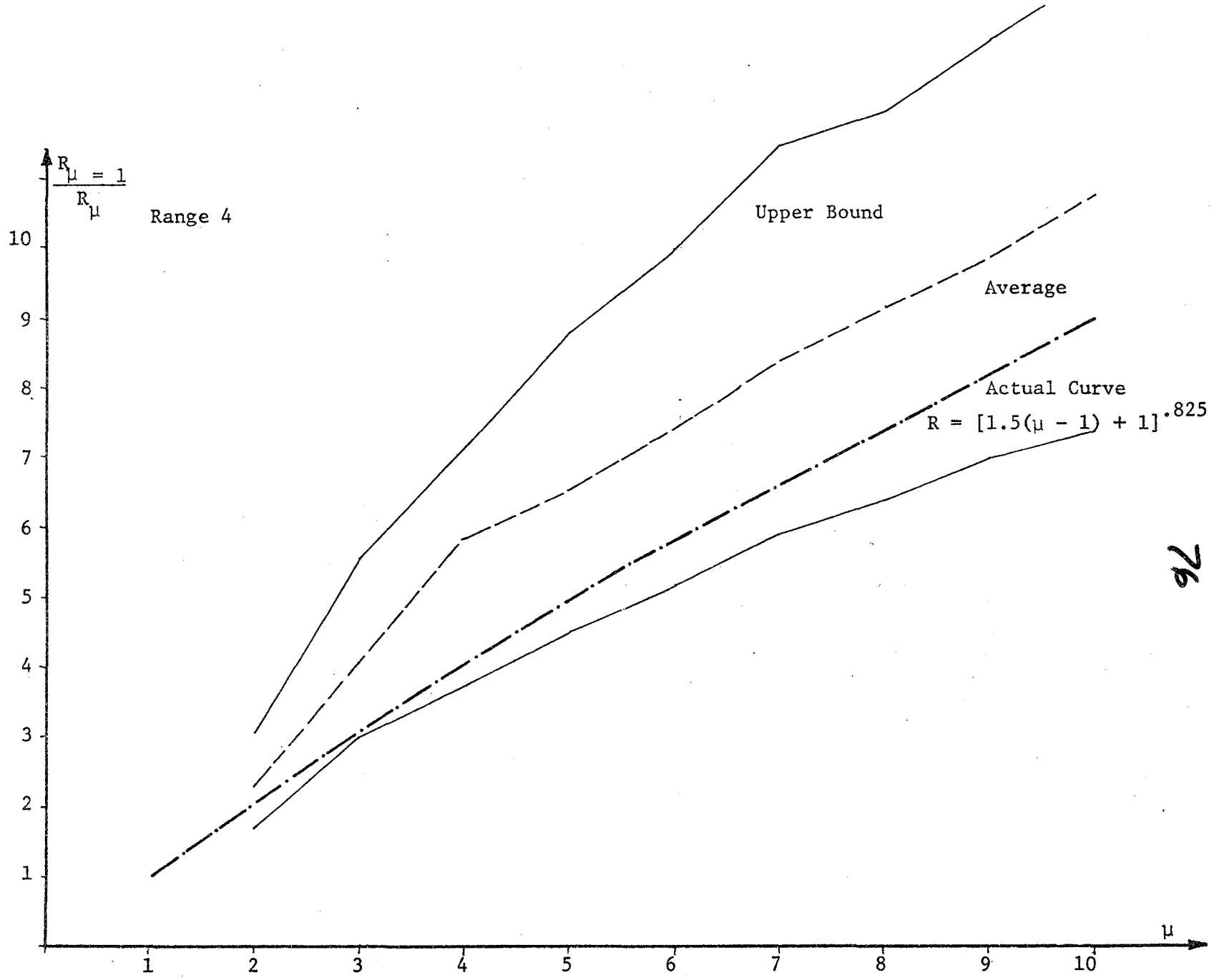
$\frac{R_{\mu=1}}{R_\mu}$
Range 4
Upper Bound
Average
Actual Curve
$R = [1.5(\mu - 1) + 1]^{.825}$
10
9
8
7
6
5
4
3
2
1
1
2
3
4
5
6
7
8
9
10
μ

Figure 4-2

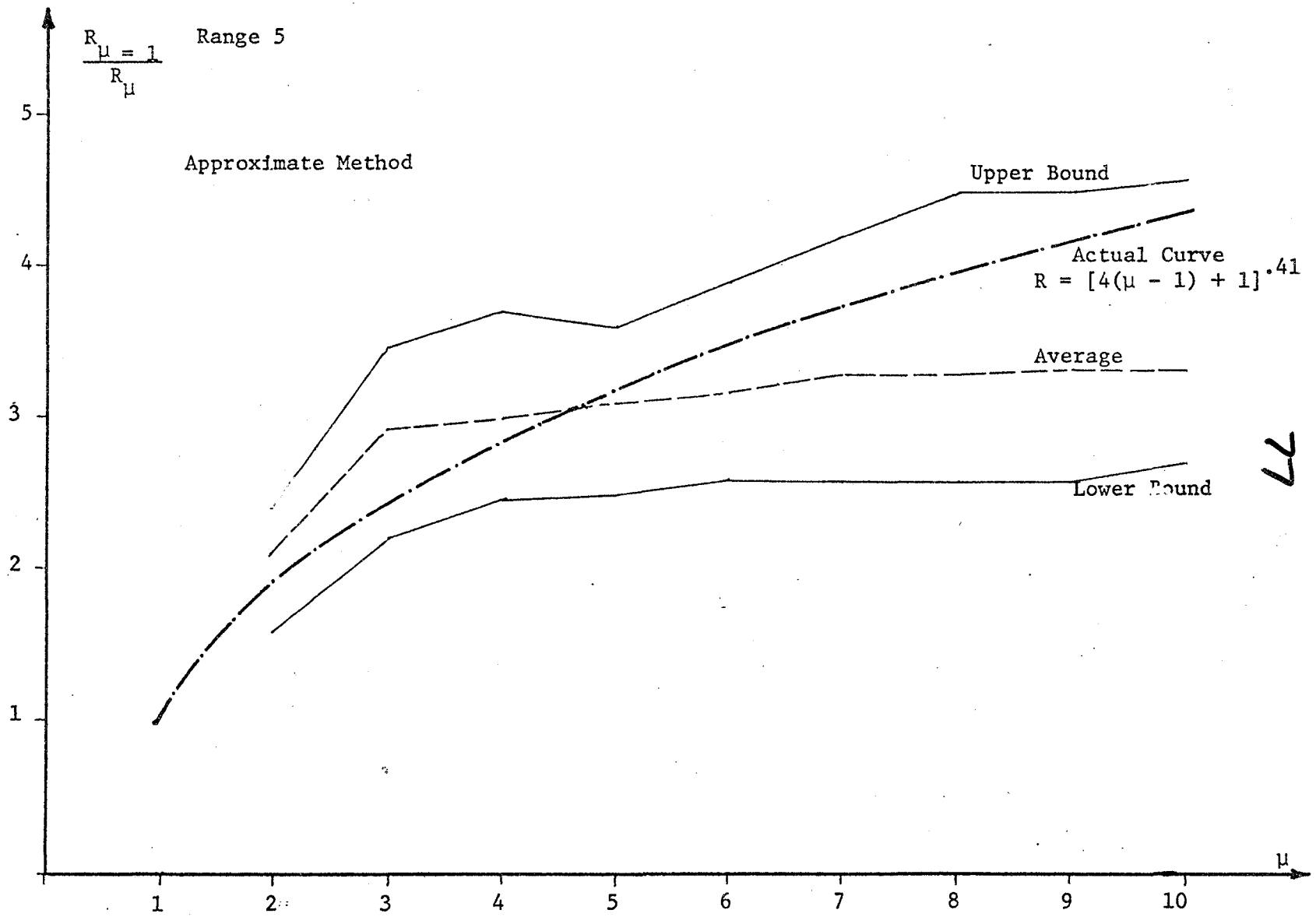
$\frac{R_{\mu=1}}{R_\mu}$
Range 5
Approximate Method
Upper Bound
Actual Curve
$R = [4(\mu - 1) + 1]^{.41}$
Average
Lower Bound
77
5
4
3
2
1
1
2
3
4
5
6
7
8
9
10
μ

Figure 4-3

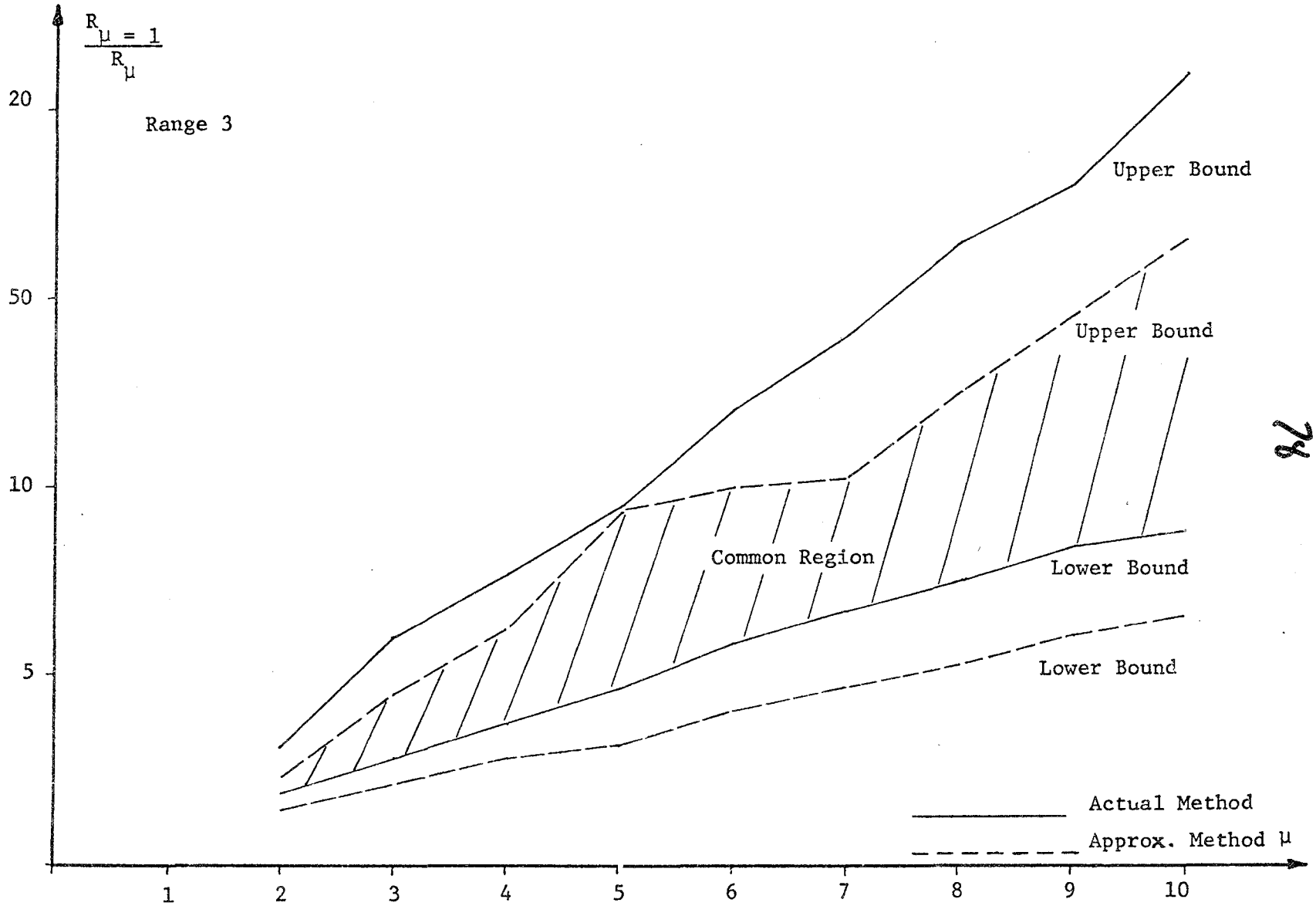
$\frac{R_{\mu=1}}{R_\mu}$
Range 3
20
50
10
5
Upper Bound
Upper Bound
Common Region
Lower Bound
Lower Bound
Actual Method
Approx. Method μ
1
2
3
4
5
6
7
8
9
10

Figure 4-4

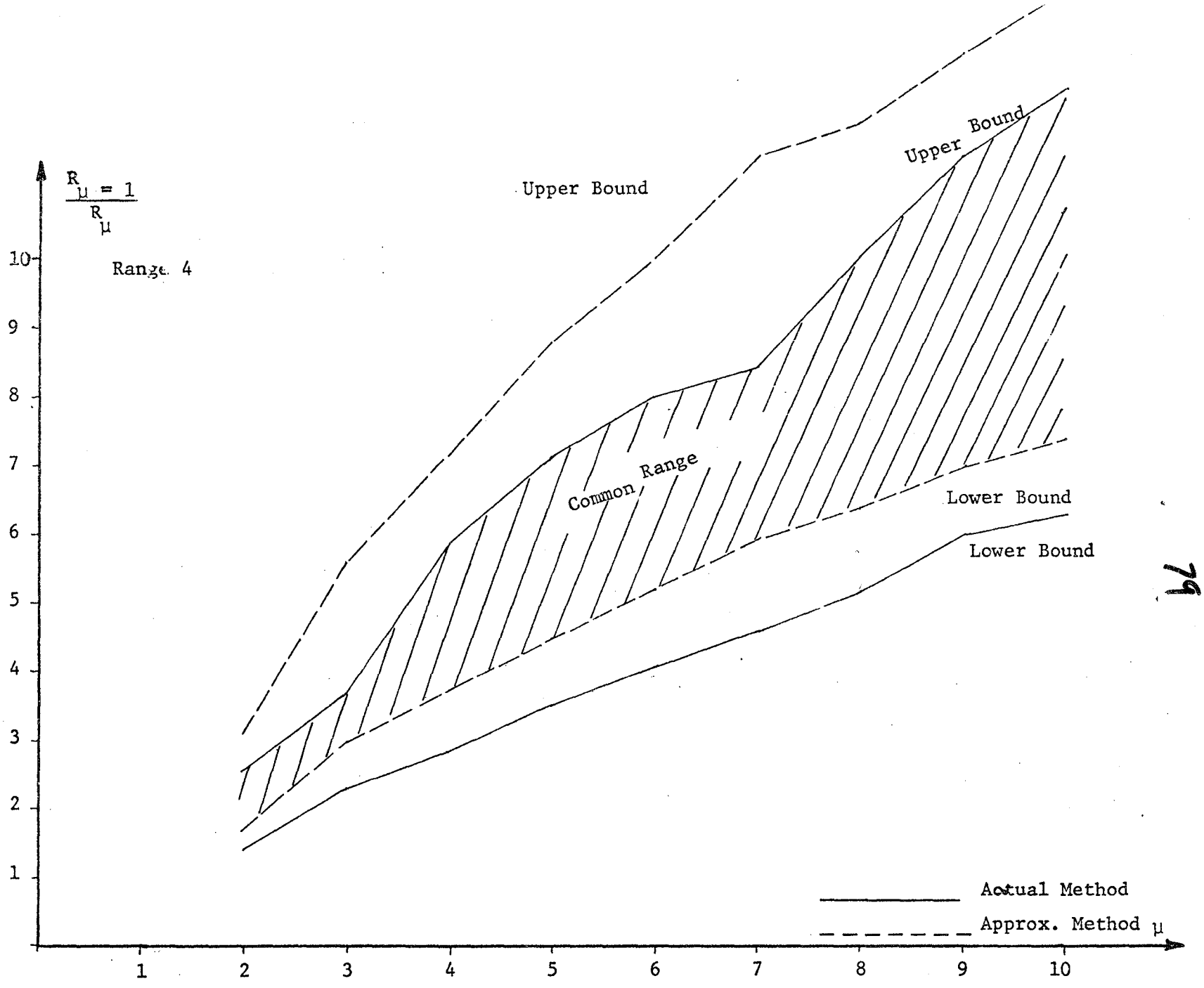
$\frac{R_{\mu=1}}{R_{\mu}}$
Range 4
Upper Bound
Upper Bound
Common Range
Lower Bound
Lower Bound
Actual Method
Approx. Method
μ
1
2
3
4
5
6
7
8
9
10

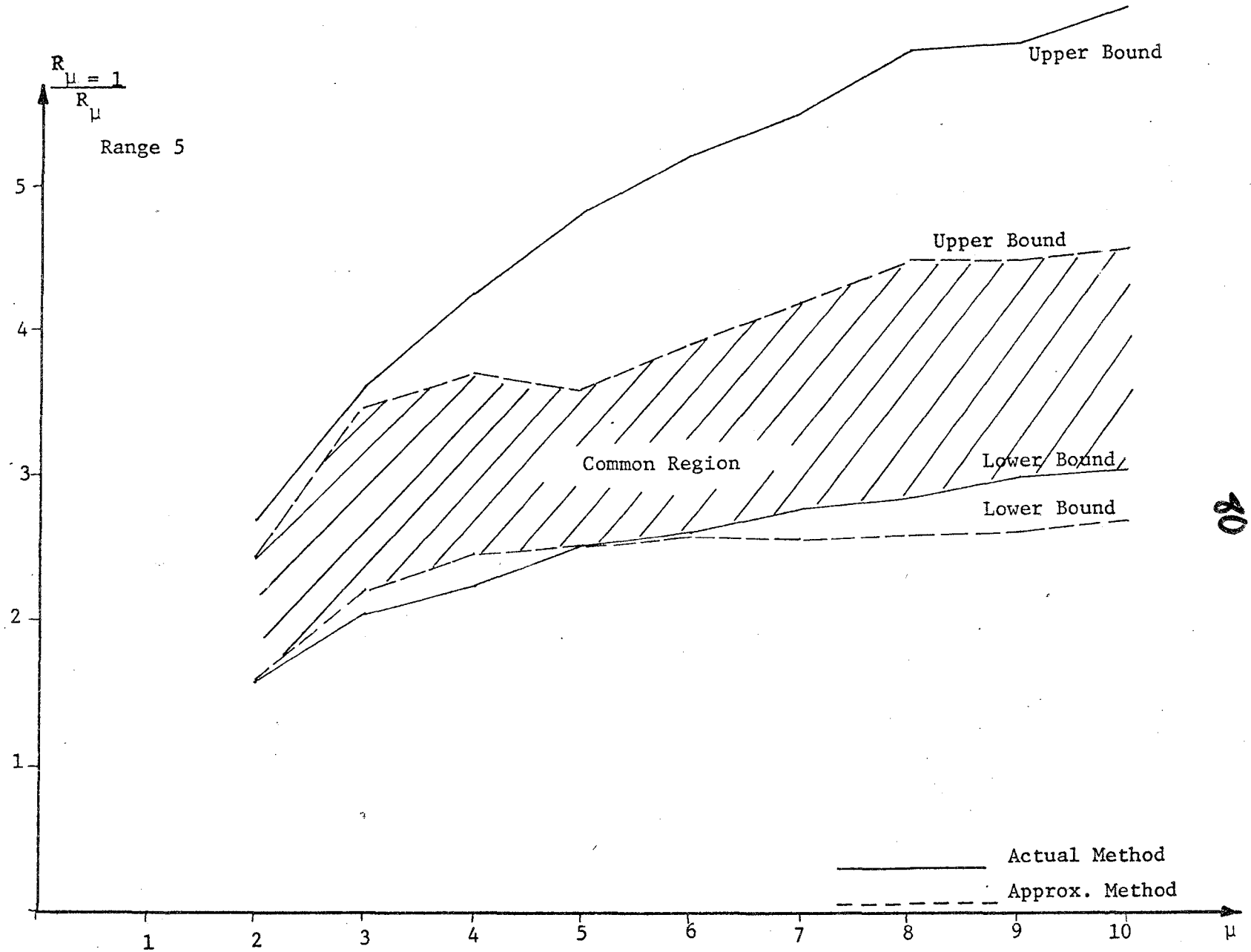
$R_{\mu=1}/R_{\mu}$
Range 5
Upper Bound
Upper Bound
Common Region
Lower Bound
Lower Bound
Actual Method
Approx. Method
1
2
3
4
5
6
7
8
9
10
μ

Figure 4-6

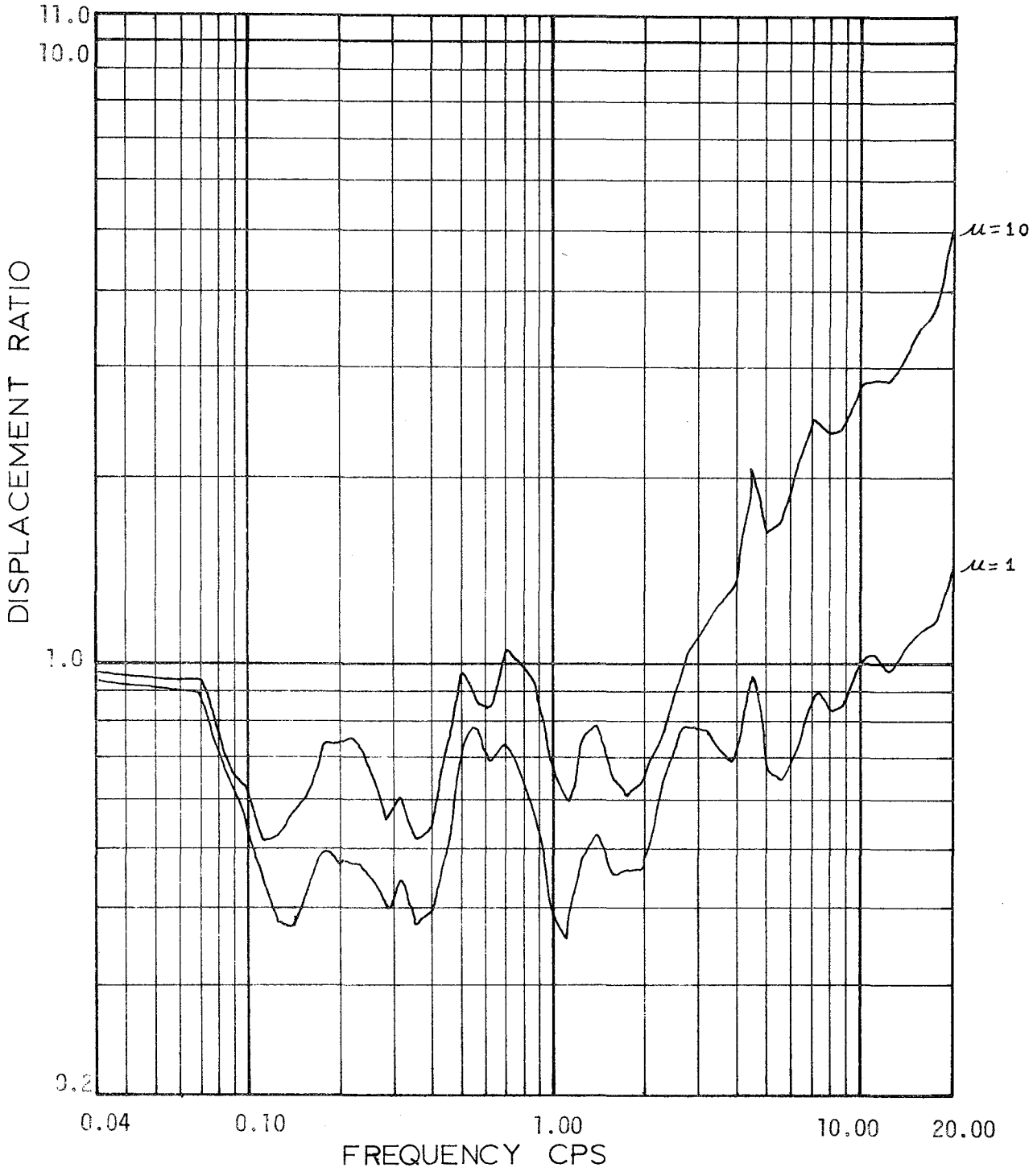
11.0
10.0
1.0
0.2
DISPLACEMENT RATIO
μ=10
μ=1
0.04
0.10
1.00
10.00
20.00
FREQUENCY CPS

FIGURE 4.7

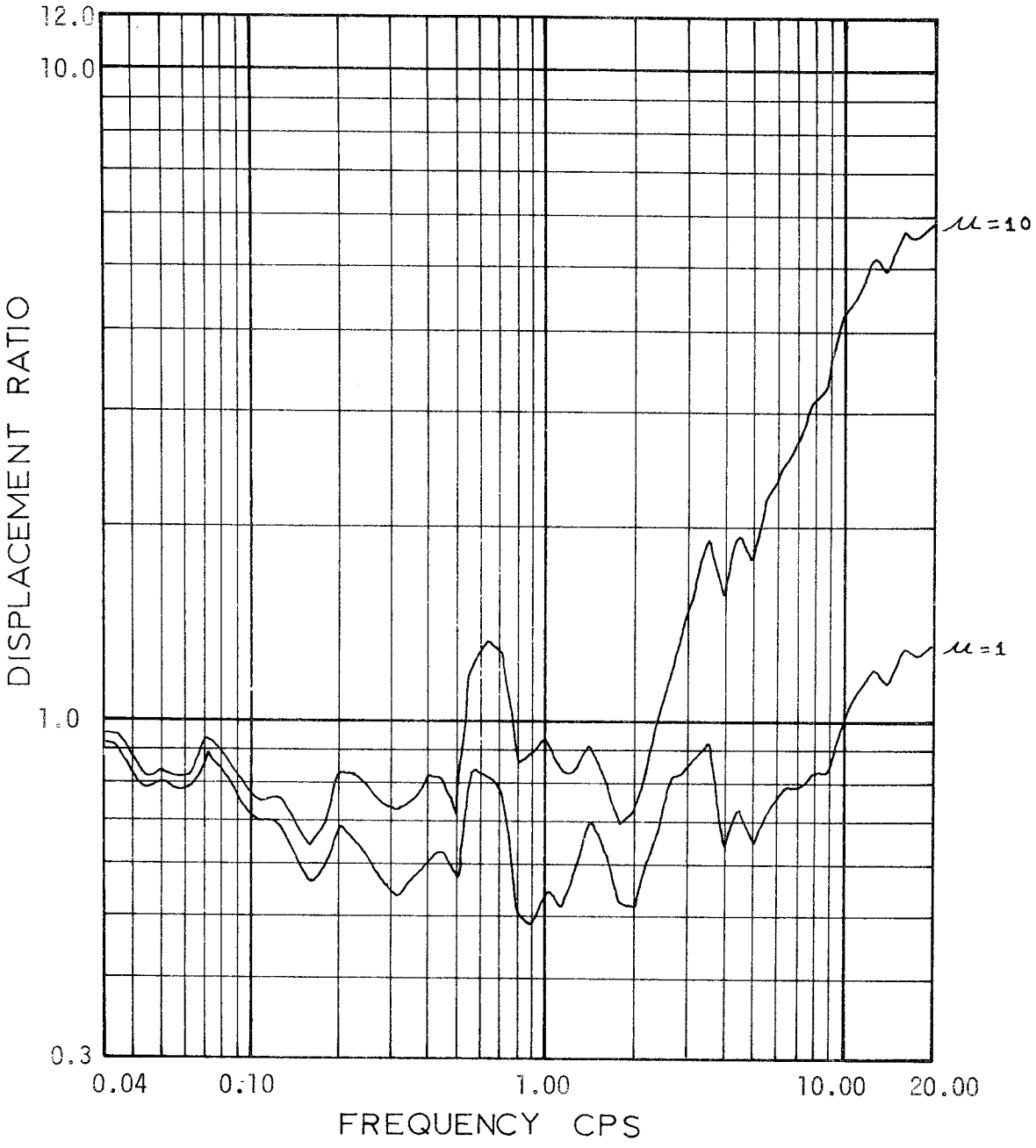
12.0
10.0
1.0
0.3
DISPLACEMENT RATIO
μ=10
μ=1
0.04
0.10
1.00
10.00
20.00
FREQUENCY CPS

FIGURE 4.8

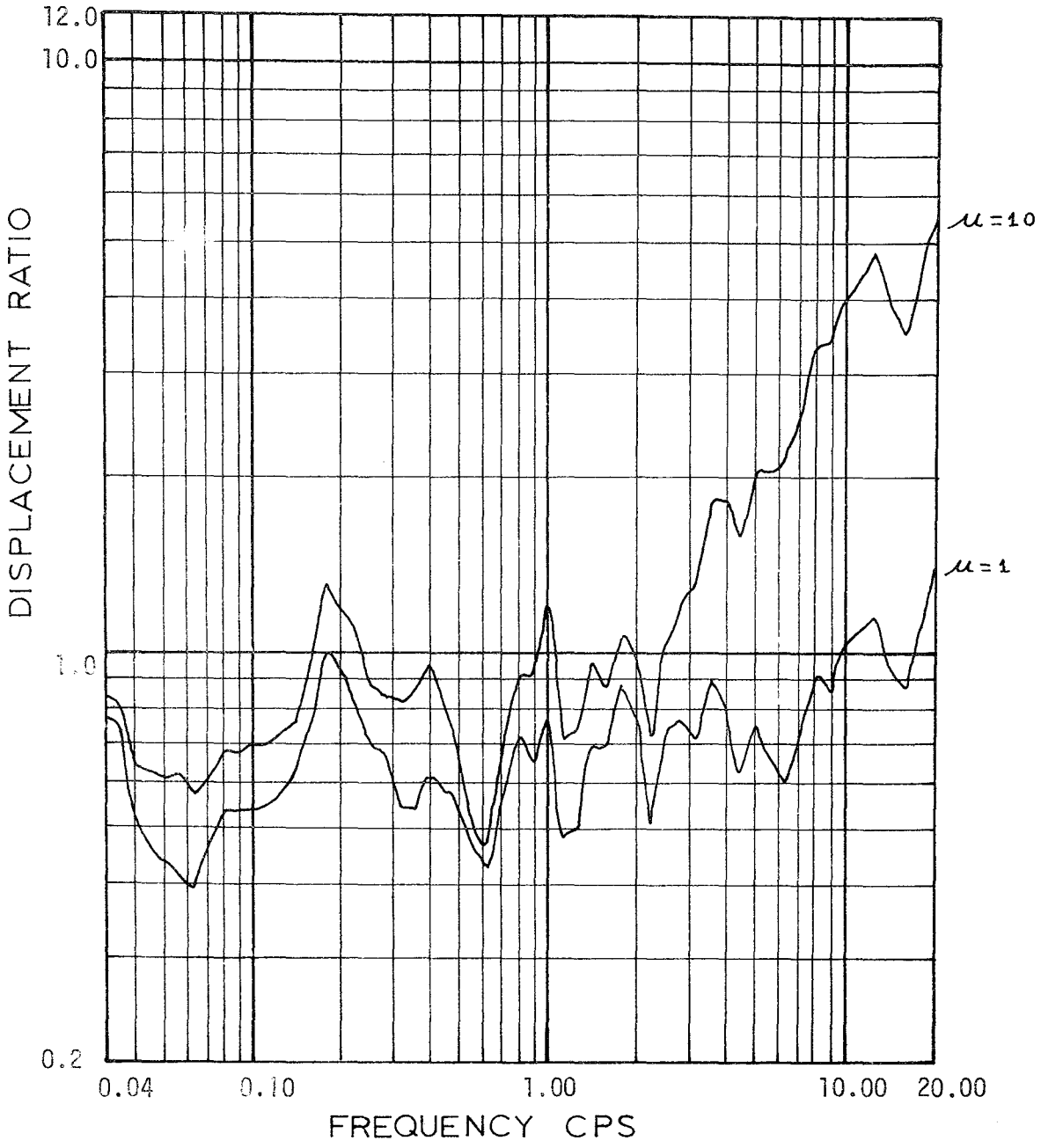
12.0
10.0
1.0
0.2
DISPLACEMENT RATIO
μ=10
μ=1
0.04
0.10
1.00
10.00
20.00
FREQUENCY CPS

FIGURE 4.9

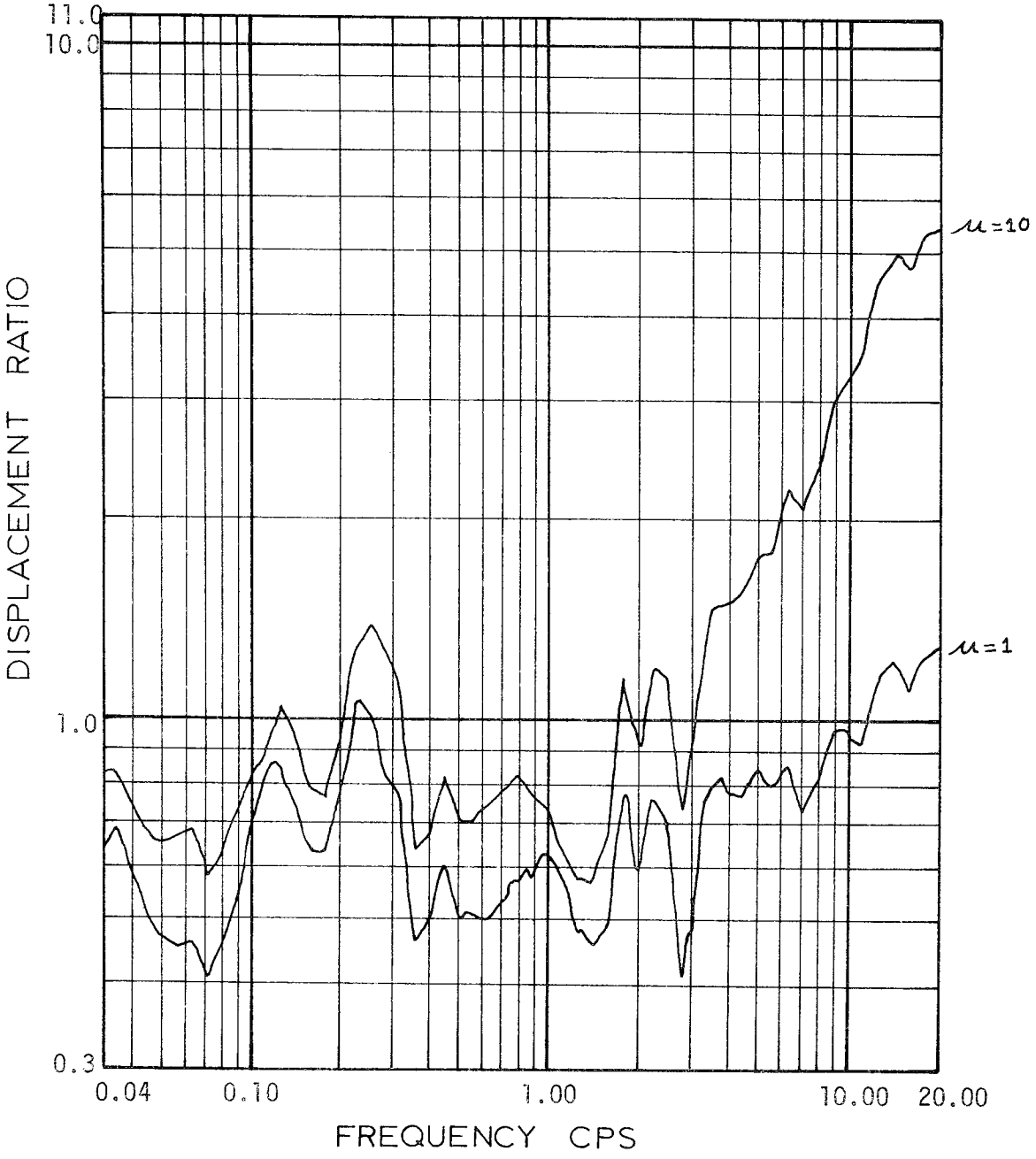
11.0
10.0
1.0
0.3
DISPLACEMENT RATIO
μ=10
μ=1
0.04
0.10
1.00
10.00
20.00
FREQUENCY CPS

FIGURE 4.10

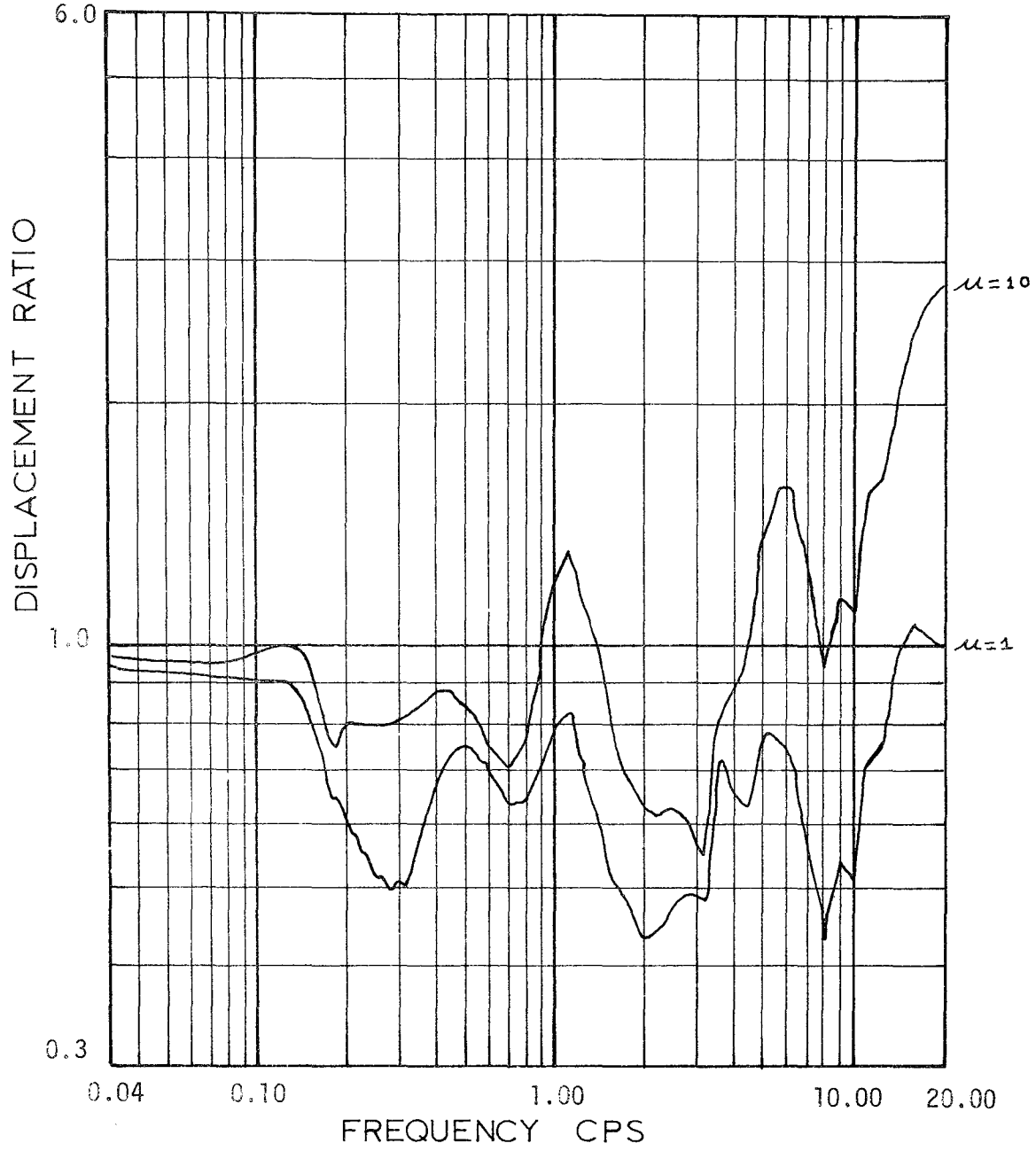
6.0
1.0
0.3
DISPLACEMENT RATIO
μ=10
μ=1
0.04
0.10
1.00
10.00
20.00
FREQUENCY CPS

FIGURE 4.11

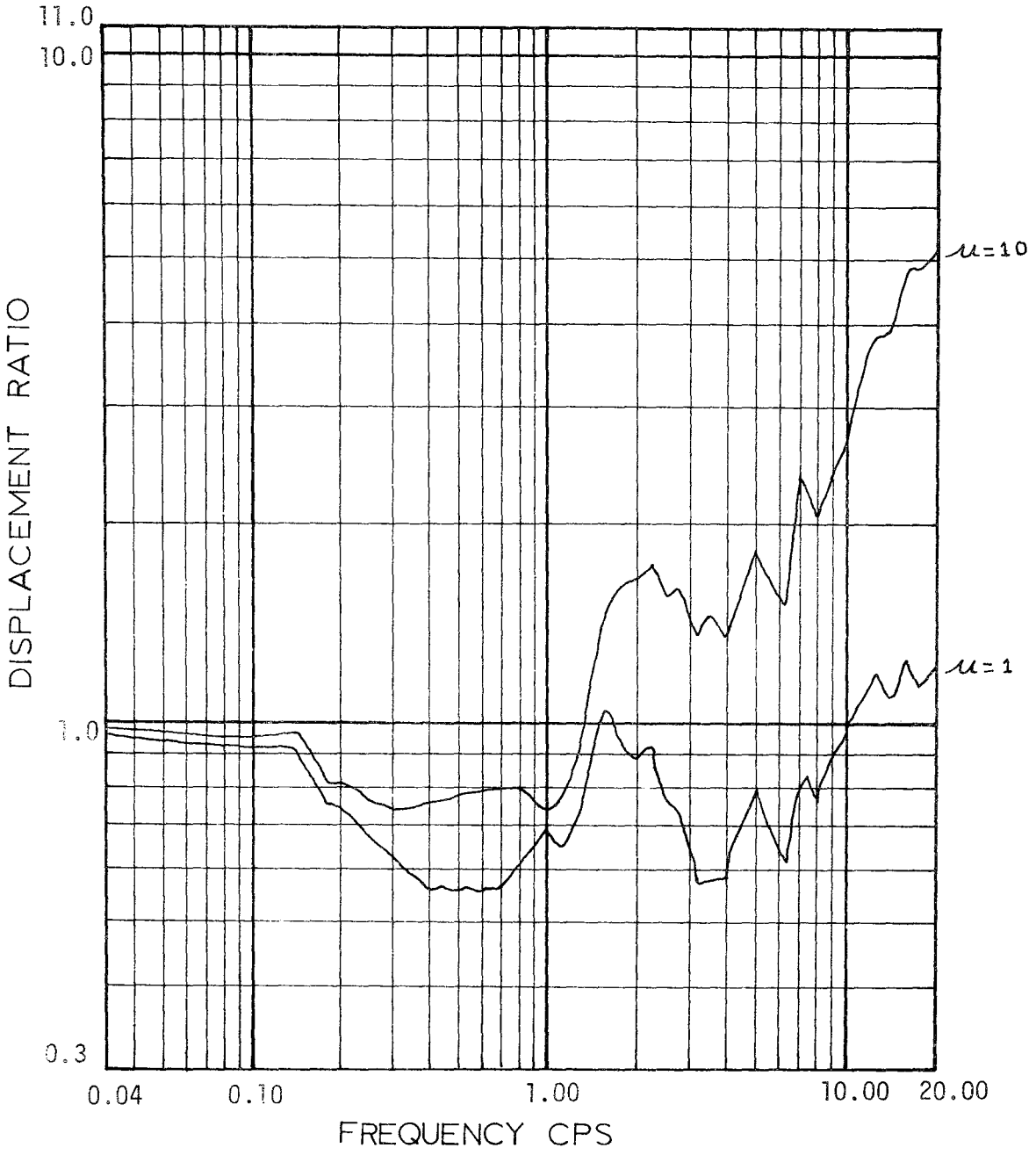
11.0
10.0
1.0
0.3
DISPLACEMENT RATIO
μ=10
μ=1
0.04
0.10
1.00
10.00
20.00
FREQUENCY CPS

FIGURE 4.12

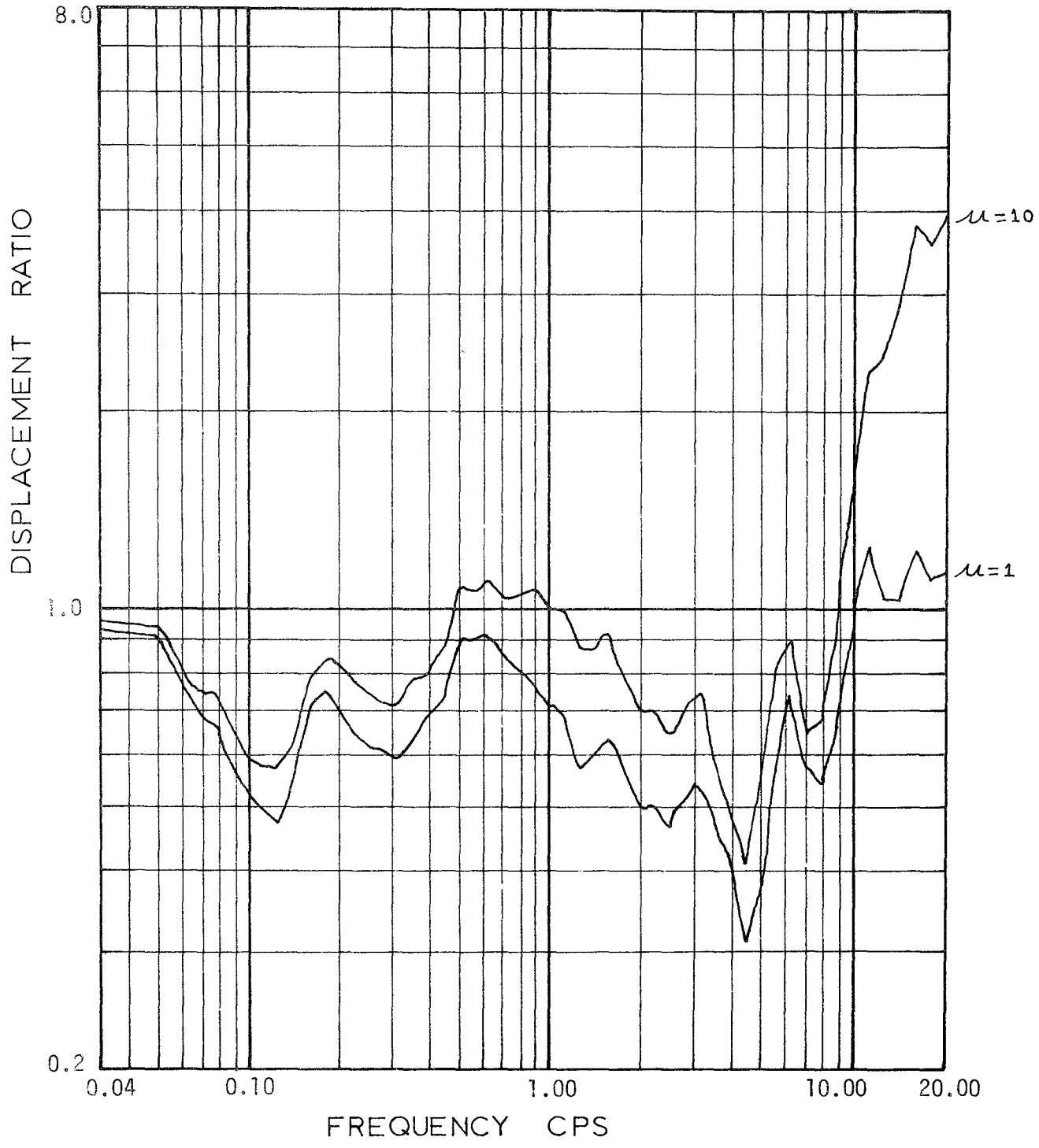
8.0
1.0
0.2
DISPLACEMENT RATIO
μ=10
μ=1
0.04
0.10
1.00
10.00
20.00
FREQUENCY CPS

FIGURE 4.13

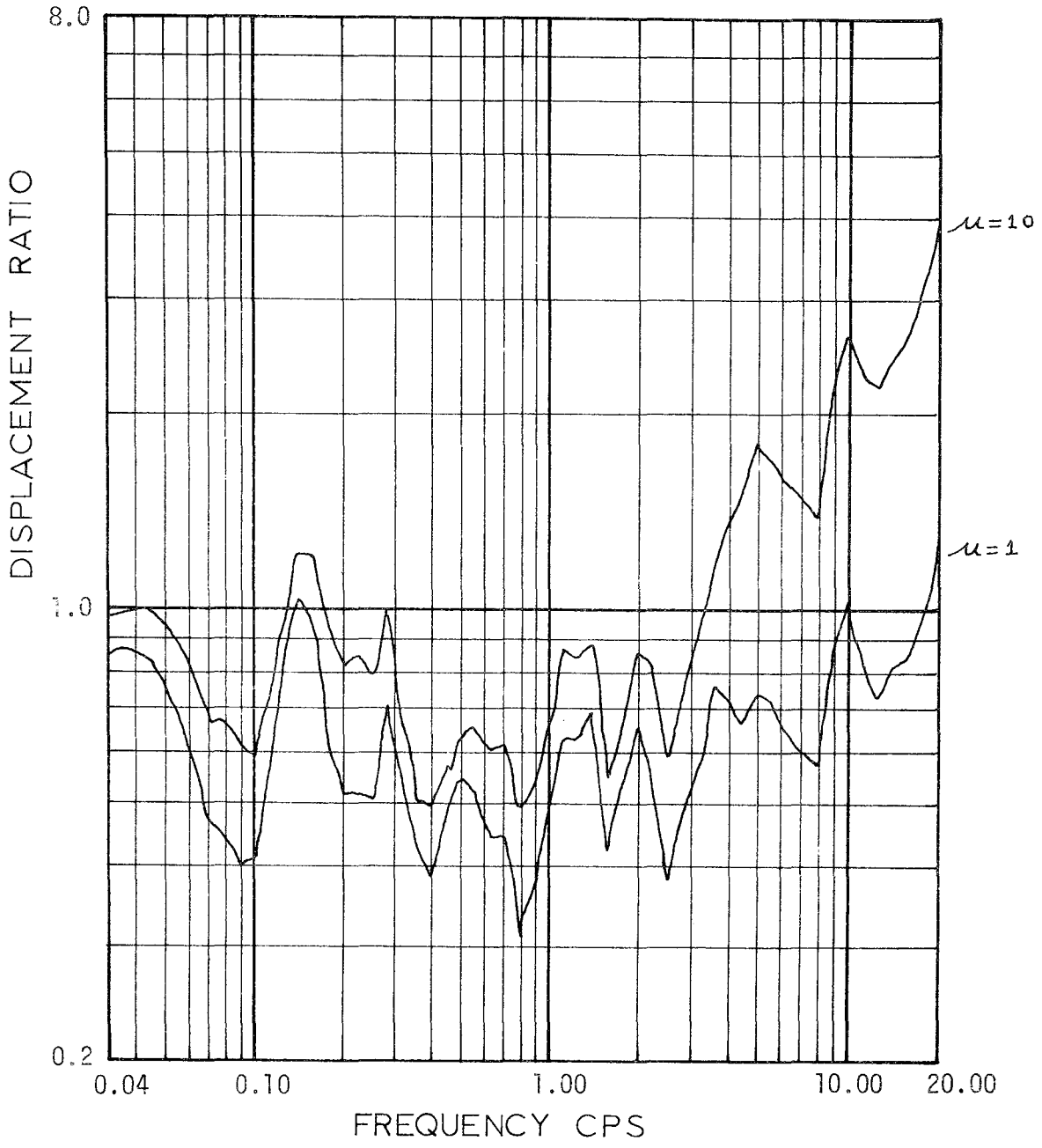
8.0
1.0
0.2
DISPLACEMENT RATIO
μ=10
μ=1
0.04
0.10
1.00
10.00
20.00
FREQUENCY CPS

FIGURE 4.14

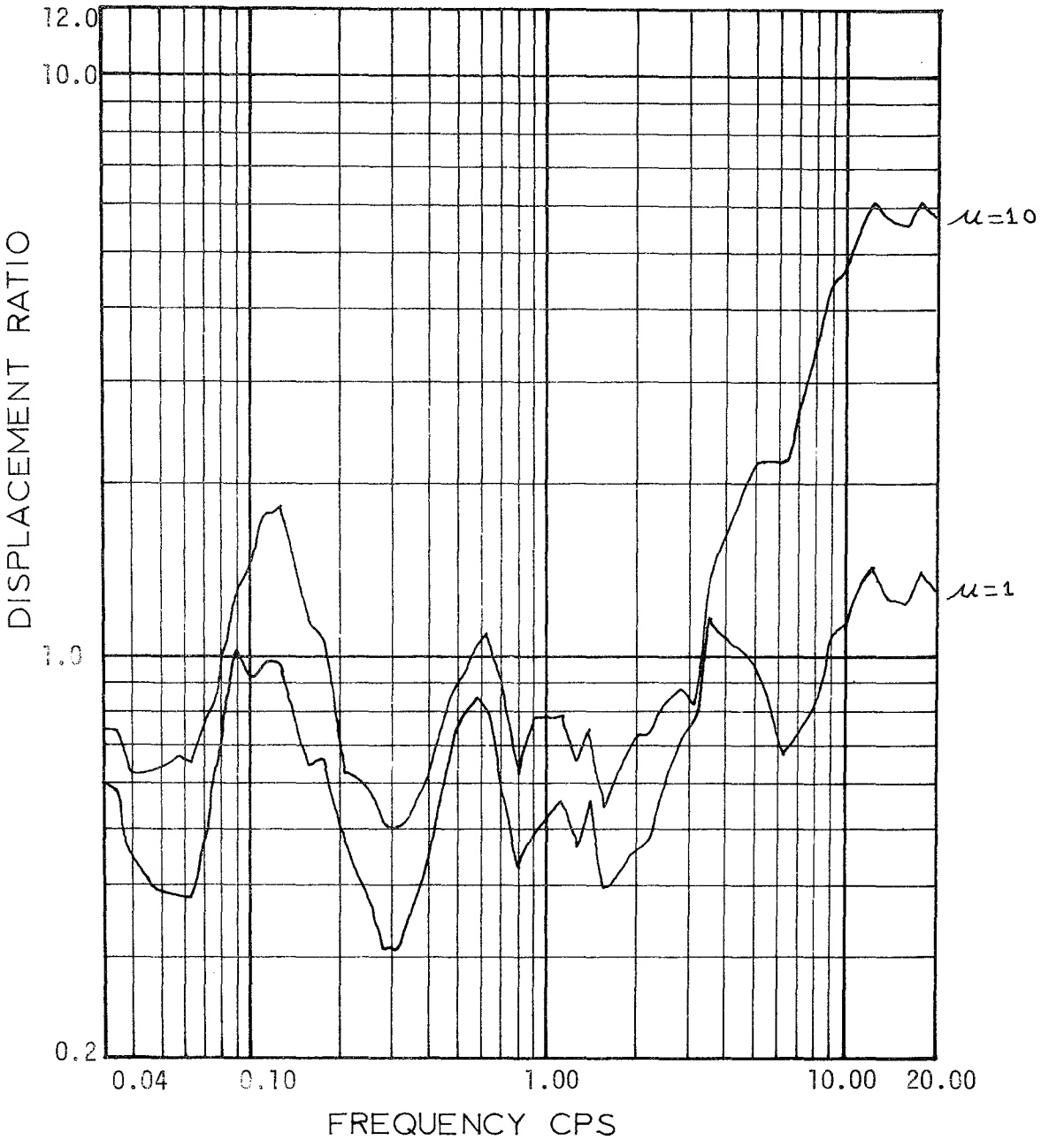
12.0
10.0
1.0
0.2
DISPLACEMENT RATIO
μ=10
μ=1
0.04
0.10
1.00
10.00
20.00
FREQUENCY CPS

FIGURE 4.15

CHAPTER 5

Conclusions and Recommendations

The purpose of this study was to evaluate two procedures often used to estimate response parameters for inelastic systems subjected to earthquakes. The first one is a set of rules suggested by Newmark to derive inelastic spectra from the elastic response spectrum. The second was a method often used, both for single and multidegree of freedom systems, replacing each inelastic spring by an equivalent linear spring with stiffness and damping functions of a characteristic strain.

Results shown in Chapter 3 indicate that Newmark's rule is always close to the average for the nine accelerograms considered or on the conservative side. Only in ranges 3 and 6 the difference (on the conservative side) might warrant a more accurate expression. Best fit relationships between R (ratio of elastic to inelastic spectrum) and ductility μ were obtained, but such a refinement is probably not warranted. It is interesting to notice, however, that the inelastic displacement may be less than the elastic displacement, particularly in range 3. The values shown in Chapter 3 would permit to obtain only average relationships as done in this work, but also maximum (lower bound) or standard deviations etc. Results are, however, limited to the set of earthquakes studied.

The second procedure investigated reproduces also fairly well the overall trend, although the agreement is not as satisfactory as with Newmark's rule. Using a characteristic ductility of 2/3 of the maximum, results for the accelerations are reasonably good, but the displacement

of the equivalent linear system is consistently smaller than that of the inelastic system. This would not occur if the displacement was simply computed as $S_d = \mu(S_a/\omega_o^2)$.

Due to limitations in computer time results were only obtained for systems with an initial, viscous damping of 5% of critical. The same programs could be used to study systems with other values of damping (0, 0.5, 1, 2 and maybe 7 and 10%). This would permit to determine if the value of viscous damping influences the previous conclusions or if they can be generalized. Continuation of the study for other values of damping would seem advisable.

REFERENCES

1. Roesset, J.M., and Garcia, F., "Influence of Damping on Response Spectra," MIT Dept. of Civil Engineering Research Report R70-4. January 1970. (Inter-American Program).

2. Blume, Newmark and Corning, "Design of Multistory Reinforced Concrete Buildings for Earthquake Motions," Portland Cement Association.

3. Veletsos, A.S., "Maximum Deformations of Certain Nonlinear Systems," Proceedings of the 4th World Conference on Earthquake Engineering, Vol. II, Chile, 1969.

4. Berg, G.V. and G. W. Housner, "Integrated Velocity and Displacement of Strong Earthquake Ground Motion," BSSA Vol. 51, 1961.

5. Roesset, J.M., Unpublished course notes for Structural Dynamics, M.I.T., 1969.

6. Anagnostopoulos, S.A., "Nonlinear Dynamic Response and Ductility Requirements of Building Structures Subjected to Earthquakes," MIT Department of Civil Engineering Report R72-54, September 1972.